Studying the inhibitory effect of oxysterols on NK-92 metabolism and cytotoxicity

A dissertation submitted to Trinity College Dublin in candidature for the degree of Doctor of Philosophy

School of Biochemistry and Immunology,

Trinity Biomedical Sciences institute,

Trinity College Dublin

2024

By Mona Shujaa Alharbi

Under the supervision of Dr. David Finlay

Declaration

I, the undersigned, declare that this work has not previously been submitted as an exercise for a degree at this, or any other University, and that unless otherwise stated, is my own work.

I, the undersigned, agree to deposit this thesis in the University's open access institutional repository or allow the library to do so on my behalf, subject to Irish Copyright Legislation and Trinity College Library conditions of use and acknowledgement.

I consent / do not consent to the examiner retaining a copy of the thesis beyond the examining period, should they so wish (EU GDPR May 2018)

X _____

Mona Shujaa Alharbi

Publication

‘25-hydroxycholesterol disrupts NK92 mitochondrial metabolism to block tumor cytotoxicity.’

Mona Alharbi……. David K. Finlay

(Manuscript in preparation)

‘Increasing the anti-cancer functions of NK-92 cells through targeting cellular metabolism’

Mona Alharbi, David K Finlay.

Poster in Irish Society for Immunology (ISI) conference, 2022

25-hydroxycholesterol disrupts NK-92 mitochondrial metabolism to block tumor cytotoxicity

Local Immunometabolism forum (IMF) ta

Abstract

NK cell-based immunotherapy has become a promising cancer treatment for cancer. One approach is the use of NK cell lines such as NK-92 as this overcomes many of the technical challenges associated with the use of human NK cells isolated from the blood. One of the major restrictions for the activity of NK cells against solid tumours are the conditions within the tumour microenvironment (TME) including adverse metabolic conditions. The Finlay lab has discovered that cellular metabolism is closely linked to NK cell anti-tumour functions, including NK cell cytotoxicity. However, little is known about the metabolic requirements for NK-92 to mediate anti-tumour cytotoxicity. This study investigated the metabolism of NK-92 cells and the importance for metabolic regulators, including mTORC1 and SREBP, in sustaining NK-92 cytotoxicity. Direct inhibition of metabolic pathways inhibited NK-92 cytotoxicity. While IL-2 signaling is required for NK92 cytotoxicity, the activity of the downstream signaling through mTORC1 and Srebp is dispensable. Interestingly, the oxidized cholesterol molecule 25-hydroxycholesterol (25-HC), a known inhibitor of SREBP activation, potentially inhibited NK-92 cytotoxicity, mitochondrial metabolism, along with observed distribution in membrane structure, seemed to occur independently of SREBP and LXR activation. 25-HC can be made by tumour associated macrophages (TAMs) that express cholesterol-25-hydroxylase. These data argue that 25-HC in the TME would inhibit NK-92 anti-tumour activity through modifying the membrane lipid order. Understanding NK92 cell metabolism will support designing better cell-based cancer therapeutic strategies in future. The data emerging from this project suggest that one strategy would be to engineer NK-92 cells to be resistant to the actions of 25-HC.

Acknowledgements

First and foremost, I am immensely grateful to my supervisor, Dr. David Finlay, for his invaluable advice, continuous support, and patience during my PhD studies. His vast knowledge and extensive experience have been a guiding force throughout my academic research and daily life. David, I extend my sincere appreciation for the opportunities, advice, support, and guidance you have provided. Working in your lab has been a pleasure, and I cannot thank you enough for the opportunities you've granted me.

I extend my gratitude to my non-thesis committee members, Prof Derek Nolan and Prof Clair Gardiner, for their valuable comments, feedback, and engaging discussions during my PhD journey.

My heartfelt thanks go to the Deanship of Scientific Research at King Saud University, Saudi Arabia, Riyadh, for their funding and supporting their research through the invitation of DSR Scholarship Support.

Studying abroad has been an incredible experience, thanks to the wonderful members past and present from the Finlay and Gardiner Labs. To all whom I've collaborated with, I am immensely grateful for the knowledge and experiences shared. I deeply appreciate the patience shown to me as I began my work in Finlay's lab. Special thanks to past members Katie O'Brien, Aisling McCrudden, Diana Moreira, Elisabeth Littwitz-Salomon, and Leonard Pelgrom for their warm welcome and immense help, which made me feel comfortable. Karen and Elena, your invaluable assistance during my initial stages and continued support have been greatly appreciated.

To the current members of the Finlay lab - Aisling Cameron, Sakshi Sankhla, Chloe Choi, Simon O'Shaughnessy, Cathal Keane, Carrie Corkish, Cristhiane Favero De Aguiar, Maxim Nosenko, Gavin Davis, Amal Alghethami, and Connor Corrigan - thank you for your unwavering support, camaraderie, and enjoyable moments shared during breaks or outside the lab.

Aisling McCrudden, your constant presence from my initial days has been invaluable. You've not only been a lab manager but also a friend. Your adept management has created a wonderful atmosphere. I cherish the inspirational sticky notes you left on my desk. Working with you has been a stroke of luck.

Chloe, thank you for your patience and for imparting almost all the techniques I've utilized in this study. Your knowledge and kindness are admirable, and I take pride in having worked with you.

Aisling Cameron, your assistance and patience, along with your prompt responses, have been invaluable to everyone.

I extend my thanks to all the staff at TBSI, especially Barry and Aoife, for their assistance with flow cytometry.

To my wonderful daughters – Rital, Abeer, and Raween – I am incredibly fortunate to have you. Thank you for your patience and daily messages; they keep me going. To my husband Nasser, thank you for your unwavering patience and boundless support.

My amazing siblings – Abeer, Saud, Huda, Dyan, Abdullah, and Zyad – thank you for your unwavering belief in me, your encouragement, support, love, and patience. I believe my parents, Shemah and Shujaa, would be immensely proud and happy for me; this moment was their dream!

Lastly, heartfelt gratitude to my best friends Juji and Claudia for their unwavering support. Juji, your exceptional support and love mean the world to me. Claudia, our 20 years of friendship speaks volumes; your support has been outstanding.

Abbreviations

25-HC	25-Hydroxycholesterol
27-HC	27-Hydroxycholesterol
2-DG	2-Deoxyglucose
7KC	7-Ketocholesterol
AA	Antimycin A
ABCG1	ATP binding cassette subfamily G member 1
APC	Antigen Presenting Cell
ATP	Adenosine Triphosphate
CAR	Chimeric Antigen Receptor
Ch25h	Cholesterol-25-hydroxylase
CLP	Common Lymphoid Progenitor
CTL	Cytotoxic T Lymphocyte
Cyp27a1	Cytochrome P450 family 27 subfamily A member 1
DC	Dendritic Cell
DEPC	Diethylpyrocarbonate
DMEM	Dulbecco's Modified Eagle Medium
DMSO	Dimethyl Sulfoxide
ECAR	Extracellular Acidification Rate
ER	Estrogen Receptor
ER	Endoplasmic Reticulum
ETC	Electron Transport Chain
FASL	Fas ligand
FASN	Fatty Acid Synthase
FCCP	Fluoro-Carbonyl Cyanide Phenylhdrazone
FCS	Foetal Calf Serum
G6P	Glucose-6-Phosphate
H.S	Horse Serum
HIF	Hypoxia Inducible Factor

HMGCS1	3-Hydroxy-3-methylglutaryl-CoA Synthase 1
HSCs	hematopoietic stem cells
IDO1	Indoleamine 2, 3-dioxygenase
IFN	Interferon
IL-2	Interleukin
ILC	Innate lymphoid cell
IMDM	Iscove’s Modified Dulbecco’s Medium
INSIG	Insulin induced gene 1 protein
ITAM	Immunoreceptor Tyrosine-Based Activation Moti
ITIM	Immunoreceptor Tyrosine-Based Inhibition Motif
MTG	Mitotracker Green
MTOC	Microtubule Organising Centre
mTORC	Mammalian Target of Rapamycin Complex 1
mtROS	Mitochonderial Reactive Oxygen Species
NK	Natural Killer
NK-92CRL	IL-2-dependent NK-92 cell line
NK-92MI	IL-2-independent NK-92 cell line
OCR	Oxygen consumption Rate
Oligo	Oligomycin
OxPhos	Oxidative Phosphorylation
PBMC	Peripheral Blood Mononuclear Cells
PCR	Polymerase Chain Reaction
qPCR	Quantitative Real Time
R5P	Ribose-5-phosphate
Rapa	Rapamycin
ROS	Reactive Oxygen Species
Rot	Rotenone
RPMI	Roswell Park Memorial Institute
S1P	Site-2-Protease
SCAP	SREBP Cleavage Activating Protein
SCD	stearoyl-CoA desaturase

SRC	Spare Respiratory Capacity
SREBP	Sterol regulatory binding protein
TME	Tumour Microenvironment
TMRM	Tetramethylrhodamine, methyl ester
TRAIL	TNF-related apoptosis-inducing ligand

Table of Contents

Chapter 1- Introduction

1.1 The immune system: innate and adaptive immune systems

The immune system is a host defense complex including a collection of cells, proteins, and many biological processes within an organism which function to protect against various diseases. The immune system has been divided into two distinct arms, innate immunity and adaptive immunity, which are regulated cohesively in response to a specific pathogen: therefore, defects in either arm of the immune system lead to inappropriate responses. The innate immune system, including antimicrobial proteins, macrophage, neutrophils, monocyte and complement activation, is the first line of defense with non-specific protection against extracellular pathogens. The adaptive immune system, consisting of T and B lymphocytes, possesses higher specificity which is mediated by antigen-specific recognition of pathogen. [1, 2, 3]

Innate immunity consists of several non-specific defense mechanisms including natural barriers (e.g. skin, low pH in the stomach, digestive enzymes and phagocytosis), immune cells (e.g. Macrophage, Neutrophil, and Natural Killer (NK) cells) and biochemical cascades (e.g. complement Activation). Innate immune cells rely on pathogen recognition receptors (PRRs) to identify pathogen, allowing a limited number of immune cells to recognize and respond rapidly to a broad range of pathogens that share common structures known as pathogen associated molecular patterns (PAMPs). Examples of PAMPs including bacterial cell wall component such as Lipopolysaccharide (LPS) and double-strand ribonucleic acid (RNA) in viral infection [2, 4]. An essential role of innate immunity is engulfing pathogens by phagocytosis as well as recruiting the other immune cells to sites of inflammation or infection by producing cytokines and chemokines, which are important for cell-cell communication and thus clearance of pathogens.

Even though the innate immunity has evolved to rapidly respond and effectively eliminate a variety of pathogens, the type of molecular patterns that can be recognizing is limited. This limitation has driven the evolution of adaptive immunity

[5]. The adaptive immune system is engaged at the same time, but it is good at clearing pathogens not cleared by the innate immune system. The function of the adaptive immune response is to identify non-self-antigen. Adaptive immunity has two types of lymphoid cells; T cells and B cells, which express the antigen receptors T cell receptor (TCR) and B cell receptor (BCR), respectively [6]. NK cells are also characterized as lymphocytes according to their morphology, the expression of many lymphoid markers, and their origin in bone marrow from common lymphoid progenitor cells (CLPCs) [6]However, NK cells generally are considered to be a component of innate immune system as they lack antigen-specific receptors on their surface. Innate lymphoid cells (ILCs) are heterogeneous group of cells that differentiate from CLPCs, but unlike T/B cells, they lack antigen receptors. NK cells are one of the five major group of ILCs which are divided on basis of their cytokine production and the transcription factors required for their development [7]

In recent years, there has been growing interest in innate immunity, because of its powerful anti-tumor capacities that can be triggered in the early stage of tumor formation. NK cells as defined by Herberman in 1975 are cytotoxic lymphocytes that exert a natural cytotoxicity toward tumor target and produce a wide range of cytokines that modulate the adaptive immunity [7], [8]. Considering the crucial role of NK cells in cancer biology, they have emerged as exciting tool for cancer therapy.

1.2 Natural Killer cells

Natural Killer (NK) cells were discovered almost 50 years ago. NK cells are large granular lymphocytes and derive from bone marrow. They are well-known to moderate the function of innate and adaptive immune systems. They represent 5-10% of the lymphocytes peripheral blood and possess cytotoxic effector molecules and the ability to identify and kill a wide range of various cancer cells [10], [11]. NK cells are identified as CD3 negative lymphocytes that express CD56 in human or NKp46 in mice [9], [10]. NK cell have receptor families to tune NK effector

responses, and these including inhibitory CD94/NKG2 receptors that identify non-classical MHC, and inhibitory KIR receptors that identify classical MHC, and activating Natural Cytotoxicity Receptors (NKp44, NKp46, and NKp30) [11], [12].Functionally, NK cells identify transformed cells and viral-infected cells and kill them by producing and releasing several effectors molecules like perforin and granzyme B. Moreover, NK cells also mediate antibody-dependent cellular cytotoxicity (ADCC) toward antibody bound target cells. NK cells also coordinate other cells of the immune system through releasing a range of cytokines and chemokines [13].

1.3 Development of NK Cells

NK cells differentiate from hematopoietic stem cells (HSCs), the common precursor for many immune cell subsets [14], [15]. The development of NK cells from multipotent hematopoietic stem cells is a complex process that is guided by external environmental factors as well as intrinsic responsiveness precursor cells to pathologic challenges. In particular HSCs give rise to different types of blood cells including NK cells through a process known as hematopoiesis which occurs in the bone marrow [16]. The first stage of the hematopoiesis process occurs when HSCs give rise to hematopoietic lineages with one of the precursors being common lymphoid progenitor (CLP). The CLP then differentiates into any lymphocytes subset and it is IL-2 a selectively enhances their development towards NK cells [16]. To respond to IL-2 cells must express CD122 (the IL2 and IL-15 receptor common β chain) and CD132 (the common ɣ chain). The acquisition of CD122 is then a hallmark of the NK cell population and commits lineage negative lymphoid precursors to the NK cells lineage. Then, immature cells must undergo an education process to become a functional mature NK cell. This involve engaging of NK cells inhibitory receptors with cognate major histocompatibility complex (MHC) class I ligands on surrounding cells. Cells that not able to ligate their inhibitory receptors through this process become anergic as a protective mechanism to avoid NK cell self-reactivity [17] [20] [21] [22].

1.4 NK Cells Phenotype

Recent studies established that human NK cells can be defined into two subsets $CD56^{dim}$ and $CD56^{bright}$ based on a comparative expression of CD56 (adhesion marker mediating homotypic adhesion) and CD16 (or FcγRIIIA, low-affinity receptor for the Fc portion of immunoglobulin G, IgG). Most of our knowledge about NK cells which are acquired from mouse bone marrow or spleen, and human peripheral blood mononuclear cells (PBMC). These cells are known as conventional NK cells (cNK) [18], [19]. Currently, many studies have started providing insight into tissue-resident NK cells (trNK) [20]. Here, I will give a brief description of dichotomy between cNK and trNK cells in term of their phenotype.

1.4.1 Conventional NK cells (cNK)

Based on the expression of CD56 and CD16, cNK cells consist of two-significant subsets $CD56^{bright}$ $CD16^{-}$ and $CD56^{dim}$ $CD16^{+}$. NK cells $CD56^{dim}$ $CD16^{+}$ subset represents about 90% of CD56+ NK cells in peripheral blood, with $CD56^{bright}$ $CD16^{-}$ subset accounting for the remaining ~10% [21]–[23]. Functionally, $CD56^{bright}$ subset has an immunoregulatory function, while $CD56^{dim}$ subset plays an essential role in cell cytotoxicity [24].

cNK cells receptors are categorized as inhibitory (mainly, Killer Ig-like receptors (KIR) and the heterodimeric C-type lectin receptor (NKG2)) and activating (notable, natural cytotoxicity receptors (NCR) NKp46, NKp30, NKp44, and the C-type lectin-like activating immunoreceptor, NKG2D. The integration of signals from these activating and inhibitory receptors controls the function of NK cells, including the cytotoxic capacity and the release of a range of cytokines and chemokines [21].

KIR on cNK cells, can recognize healthy cells via interactions with the major histocompatibility Class I (MHC-I), receptors that are expressed on the surface of most healthy cells. Once ligated KIR induce suppressive signaling pathways that prevent cNK cell activation and the induction of their killing activity, thus protecting healthy cells [25]. These KIR illustrate the hypothesis of “missing self” which was

presented in 1986 by Dr. Klas Karre [26]. It proposes that NK cells have a mechanism that empowers them to recognize information that presents in the host, but that is missing on NK cell targets. Upon encounter with transformed cells in which MHC-I molecule expression is downregulated or lost “missing self”, NK cells no longer receive inhibitory signals leading to the activation of cytotoxicity and cytokine production.

Even though missing self-theory is important, the activation of NK cells is dependent on the balance between self-signal (inhibition) and stress signals (activation) meaning if there is high expression of ligand for activating receptors then NK cells will be activated even if the MHC-class I is still expressed (**Figure 1.1**).

1.4.2 Tissue-resident NK cells (trNK)

Compared to cNK tissue-resident NK exhibit distinctive tissue-specific markers and are developmentally less mature. These differences are likely due to the local microenvironment at the tissue site [27], [28].

Expression of activating receptors such as NCRs and NKG2D occurs in both cNK and trNK, and both recognize induced self -ligands or antigen-specific ligands suggesting that trNK has the same activation mechanism as cNK [29]. trNK express different levels and types of KIR comparing with cNK, which means there is functional difference between cNK and trNK at the level of inhibitory receptors. Unlike cNK cells trNK express CD69; type II C-lectin membrane receptor, CXCR6; chemokine receptor, CD103; an integrin subunit that forms αEβ7 and binds to the cell adhesion molecule E-cadherin, CD49a; an α1β1 integrin receptor α-subunit that attach to collagen IV, all of which are well-established to be key markers of tissue recognition [30], [31]. Unlike human peripheral blood $CD56^{bright}$NKs, $CD56^{bright}CXCR6^{+}$ trNKs have increased levels of CD98 (the amino acid transporter) but expressed lower levels of Glut1. This interesting finding suggests potential differences in their metabolism [32].

Upon activation, NK cells can seek out and destroy tumor cells by several mechanisms, including directly killing abnormal cells by identifying markers of stress on the surface of cancer cells. Then, releasing toxic granules containing granzyme and perforin or by expression of Tumor necrosis factor (TNF) family member on the surface of NK cells such as FASL and TNF-related apoptosis-inducing ligand (TRAIL). These death ligands induce tumor cell apoptosis by interacting with corresponding receptors, FASL and TRAIL receptors. Additionally, NK cells can work in combination with antibodies, which have identified a specific antigen expressed by cancer cells and kill the cancer cells through ADCC [21]. Further details on the mechanisms of how NK cells kill against target cells will be provided.

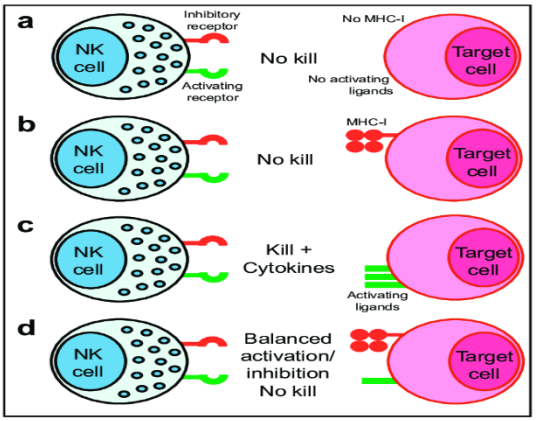

Figure 1. 1 Self-missing and self-recognition molecular basis by NK cells [33]**.**

(a)NK cells do not respond if the target cells do not express ligands for activating and inhibitory receptors. (b)If the MHC-I on target cells binds to inhibitory receptors on NK cells in absence of ligands for activating receptors, then no cytotoxicity will occur. (c) downregulation of MHC-I expression and expression of ligands for activation receptors lead to strong cytokine production and cell cytotoxicity. (d) NK cells responses can be regulated by balance between inhibitory and activating signaling.

1.5 NK cell functions

NK cells are named 'natural' killing as they were first identified for their capacity to kill without any prior activation, unlike to cytotoxic T cells, which need instructions from antigen presenting cells. In addition, NK cells secrete cytokines such as Interferon-gamma (IFNγ) and Tumour necrosis factor- α (TNF-α), which control other immune cells such as DC and macrophages to influence the immune response [28]. NK cell recognition systems include a wide range of activating and inhibitory cell surface **(Figure 1. 2)**, the engagement of which, controls the NK cell activities. Thus, the binding of these receptors or the signaling that received by receptors, determines whether a cell is targeted for killing and NK cell cytokine secretion [34].

A fundamental role of NK cells is termination of cells with downregulated or absent MHC-class I expression which normally bind to a set of inhibitory receptor (KIR) on NK cell surface leading to suppress NK cell function [26]. Aside from MHC molecules downregulating expression, cancer cells might overexpress ligands that bind to NK cell activating receptors. For example, MHC class I polypeptide-related sequence A (MICA) is a ligand that bind to the activating NKG2D receptor. Even though, the majority of ligand for activating receptors are

express on cell membrane, some of them are soluble such as the complement factor P (properdin) which binds NKp46 leading to important signaling during bacterial infections. In addition, many cancers cell type secretes Platelet derived growth factor DD (PDGF-DD) which ligates to the activating NKp44 receptor on NK cell, leading to stimulate the secretion of IFNγ and TNF [7], [35]. Another mechanism that involves in target recognition is CD16 receptor-mediated mechanism which attaches to the immunoglobulins constant region (Fc). The binding of CD16 with antibodies that coated surface membrane antigens of the cells, triggers phosphorylation of the immunoreceptor tyrosine-based activation motif (ITAM) domains of the high-affinity receptor of IgE (FcεRIγ) and CD3ζ in NK cells leading to induce a signaling cascade that eventually results in killing of the antibody-coated cell, a process called ADCC [36], [37].

When NK cells confront a prospective target cell and become activated, a synapse is formed with the target, and the lytic granules are release into synapse, called degranulation. The polarization of the lytic granules needs further signals from the synapse. The main key effectors granules of cytotoxicity are perforin, which makes pores on the cell membrane of the target cells, and granzymes, which pass thorough the pores and induces caspases leading to apoptosis of target cells. The expression of CD107a on cell surface, also known as lysosomal-associated membrane protein 1 (LAMP1), can be utilized as a marker for the degranulation, the process of releasing of lysosomal-related organelles **(Figure 1.3).**

Another mechanism for direct killing of NK cells is through expression of FAS ligand (FASL) and TNF-related apoptosis-inducing ligand (TRAIL) **(Figure 1. 4)** [7], [38].

Engagement of activating receptors (except for CD16 ligation) is not enough to induce cytokine secretion or cytotoxicity in naïve NK cells. Pre-activating NK cells with cytokine is key for triggering the effector function of NK cells. NK cells can be activated by exposure to IL-2 which trigger signaling from activating receptors. Additionally, IL-15, that signals via the receptor which shares the

signaling β- and γ-chain with IL-2 receptor, activates NK cells and induce their proliferation and survival. Also, IL-2, IL-12 and IL-18 when used in combination, can activate NK cells and strongly induce production of IFNγ [39], [40].

In addition to their cytotoxic ability, NK cell can produce various cytokines, chemokines, and growth factors, including IFNγ, FLT3L, TNF, CC chemokine ligand 3 (CCL3), CCL4 and CCL5, lymphotactin (XCL1) and granulocyte-macrophage colony-stimulating factor, thus NK cells can control the activity of other immune cells [35], [41]. For example, release of CCL5 and XCL1 influence DCs, FLT3L increases the amount of stimulatory DCs in the tumor microenvironment, and IFNγ triggers T helper 1 cells polarization while also inducing MHC class II molecules on antigen-presenting cells and activates macrophages [7].

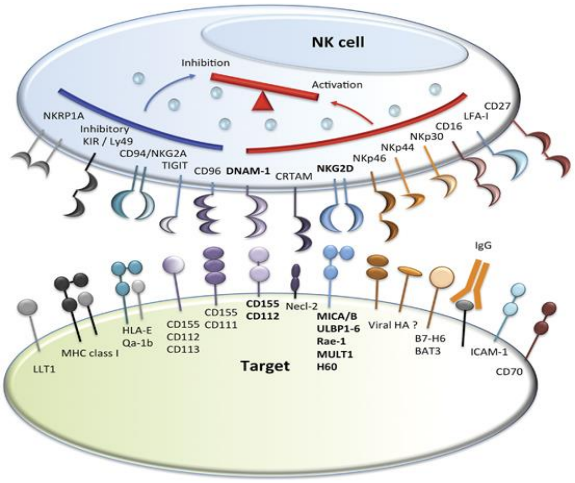

Figure 1. 2 NK cell receptors and their associated ligand on the target cells.

Most of inhibitory and activating receptors on NK cells and their associated ligand on the target cells are illustrated. BAT3, human leukocyte antigen (HLA)-B-associated transcript 3; CRTAM, class I-restricted T-cell-associated molecule; HA, hemagglutinin; HLA-E, HLA class I histocompatibility antigen, alpha chain E; IgG, immunoglobulin G; LFA-1, leukocyte function-associated antigen-1; LLT1, lectin-like transcript 1; TIGIT, T cell immunoglobulin and ITIM domain [18]

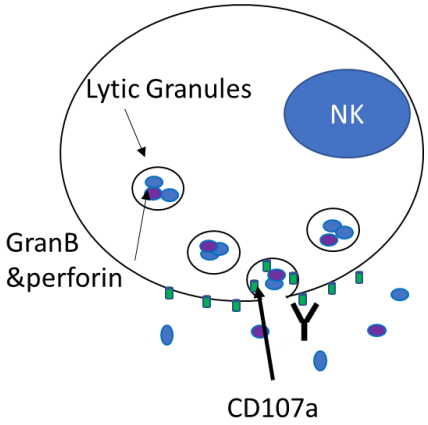

Figure 1. 3 Schematic diagram illustrate the NK cell degranulation.

NK cell release the content of lytic granules (Granzyme B and perforin) in process called degranulation. These lytic granules moved to and fuse to NK cell membrane leading to secrete their content on the outside of the cells.

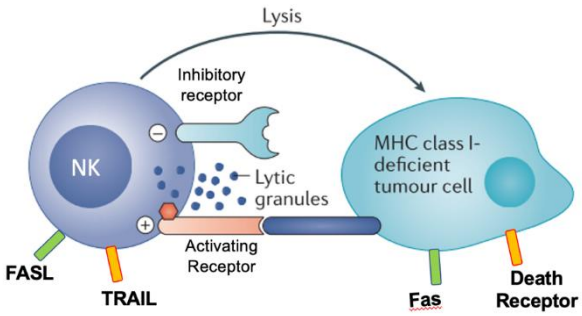

Figure 1. 4 NK cell response-mediate apoptosis to tumour cells.

The NK-cell response to tumor cells. NK cells eliminate tumor cells via engagement of activating receptor; Fas (CD95)-Fas ligand (CD95L) interaction; and release of perforin and granzyme B molecules (lytic granules), which cause necrosis/apoptosis of the tumor cell

1.6 NK cells in Tumour microenvironment

The tumor microenvironment (TME) contributes conditions that induce tumor progression. Many studies provide evidence that the TME inhibits NK cell function through the production of soluble modulators known as immunosuppressive factors, low nutrient levels, and hypoxic conditions which negatively affect proliferation, maturation, and the effector functions of NK cells [42].

Transforming growth factor beta (TGF-β) is a cytokine generated in the TME by Treg, tumor cells, and myeloid-derived suppressor cells (MDSCs). This is well-known to inhibit the extension and function of effector cells and to induce the Treg proliferation [43]. TGF-β inhibits NK cell function directly or indirectly, by regulating and stimulating other immune cells such as regulatory T cells (Treg), and MDSC to generate further immunosuppressive molecules. As a direct consequence, TGF-β limits NK cell function, such as cytotoxicity and production of IFN-γ, by impairing T-bet transcription factor (SMAD3) and NKp30 and NKG2D downregulation, and its ligand MICA in cancer patients [44]–[46].

Additionally, TGF-β produced by NK cells inhibit NK cell metabolism and function [47]. Moreover, TGF-β inhibit $CD56^{dim}$ recruitment and favor that of $CD56^{bright}$ [46]. It entails the modulation of chemokines to decrease the expression of a set that attracts $CD56^{dim}$ NK cells (CXCL1, CXCL2, CXCL1, and CXCL8) while increasing the expression of chemokines that guide the migration of $CD56^{bright}$ (CXCL9, CXCL10, CCL5, and CXCL19). The predominant population of NK cells in TME in several cancer diseases is $CD56^{bright}/CD16^{low}$ such as ovarian and lung cancer patients. Based on this fact, TGF-β might be consider a target for triggering NK cell-mediated antitumor immune system [48].

Another fundamental reason leading to NK cells dysfunction in cancer is damaged cellular metabolism. The TME is known to be restrictive in nutrients such as glutamine and glucose which are very important for NK cell metabolism. In human NK cells elevated levels of glycolysis and oxidative phosphorylation (OXPHOS) are associated with release of IFN-γ by cytokines activation [49]. In mice, NK cells OXPHOS is a primary pathway in the steady state, rather than glycolysis. However, NK cells that activated by IL-2/IL-12 have a superior preference for glycolysis. Glycolysis is a crucial metabolic pathway in activated NK cells for their function. One study identified a mechanism involving TGF-β: lung tumor increased the expression of fructose bisphosphates1 (FBP1), the gluconeogenesis enzyme, in tumor-infiltrating NK cells leading to dysfunctionality of NK cell by impairing of NK cells viability and glycolysis. To restore the NK cells dysfunctional phenotype, pharmacological inhibition of FBP1 was used during tumor promotion but not progression [50]. Other potential molecules that can inhibit NK cell metabolism are physiological products of cholesterol oxidation via enzymatic process, 25-hydroxycholesterol and 27-hydroxycholesterol, that inhibit the SREBP transcription factor process and activation, which is a key regulators of NK cells metabolism [51], [52]. Further evidence supporting the role of impaired cellular metabolism leading to NK cell dysfunction is derived from studies conducted on obesity in both murine and human models. NK cell from obese humans and mice are loss their responses to

tumor target cells regarding production of IFN-γ, granzyme B and perforin and cytotoxic capacity [53].

This observation in dysfunction of metabolism has linked to peroxisome proliferator-activated receptor (PPAR)-directed lipid accumulation in NK cells; as a result, gene expression is altered with downregulation of mTORC1 and cMyc signaling, as well as decreased levels of both glycolysis and OXPHOS. Consequently, NK cells that come from obese human and mice decline to eliminate tumor cells due to their inability to form synapses with target cells as this event is energy consuming [54], [55].

Another condition that causing NK cell dysfunction in TME is hypoxia. Hypoxia led to decrease of NKp46, NKp30, NKp44, NKG2D, granzyme B and perforin [56]. Exposure to IL-2 can restore NK cells cytotoxicity in multiple myeloma by upregulating NKG2D expression. Beside hypoxia, tumor cells produce a huge amount of lactic acid in the TME, which causing acidosis and immunosuppression. The accumulation of lactic acid has associated with decreased NK cell cytotoxicity and reduction of NKG2D expression [57], [58]. Moreover, the acidification induced apoptosis of liver-resident NK cells in colorectal cancer liver metastases. Neutralization of the TME restored effector NK cell functions such as cytotoxicity through inducing NKG2D expression [59].

1.7 NK cell immunosurveillance

The immune surveillance theory was first introduced by Thomas is 1959 [60]and states that the immune system is constantly guarding the body from abnormal cells (tumor) which are identified by the body as foreign, and that immune responses terminate tumor cells before they become detectable clinically. Even though, this definition of immune surveillance remains controversial, various studies support it. Tumors that are infiltrated by various immune cells, including CD8+ T lymphocytes, NK cells, and macrophages, tend to exhibit significantly better survival rates in cancer patients compared to tumors with limited immune cell infiltration [61]. This suggests that immune cells play a fundamental role in the development of survival

outcomes in cancer patients. Secondly, immune responses become less efficient in old people and neonatal period, which put them at a risk for bacterial and viral infections development, consequently resulting in increased mortality. Additionally, the incidence of cancer is higher in people with immunodeficiencies such as AIDS patients compared to people with normal immune functions [62],[67].

Impaired T cell function or any other part of the adaptive immune system particularly affects immune surveillance. However, innate components of the immunity, involving NK cells, also play a crucial role.

Upon activation, NK cells produce many cytokines and chemokines, many of which have potent anti-tumor activities in addition to enhancing other innate and adaptive immunity responses [64]. There are several advances in research which support the ability of human NK cells to limit cancer progression.

The first area which supports the significant important role of NK cell in immune surveillance are the potential mechanisms that govern NK cell recognition of tumor cells. NK cells are well-known to express CD16 that enhances ADCC. ADCC is an important key mechanism involving in the action of many monoclonal antibodies that recently used in clinical cancer immunotherapy [65]. Many NK cells activating receptors have recognized and characterized to their contribution to natural cytotoxicity [66], [67]. One significant group of these receptors is a natural cytotoxicity receptor (NCRs). For instance, NKp46 and NKp30 are expressed in all peripheral blood NK cells, while NKp44 expression is induced in response of IL-2 stimulation. Upon ligation, these receptors trigger NK cell-mediated lysis of many different cancer cells [65]. Beside these receptors, many activating receptors including NKp80, CD59, CD11a/CD18 and CD2 are well characterized and have significant important costimulatory function in activation of NK cells and thus tumor cell recognition. In addition to activating receptors, the cytotoxicity of NK cells is controlled by signals driven by inhibitory receptors [68]. Most of these receptors bind to classical or nonclassical MHC class I molecules expressed normally on most healthy cells but which are commonly downregulated on transformed tumor cells as a mechanism to evade killing by CD8 cytotoxic T cells [69], [70].

KIR and CD94/NKG2A in human, play an essential role as HIL-A class I-binding inhibitory NK cell receptors. KIR identify selected HIL-A, B and C alleles, while CD94/NKG2A receptors identify HIL-A class E molecules [71]. The arrangement or replacement (clonal location) of KIRs results in a system allowing NK cells to recognize cells the expression absence of single MHC class I alleles. Therefore, each individual has a collection of NK cells with different proportions of cells that can sense modifications in HLA class I levels on transformed cells [72], [73]. The interaction between inhibitory receptors and their cognate HLA class I ligands are not only important in controlling NK cells activation but also participate to control immune tolerance to healthy tissue, a process called NK cell education [74]. In this process only NK cells that received a signal through an inhibitory receptor become 'educated' to achieve their full cytotoxic and immunoregulatory potential. This prevents NK cells lacking an inhibitory receptor being released to cause damage to healthy cells.

Another significant concept relevant for NK cells attacking tumor cells is NK cells differentiation and functional heterogeneity of NK cells subsets. During the process of differentiation from $CD56^{bright}$ to $CD56^{dim}$ cells, NK cells go through series of phenotypic and functional changes mainly in receptor expression. $CD56^{bright}$ are less cytotoxic and have a fundamental regulatory function with powerful ability to produce cytokines, while $CD56^{dim}$ subsets are more cytotoxic cells. This functional division is mostly outcome of differing responses to extrinsic stimulation [73], [75]. Thus, while $CD56^{bright}$ NK cell respond to cytokines, $CD56^{dim}$ respond to consequence via activating receptors; therefore, they are more responsive to stimulating agent by cancer cells that express particular ligands.

Based on previous findings there are many mechanisms triggering the anti-tumor responses of NK cells. Better understanding of the mechanisms that adapted by TME to inhibit NK cells effector functions and how they can be restored is of essential to develop NK cancer-immunotherapeutic strategies and would give insight into harnessing the anti-tumor characterization of NK cells for cancer immunotherapy.

1.8 NK cells adoptive transfer immunotherapies

Adoptive transfer cellular immunotherapies have involved many types of immune cells, including cytotoxic T lymphocytes (CTLs), DCs, and NK cells. Even though there are many current developments in CTL and DC therapies, clinical applications are a bit limited due to a failure in characterizing cancer antigens and the restricted use of autologous cells [76]. Unlike DC and CTL therapies, NK cells, which are a fundamental part of tumor immunosurveillance, have anti-tumor activity that is independent of specific tumor antigens. NK cell activation is controlled by the interaction of NK receptors with target cells leading to the release of cytotoxic granules molecules such as perforin and granzymes to immediately lyse target cells in similar fashion to triggered cytotoxic T cells but without prior sensitization. Recently clinical trials have investigated the overall safety of the infusion of NK cells even in allogeneic setting. Because of the viability of using allogeneic NK cells, that can rapidly act against tumor cells, many efforts are ongoing to engineering NK cell-based cancer immunotherapies [77]–[79].

A major NK cell-based therapy approach is the transfer of unmodified allogeneic and autologous NK cells. The first clinical trials for this approach were in 1980 utilizing adoptive cellular therapy was based on delivery of lymphokine-activated killer (LAK) cells which were autologous peripheral blood mononuclear cells stimulated exogenously with IL-2 *in vitro* for few several days (5 to 7 days) to trigger killer cells [80], [81]. High-dose IL-2 was administrated to activate autologous NK cells *in vivo,* but this had significant side-effects leading to a capillary leak syndrome [80], [82]. Following the discovery of inhibitory KIR and their role in avoiding NK cells killing of self-cells, researchers started to investigate the possibility of utilizing allogeneic donor cells as opposed to autologous cells. However, there remain significant limitations to strategies involving expanded of *ex vivo* autologous or allogeneic NK cells [83]. NK cells extracted from patients with cancer are often dysfunctional and while allogeneic NK cells are efficacious in hematological cancers, they show very limited therapeutic benefits for solid tumors.

This is due to the high level of heterogeneity of solid tumors and the harsh tumor microenvironment, including high levels of TGF-β and hypoxia which inhibit the activation of NK cells activities [84]. Therefore, several strategies have been investigated for improving the effect of adoptively transferred NK cells to treat solid cancers.

Some investigators have taken the approach to use an NK cell line that can be expanded easily *in vitro* to large numbers under conditions of good manufacturing practice (GMP) abd that display potent cytotoxicity against cancer cells. The most important feature of this approach is that a NK cell line could be engineered for increased antitumour activities and can easily expanded and maintained *in vitro,* thus readily available for the treatment of cancer patients on mass [85]. There are seven malignant NK cell lines including NK-92, NKL, YT, HANK-1, KHYG-1, NK-YS and NKG. Figure 1.5 shows a list of these NK cell lines that were established for clinical application.

Table 1.1 Established NK cell lines for clinical applications

NK cell line	Disease	IL-2 Dependency	Reference
NK-92	Non-Hodgkin's lymphoma	Yes	[86]
NKL	Large granular lymphocyte leukemia	Yes	[87]
NKG	non-Hodgkin's lymphoma	Yes	[88]
YT	Acute lymphoblastic lymphoma and thyoma	NO	[89]
HANK-1	Nasal-type' NK/T cell lymphoma	Yes	[90]
KHYG-1	NK cell leukemia	Yes	[91]
NK-YS	NK cell lymphoma/leukemia	Yes	[92]

1.9 Genetically modified NK-92 cells, a promising Off-the-shelf cancer immunotherapy

NK-92 cell line.

NK-92 cell lines were established in 1994 from the peripheral blood of a 40-year-old male patient diagnosed with acute progressive non-Hodgkin's lymphoma. This cell line is positive for CD56, CD2, CD57 and negative for CD3 and CD16 and thus incapable of mediating ADCC [86]. NK-92 cell express a high number of activating receptors including NKp30, NKp46, 2B4, NKGD/E and CD28 and express a high level of cytotoxicity molecules such as perforin, granzyme, TRAIL, FASL and TNF-α. On other hand, they express a low number of inhibitory receptors, lacking almost all of inhibitory KIRs [93].

The proliferation of NK-92 cell line is highly dependent on the presence of recombinant IL-2. Recent studies showed that IL-2 deprivation led to a decline in cytotoxicity within 24 hours and cell death within 72 hours. However, IL-2 can cause unwanted side effects when given to patients such as vascular leak syndrome. Therefore, NK-92 cells have been engineered to express IL-2 in the endoplasmic reticulum so that they able to support their own growth and make them more compatible with clinical applications [94].

NK-92 cells have characteristics of both primary NK cells and cancer cells and thus can behave differently to what might be predicted e.g. [95]. CD94 inhibitory receptor and LIR-1 receptors are both expressed on NK-92 cell line, yet the engagement of these receptors does not have a major effect the cytotoxicity of NK-92 cells [96].

In addition, NK-92 cells have been used in studies with SCID mouse models and in human clinical trails. NK-92 cell showed a high cytotoxic activity against several human malignant cell *in vitro* and *in vivo.* Following successful preclinical studies in

mouse model, NK-92 cells were used in direct infusions of cancer patients [97].

NK-92 cell have gained FDA approval for the treatment of patients with renal cell carcinoma and acute malignant melanoma in United States and Europe. This cancer therapy is safe and shows significant anti-tumor efficacy against these malignancies. For these human infusions, NK -92 cell are irradiated with 5 Gy to prevent the NK-92 cells from undergoing any further cell division once transferred into the patient. *In vitro* test have shown that NK-92 cytotoxic activity is maintained after up to 10 Gy irradiation for 48 hours [98], [99]. Moreover, no toxicity against non-malignant allogenic cells has been detected. Accordingly, this data suggests that infusion with NK-92 cells is safe and an excellent candidate for adoptive cellular immunotherapy. Thus far, NK-92 cell line is the only NK cell line that has entered clinical trails and it will serve as a platform for the future of NK cell-based cancer immunotherapy studies.

Gene modified NK-92 cell line.

Genetic modification of NK-92 cells might give new possibilities for tumor immunotherapy by increasing NK-92 cell functions, enhancing their specificity and providing them with additional capacities. This genetic modification could be approached through a different strategy either by triggering NK-92 cell proliferation, survival by cytokine gene manipulation, targeting specific target of tissue or malignant cells for NK cells. Activating receptor overexpression or blocking of inhibitory receptors could also enhance the cytotoxicity capacity of NK cells. Using of chimeric antigen receptor (CAR) targeting a specific tumor antigen can deliver specificity towards the tumour cells and additional activating signalling. Currently, there are many gene-modified NK-92 cell lines that are being tested for tumor immunotherapy [100].

The parental NK-92 cell line does not express CD16 (FcγRIIIa receptor), thus they cannot mediate ADCC. There are two variants of CD16, the high affinity variant which has valine substitution for phenylalanine at position 158 and low affinity

variant. It has been shown that patients expressing high affinity CD16 receptor has better response improvement to treat with monoclonal antibodies such as lymphoma, breast cancer, and colon cancer [101], [102].

This provides the rationale for a treatment that combines IgG1 antibodies (mAbs) against a specific tumor antigen with infusions of NK-92 cells engineered to express the high affinity FcγRIIIa receptor (haNK).

The term taNK refers to engineered 'targeted' NK-92 cells. These cells are transfected with a gene that that expresses a CAR that specifically and directly targets a tumor antigen. A large number of studies have showed that these NK-92 CARs (taNK) have superior efficacy to the parental NK cells [6].

The T-haNK cell line combines features of both the haNK and taNK platforms. The outcome is a cell that is capable of innate, ADCC and CAR directed killing. The t-haNK cell line is intended to be administered in combinations with antibodies, so that it could effectively target either two proteins in the same cancer or two different antigen-binding site of the same cancer protein (NantKwest: https://nantkwest.com/technology/).

The main goal of CAR-NK cells is triggering the anti-tumor effects of the cells and developing tumor cell targeting via new activation pathway. A CAR comprises a fragment of a single-chain FV (scFv) derived from an antibody for a specific surface antigen, connected through a single transmembrame region to a intracellular transducing chain that mimics the γ chain of the FcεRI receptor or the CD3ζ chain of an antigen receptor, thus enhancing a cytolytic response via intracellular signaling biomolecules.

Unlike T cells, NK cells do not express antigen specific receptors. Even though many of tumor such as melanoma or carcinomas do not express MHC class I, NK cells could not respond to them. Thus, one of the approaches to enhance the therapeutic potential of NK cells against a wide range of tumors cells is genetically modifying NK cells to identify antigen-tumor targets. Based on the approach of generating tumor specific T cells by modification of gene receptor, NK cells can be directly

targeting tumor antigen by engineering the expression of CAR genes [103]. NK-92 cells have been successfully modified to express CARs targeting antigens that specifically expressed on the cell surface on tumor cells such as CD19, CD20, and HER-2/neu. These CARs then enhance the activation and cytotoxic activity of the modified NK cells towards the tumour cells [104]. Another strategy is improving the targeting of NK receptors such as NKG2D. The NKG2D receptor is an important NK cell surface activating receptor [105]. Therefore, a NKG2D CAR can identify and bind 90% of human tumors. Nevertheless, there are concerns that this treatment could raise off-target cytotoxicity as NKG2D ligands are also enhanced on cells during inflammation [106]. NK-92 NK-cell-based cancer immunotherapy show great potential as a treatment for cancer. NK cell lines are more flexible than autologous or allogenic activated NK cells regarding expansion to generate large number. Among other types of NK cell lines, NK-92 cell lines are consistently shown high cytotoxic activity. Only NK-92 cells have been successfully genetically modified for enhanced functionality, such as to identify a specific antigen on tumors cells or for combined use with therapeutic antibodies via ADCC. Additionally, NK-92 cells have been infused into patients with progressed cancer and substantial clinical benefits with limited side effects.

Overall, using NK-92 cell-based cancer immunotherapy appears to be encouraging in the treatment of various types of tumors including solid tumor. Growing number of studies have been investigated new strategies to genetically modified NK-92 cell line to make them more resistant to the metabolically restrictive TME and so more efficacious against solid tumours.

1.10 Tumor microenvironment as a metabolically restrictive site

One of the major restrictions for the activity of NK cells is the immunosuppressive TME. Tumor cells manipulate the environment for tumor proliferation, while suppressing anti-tumor immunity including the activity of NK cells. The metabolism of NK cell will also be impaired in the TME due to the limited availability of nutrients and oxygen, and higher concentration of tumor metabolites such as lactic acid.

Thus, NK cell metabolic restriction is likely to be one mechanism that inhibits their effector functions.

Therefore, engineering NK cells to maintain their cellular metabolism in the TME could be a potential route towards improving NK cell immunotherapy against solid tumors. There are many potential effects of the TME on the metabolism of NK cells that would have an impact on NK cell effector functions.

One of the main sources of energy for NK cells is glucose and its consumption is remarkably increased following activation. NK cells utilize glucose to produce ATP (energy) and NADPH (a key cofactor for biosynthesis) or use glucose as a source of carbon to build other biomolecules such as amino acids and fatty acid [34]. Glucose deprivation inhibits anti-tumor activity of T-cells and the metabolic changes in the TME can control cancer development by effecting on the specific responses in antigen tumor-infiltrating T cells. Accordingly, it is reasonable that glucose deprivation in the TME might reduce NK cells glycolysis and thus impact on their effector functions [24], [48]. NK cells isolated from lung tumors have lower glycolytic level alongside lower production of cytokine and weak cytotoxicity. In the same study, it was found that the glycolysis is inhibited due to increase the expression of fructose-1, 6-bisphosphatase (FBP1) in lung TME NK cells. Interestingly, the effector function of NK cells can be restored by inhibiting FBP1 which give a good example of how manipulate NK cells metabolism can improve the anti-tumor function [111].

On another note, based on the metabolic reprogramming analyzing of cytokine-stimulated NK cells, it has been found that sterol regulatory element-binding proteins activity (SREBP) is fundamental transcription factor that regulates and maintain higher level of glycolysis and in doing so effector functions including cytotoxicity, IFNγ, and granzyme B production. Notably, molecules that inhibit SREBP can be enriched in the TME e.g. there are some SREBP inhibitors, including cholesterol, and oxysterols such as 27-hydroxycholesterol, which can be present at high level in patients with breast, colorectal and gastric cancers [34]. Additionally, amino acids are another significant fuel for NK cells. In the TME, it was found that amino acid

consumption was increased, and levels of glutamine can be depleted [108]. It was also found that low levels of arginine impact on the IFNγ, production and proliferation of NK-92 cells line as well as human primary NK cells [109]. Moreover, it is notable in a leucine, arginine or glutamine depleted microenvironment, mTOR signaling, which plays an essential role in the glycolytic pathway modulation, can be inhibited. The inhibition of mTOR signaling cascade also impairs the effector functions of NK cells [110]. The transport of amino acid via SLC7A5 is important to sustain the expression of cMyc, a transcription factor important in regulating NK cell metabolism [111]. Thus, this data reinforces the concept that amino acid availability could be important for NK cell effector functions within the TME. Hence, this study proposes that manipulating amino acid metabolism might activate NK cell-based therapies by limiting the tumor's fuel supply without affecting NK cell functions. [112]. Nevertheless, it is crucial to deeply investigate the metabolic requirements of NK cells to increase our knowledge of how we could possibly modify NK92 cells to be more resistant in metabolically restrictive TME and thus protect their effector functions. Ultimately, understanding of NK92 cell metabolism would participate in designing better cell-based cancer therapeutic strategies in future.

Aim

This study is designed to investigate the metabolism and function of NK-92 cell lines. Our aim is to pinpoint the metabolic key regulators that sustain the cells' effective killing mechanism against tumor cells, utilizing inhibitors targeting factors such as mTORC1, Srebp, and cMyc. Additionally, we plan to explore the potential mechanism behind the oxysterol-mediated inhibition of NK-92 cells. The ultimate goal is to comprehend the metabolic requirements of NK-92 cells and subsequently target various metabolic and signaling pathways to enhance their resistance in the harsh tumor microenvironment (TME).

Objectives

1. Identify the key signaling pathways essential for NK92 cytotoxicity.
2. Characterize metabolic flux rates in the NK92 cell line.
3. Determine the effect of oxysterols (25-HC and 27-HC) on NK-92 cytotoxicity.
4. Investigate the potential mechanisms by which oxysterols impact the effector function of NK-92 cells.

Chapter 2 - Materials and Methods

2.1 Materials

2.1.1 Chemicals

IL-2 is Teceleukin, and it obtained from NCI preclinical repository. L-glutamine and Penicillin Streptomycin were purchased from gibco. Heat-inactivated FBS weas purchased from biosera. Activated Horse serum, Folic acid and myo-Inositol were purchased from SIGMA. 25-hydroxycholesterol (25-HC), Dimethyl-sulfoxide (DMSO), β-Mercaptoethanol (β-ME), glucose, 2-deoxyglucose (2-DG), Rotenone, Antimycin-A, Oligomycin, Fluoro-Carbonyl Cyanide Phenylhyrazone (FCCP), and Triton-X were obtained from Sigma-Aldrich. Cell-Tak was purchased from Corning. Roswell Park Memorial Institute (RPMI) 1640 Medium was obtained from Gibco. Dulbecco's phosphate buffered saline (PBS) was purchased from Invitrogen/biosciences. Seahorse XF media and calibration buffer were purchased by Agilent technologies. Qscript cDNA was purchase from Quanta Biosciences Cytofix/Cytoperm, Glogi plug, Calcein-AM and Perm/wash were purchased from BD biosciences. SYBR green was purchased from SIGMA. RNeasy RNA purification mini kit was obtained from Qiagen. Rapamycin was purchased from Fisher scientific. Ethanol was obtained from school stores. PF429242 was purchased from Adoog Bioscience. Tris-base, Glycine, and Ammonium persulfate were purchased from Fisher Bioreagent. Ponceaus S, Acetic acid, and Glycerol were purchased from Sigma-Aldrich. Sodium dodecyl sulfate (SDS), 30% Acrylamide, Bovine Serum Albumin (BSA) were purchased from SIGMA. Unstained protein marker was obtained from Thermo Scientific. Bromophenol blue was obtained from Fluka, , dimethyl-sulfoxide (DMSO), PF429242 was purchased from Adooq Bioscience. 7-ketocholesterol was purchased from Avanti Polar Lipids,

2.1.2 Equipment

Falcons (15 ml and 50 ml), tissue culture plates (6, 24, 48 and 96 well), tissue culture flasks (25cm^2, 75cm^2), Transfer pipettes, pipette tips, pasture pipettes, absolute

qPCR seals PCR plates were purchased from Thermo Fisher. P1000, P200, P20, P10 pipettes are from GILSON. MicroAmp Fast 96-well reaction plates (0.1ml) for PCR were from Applied Biosytems. 96-well flat black polystyrene plates were purchased from Costar. Haemocytometers were purchased from Hausser Scientific. XF 96-well microplate and cartridges were obtained from Agilent Technologies. Steri-cycle Co_2 incubator was from Thermo Forma. Seahorse XF-96 Metabolic Flux Analyzer was from Agilent Technologies. . ABI 7900HT Fast qRT-PCR machine and QuantStudio 3 Real-Time PCR System were from Applied Biosystems. FLUOstar OPTIMA Microplate Reader was from BMG LABTECH. Nanodrop Spectrophotometer ND-1000 was from Labtech Internaltional. FACS LSR Fortessa, 5 ml FACS tubes were from BD. FloWjo™ software was from TreeStar. GraphPad Prism 9.00 was from GraphPad Software, Steri-Cycle CO_2 incubator was from Thermo Forma. Power Source 300 V was obtained from VWR International, . FlowJo™ software was purchased from TreeStar. ImageJ software was obtained from NIH.

2.1.3 Cell lines

NK-92, IL-2-dependent Natural Killer Cell line derived from peripheral blood mononuclear cells from patient with non-Hodgkin's lymphoma ((ATCC® CRL-2407™), NK-92 IL-2-independent cells ((ATCC® CRL2408™) and K562, a human chronic myelogenous leukemia cell line was from the American Type Culture Collection (ATCC).

2.1.4 Antibodies

Flow Cytometry antibodies

All antibodies and stains that were used in flow cytometry are listed in **Table 2.1**

Western blot antibodies

Western blot antibodies raised against S6 ribosomal protein, phosphate-S6 S235/236, and β-actin (loading control). See **Table 2.2**

Table 2.1: Flow cytometry stains and antibodies

Target/stain	Fluorophore	Clone	Source	Dilution
CD56	BV786	NCAM1	BD Biosciences	1/100
CD3	BV605	SK-1	BD Biosciences	1/100
NKp46	Pacific Blue	9E2	Biolegend	1/100
NKp30	PE	P30-15	Biolegend	1/100
FASL	PE	NOK-1	Biolegend	1/100
Granzyme B	PE-CF594	GB11	BD Biosciences	1/100
LD Near-IR	APC-Cy7	-	ThermoFisher	1/1000

Table 2.2: Western blot antibodies

Antibody	Source	Dilution	2° Ab
S6 ribosomal protein	Cell signaling	1/5000 in 5% BSA/1X TBST	mouse
Phosph-S6 S235/236	Cell signaling	1/2500 in 5% BSA/1X TBST	rabbit
β-actin	Cell signaling	1/5000 in 5% BSA/1X TBST	mouse

2.1.5 Solutions and Buffers

The composition of various buffers and solutions were used in method are listed in **Table 2.3**

Table 2.3: Buffers and solutions

Media/Buffer/solution	Compositions
NK-92 cells culture media	RPMI medium 1640 (+) L-glutamine, 0.2 mM inositol; 0.1 mM 2mercaptoethanol; 0.02 mM folic acid; 100 U/ml recombinant IL2; adjust to a final concentration of 12.5% heat-inactivated horse serum and 12.5% heat-inactivated fetal bovine serum.
Complete growth RPMI 1640 media	RPMI medium 1640 (+) L-glutamine, heat-inactivated FBS (10%), Penicillin/Streptomycin (1%), L-glutamine (2mM).
K562 cells culture media	IMDM medium 1640 (+) L-glutamine, heat-inactivated FBS (10%), Penicillin/Streptomycin (1%),

Seahorse media	10mM glucose and 2mM glutamine in seahorse basal media.
FACS buffer	2% of FBS in PBS
Washing buffer for cytotoxicity	1% of FBS in PBS
10X SDS-gel Running Buffer for 1 L volume	Tris-base = 30.29 g, Glycine = 144.13g, SDS = 10 g
4X Upper Gel Buffer – UGB for 1 L volume	0.5 M Tris-HCL, PH 8.8 (Tris-base = 189, adjust PH to 8.8 with HCL, SDS = 4 g (0.4%)
4X Lower Gel Buffer-LGB For 1 L volume	0.5 Tris PH 6.8 (Tris-base = 60.5 g, adjust PH to 6.8 with HCL, SDS = 4 g (0.4%)
Ponceau S Staining	Ponceaus S = 0.25 g, Acetic acid = 12.5 ml, Make volume up to 500 ml dH2O
4X SDS lysis Buffer	SDS powder (9%), 100% Glycerol (27%), 2-Mecraptoethanol (10%), bromophenol blue (Tip touch) make volume up to 500 ml
10X Transfer Buffer for 1 L volume	Tris-base = 30.29 g, Glycine = 144.13 g
10X TBS Buffer (PH = 7.6) for 1 L volume	Tris-base = 24.2 g, NaCl = 87.8 g, Adjust PH to 7.6
1X TBST Buffer for 1L volume	100 ml 10X TBS, 899 ml ddH2O, 1 ml Tween20
Blocking Buffer	5% BSA in 1X TBST
RNA lysis buffer	RLT buffer (Qiagen), β-ME (1%)
Cell-Tak™ for cell adhesion of cells to seahorse plate	2986.1µl Sodium Bicarbonate (0.1M), 9.29µl Cell-Tak™ (Corning), (1.85mg/ml stock), 4.65µl NaOH (1M). Recipe makes enough to coat 96 wells.

2.2 Methods

2.2.1 NK-92 cell culture.

NK-92 Cell lines subculturing.

NK-92 cells were cultured in RPMI 1640 supplemented with 0.2 mM inositol; 0.1 mM 2mercaptoethanol; 0.02 mM folic acid ; adjust to a final concentration of 12.5% heat-inactivated horse serum, 12.5% heat-inactivated fetal bovine serum, and 100 U/ml human recombinant IL2 that was added directly to tissue flask. NK-92 cryovial was quickly thawed at 36°C in water bath (not exceed 2 minutes) and transferred by Pasteur pipette to pre-cold 9 ml NK-92 media. Cells were washed once, and cell pellet was resuspended with NK-92 media. Cells viability and cells concentration/ml were determined and then cells suspension were transferred to T25 culture flask for 48 hours at 36°C. After 48 hours, cells suspension were diluted by adding fresh NK-92 media (1:2 ratio) which were transferred to T75 tissue flask. To freeze the cells down, the cells were resuspended at 4 X 10^6 cells/ml with 50% NK-92 media, 40% heat-inactivated FBS, 10% DMSO and stored at -80°C before being transferred to liquid nitrogen. NK-92 cell lines were cultured by adding fresh medium (split as 1:2 ratio) every two/three day and they were cultured at 36°C and 5% CO_2. The optimal cell density for NK-92 cell when adding the fresh media (day 0) was from 2 to 3 X 10^5 viable cells/mL and they should not exceed 5 – 6 X 10^5 viable cells/ml at the subculturing day (day 2 or day 3). NK-92 IL-2-indenendent cells were culturing without IL-2.

NK-92 Cell lines Treatment.

On day 2 or day3, NK-92 cells were pooled from one or different T75 tissue flask

into 50 ml falcon tube. Cells were centrifuge at 1400 rpm for 5 minutes at RT. Supernatant was discarded and cell pellet was resuspended with prewarmed fresh complete growth RMPI 1640 (+) L-glutamine medium. Cell was counted and adjusted to desired concentration (1 X 10^6 cells/ml) before adding the treatments. NK-92 cells were either maintained with no adding human recombinant IL-2 (- or no IL-2) or adding IL-2 (+IL-2) in the presence or absence of 25-HC (0.25, 0.5. 1, 2, and 5 μM), 27-HC (0.25, 0.5. 1, 2, 5, and 10 μM), GW3965 (2 μM), rapamycin (20nM), PF429242 (10 μM), and different 2-DG doses response (0.5, 1, 2, 5 mM) or (1, 2, 5, 10 mM) for 18 hours at 36°C and 5% CO_2. Appropriate controls were used when it was necessary.

2.2.2 K562 Cell line culture

K562 cells were cultured in IMDM supplemented with 10% heat inactivated FBS and 1% penicillin/streptomycin at 37°C. K562 cryovial was quickly thawed at 37°C in the water bath and transferred to prewarmed 9 ml IMDM. Cells were washed and cell pellet was resuspended with IMDM media. Cell viability and number was determined and cell suspension was transferred into a T75 culture flask for two days at 37°C. After 48 hours, cells were counted and adjusted to 0.5 x 10^6 cells/ml cell concentration. To freeze the cells down, the cells were resuspended at 1 x 10^7 cells/ml with IMDM culture media supplemented with 5% DMSO and stored at -80°C overnight before being transferred into liquid nitrogen.

2.2.3 Flow Cytometry

Extracellular Staining

For FACS analysis, NK -92 cells were transferred to labelled FACS tubes and 1 ml

of cold FACS buffer was added to each tube. Cells were centrifuged at 1400 rpm for 3 minutes at RT. Supernatant was discarded and cell pellets were gently mixed. Samples were incubated for 20 minutes at 4°C in the dark with LD staining. After 20 minutes, cells were stained with surface-targeted antibodies for a further 20 minutes in the dark at 4°C. Cells were then washed with 1 ml of FACS buffer and centrifuged at1400 rpm for 3 minutes. Samples were resuspended in FACS buffer before acquisition by flow cytometry (FACS Fortessa (BD)). Samples were analysed using FACS Diva software and data analysed using FlowJo™(TreeStar). Live NK-92 cells were gated according to their forward scatter (FSC-A) and side scatter (SSC-A), single cells were gated according to their FSC-W and FSC-A, live cells were gated based on their negativity for Zombie™ NIR viability dyes and cultured NK cells were identified as CD56+,CD3- cells. Gating strategies are described in **Figure 2.1**. Comparing human NKcells with NK-92 cell displayed in **Figure 2.2.**

Intracellular Staining

For intracellular staining, exocytosis was blocked using golgi plug (BD Biosciences) four hours prior to the end of the treatment period. Cells were firstly stained for surface makers as outlined above. Subsequently, cells fixed and permeabilised using the Cytofix/Cytoperm kit from BD Biosciences according to manufacturer's instructions for 20 minutes in the dark at 4°C. After, cells were washed with 1 ml of 1x Perm Wash (BD Biosciences) and centrifuged at 1400 rpm for 3 minutes. Supernatant was discarded and cell pellet was dislodged in intracellular antibodies for 20 minutes at 4°C in the dark. After incubation time, cells were washed with 1 ml FACS buffer and centrifuged at 1400 rpm for 3 minutes. Supernatant was discarded and the cell pellet was resuspended in FACS buffer before acquisition by flow cytometry. Samples were analysed using FACS Diva software and data analysed using FlowJo™(TreeStar).

MitoTracker™ Green Staining

MitoTracker™ Green was used as an indicator of mitochondrial mass. Cells were washed from stimulation media and added to a 96-well U-bottom plate. Cell suspensions were then resuspended in media containing MitoTracker™ Green (100 nM, Invitrogen) for 30 mins prior to surface staining and analysis. Analysis was carried out using FACS Fortessa (BD, 488 nm laser, 530/30 BP filter for detection of MitoTracker™ Green).

TMRM Staining

Tetramethyl rhodamine (TMRM) was used as an indicator of mitochondrial inner membrane potential. Cells were washed from stimulation media and added to a 96-well U-bottom plate. Cell suspensions were then resuspended in media containing TMRM (100 nM, Invitrogen) for 30 mins prior to surface staining and analysis. Oligomycin (2 µM, Sigma) and FCCP (20 µM, Sigma) were used as positive and negative controls respectively. Analysis was carried out using FACS Fortessa (BD, 561 nm laser, 582/15 BP filter for detection of TMRM).

MitoSOX™ Red Staining

MitoSOX™ Red was used as an indicator of mitochondrial reactive oxygen species production. Cells were washed from stimulation media and added to a 96-well U-bottom plate. Cell suspensions were then resuspended in media containing MitoSOX™ Red (1.5 µM, Invitrogen) for 30 mins prior to surface staining and analysis. Rotenone (400 nM, Sigma) was used as a positive control. Analysis was carried out using FACS Canto (BD, 488 nm laser, 585/45 BP filter for detection of MitoSOX™ Red).

Di-4-ANEPPDHQ Staining

Cells were washed from stimulation media and added to a 96-well U-bottom plate. Cell suspensions were then resuspended in FACS buffer containing Di-4-

ANEPPDHQ (0.5 µm, Invitrogen) and the required antibodies for surface staining for 20 mins at 4 °C. The stained sample was then washed from FACS buffer and resuspended in FACS buffer for analysis. Samples were measured within 30 mins to prevent internalisation of the membrane dye Di-4-ANEPPDHQ using FACS Canto II (BD, 488 nm laser, 530/30, 585/45, 670-735, 780/60 BP filter for Di-4-ANEPPDHQ detection). The mean fluorescence intensities (MFIs) were then used to calculate the ratiometric general potential (rGP) of the dye which is an indicator of the order of the plasma membrane according to the following formula:

$rGP=(MFI_{530}-MFI_{670})/(MFI_{530}+MFI_{670})$

where MFI_{530} indicates the MFI of Di-4-ANEPPDHQ detected in 530/30 BP filter and MFI_{670} indicates the MFI of Di-4-ANEPPDHQ detected in 670-735 BP filter.

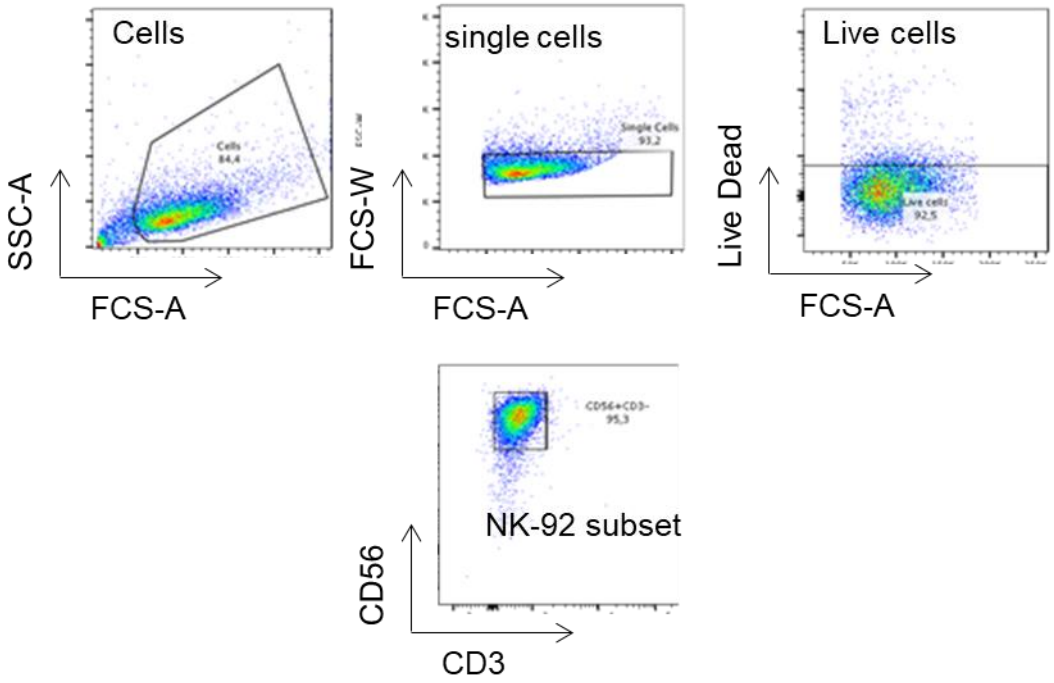

Figure 2.1: Gating strategy of NK-92 cells

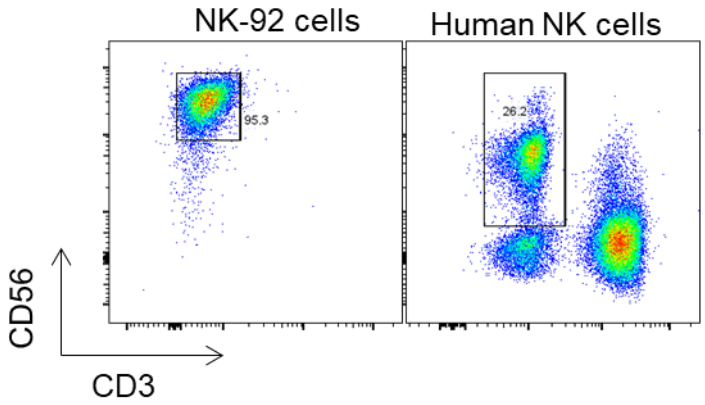

Figure 2.2: Comparing between human NK cells and NK-92 cells.

2.2.4 Protein Analysis

Protein Extraction

After 17 hours treatment, 1 X 10^6 NK-92 cells/condition were counted and centrifuged cells at 1400 rpm for 5 minutes. Cells pellet were lysed in 1X SDS-PAGE sample buffer. Samples were heated to 90°C for 10 minutes before freezing at -80°C for subsequent use.

Sodium Dodecyl-Sulphate Poly-Acrylamide Gel Electrophoresis (SDS PAGE)

Cell lysate prepared in 1XSDS sample buffer were separated based on their molecular weight. Gel were run using the AE6450 system from Atto Corporation. The recipe for 10% acrylamide gel for one gel is shown in **Table 2.4**

Table 2.4: 10% acrylamide gel composition

Component	Volume (ml)
miliQ-H_2O	2.5
30% acrylamide	2
4X LGB	1.5
30% APS	0.01
TEMED	0.06

Western blot

For the transfer of protein onto nitrocellulose membrane, SDS-PAGE gels were removed from the running plates and assembled into a gel-membrane sandwich as dictated in the manufacturer's protocol of the transfer apparatus. Nylon sponge pads, Whatmann 3-MM chromatography paper and Hybond-C extra Nitrocellulose membrane (Amersham Biosciences) were soaked in transfer buffer containing 10% methanol. The sandwich was loaded into the transfer apparatus with the nitrocellulose membrane closest to the anode. Proteins were transferred at 45V for 2 hours or 15V overnight on ice. To determine quality of transfer, membranes were stained with Ponceau S solution for 30 seconds, before gently rinsing with water. Membranes were blocked in a 5% BSA/TBST solution for 45 minutes at room temperature. Membranes were washed three times in 1XTBST for 5 minutes/washing before subsequent incubation in primary antibody (see table 2.2) overnight at 4°C. After this incubation, membranes were again washed three times for 5 minutes/washing in 1XTBST. Membranes were then transferred to appropriate secondary antibody (1/5000 in 5% 1XTBST) for 1 hour at 4°C. After this incubation

period, membranes were again washed twice for 5 minutes in 1XTBST. Pierce ECL 2 Western Blotting Substrate (Thermo Scientific) was applied to the membrane and luminescence assessed by GelDoc XR+system.

2.2.5 RNA Analysis

RNA Isolation

Following 18 hour treatment, 1 x 10^6 NK-92 cells were centrifuged at 1400 rpm for 3 minutes and resuspended in 600µl RTL buffer containing 1% 2-Mercaptoethanol.The RNeasy mini kit (Qiagen) was used to isolate the RNA according to the manufacturer's protocol. RNA quality and quantity were assessed using a Nanodrop ND-1000 (NanoDrop® Technologies).

cDNA Synthesis

1µg of isolated RNA were made up to 16 µl with ddH20 and added to 4 µl of qScript cDNA Supermix (5x) (Quanta BioSciences), which contains the reverse transcriptase enzyme required to carry out the reaction. The reverse transcription was carried out in Techne's 3Prime Thermal Cycler at the following incubation times:

Time (minutes)	**Temperature (°C)**
5	25
30	42
5	85
Hold	4

Primers Design

Primers for quantitative real time PCR (qRT-PCR) were designed using Primer BLAST software located on the NCBI website (https://www.ncbi.nlm.nih.gov/tools/primer-blast/) and parameters for primer design were set such that they fulfilled the following requirements:

- GC content of between 40-60%
- At least one GC clamp at one end of the primer
- Spanning an exon-exon junction
- Have at least three mismatches to other sequences in the gene of interest
- To have less than 1°C between melting temperatures
- An optimum Primer melting temperature of 60°C
- Forward and reverse primers to be similar length Primer sequences generated by BLAST were verified using Ensemble genome browser (http://www.ensembl.org/index.html).

RT-qPCR products were ran on an agarose gel to confirm he specificity of the primers. Sequence of primers used for qRT-PCR are listed in **Table 2.5**

Table 2.5: PCR primer sequences

Gene name	Sequence
Human Srebp1 forward	5'-GGTCCCGGTCCTGCT-3'
Human Srebp1 reverse	5'-CAGCTTCTCCGCATCTACGA-3'

Human Srebp2 forward	5’-GGCATCGACCTAGGCAGTC-3’
Human Srebp2 reverse	5’-GGCTCATCTTTGACCTTTGC-3’
Hmgcs11 forward	5’-TCTCTATCCTTCACACAGCTCTTTC-3’
Hmgcs11 reverse	5’-CTGTGCAGAAGCCCATCTTG-3’
Scd1 forward	5’-AGCCCTGTATGGGATCACTTTG-3’
Scd1 reverse	5’-GCCCATTCATAGACATCATTCTGG-3’
Fasn forward	5’-TCGTGTTGACTTCTCGCTCC-3’
Fasn reverse	5’-CCATCTCTCAAGACCACGGC-3’
Abcg1 forward	5’-GGAGCCCAAGCGCAG-3’
Abcg1 reverse	5’-GAGTAACTGCTGGCATTCATGG-3’

Quantitative real time PCR

Quantitative real time PCR (qRT-PCR) was performed in triplicates per condition in a 96-well plate using iQ SYBR Green-based detection (VWR) on a QuantStudio 3 Real-Time PCRSystem (Applied Biosystems). Each 10 µl PCR reaction consists of the following:

Component of the reaction	**Amount in µl**
cDNA - Templete	0.5
SYBR Green supermix	5
Nuclease free water	3.7
Each of forward and revers	0.5

Stage	**Temperature (°C)**	**Time (seconds)**	**Cycles**

The 96-well plate was sealed with an Absolute qPCR seal (MSC) and ran under fast cycle conditions:

1	95	60	1
2	95	1	35
2	57	20	35
3	95	15	1
3	55	30	1
3	95	15	1

For analysis of qRT-PCR data, genes of interest were normalised to an average of three internal control gene -human RPLP0. The relative mRNA content of samples was calculated according to the following equation:

Rel. mRNA expression =2^(ct_{uc}-ct_{us})/ 2^(ct_{rc}-ct_{rs})

Where **ct** is the threshold cycle, **u** is the mRNA of interest, **r** is the reference gene, **uc** is the sample every other sample is made relative to and s is every other sample.

2.2.6 Proteomics Dataset

The quantitative-proteomics dataset was generated at the University of Dundee on NK-92 IL-2 independent cells. Each copy number of each protein provided is based on an treatment NK-92 with and without of 25HC (1,2µM) . To sort out dead cells, SACSAria Fusion Cell Sorter was used. Cells were spun down and then stored at -80 °C until further preparation. Proteomics dataset was then carried out at the University of Dundee according to the method previously described [113]. Quantitation of protein expression of SREBP target genes, and pathway enrichment analysis were estimated.

2.2.7 Seahorse Metabolic Flux Analysis

A Seahorse XFe96 Metabolic Flux Analyser (Agilent Technologies) was used for real-time analysis of the extracellular acidification rate (ECAR), as a measure of glycolysis and oxygen consumption rate (OCR), as an indicator of Oxidative Phosphorylation of NK-92 cells cultured under various conditions. One day prior to analysis, the seahorse cartridge plate was hydrated using 200 µl of sterile water per well and placed in a non CO_2incubator at 37°C overnight according to manufacturer's instructions. On the day of analysis, wells of the 96 well seahorse plate were coated with 25 µl of Cell-Tak solution (Corning) and incubated at room temperature for 20 minutes before being washed twice with sterile DEPC water (200 µl.well). For analysis, NK-92 cells were washed from NK-92 cell culture media and resuspended in seahorse media containing 50mM glucose and 2mM L-glutamine. Cells were seeded at 150,000 cells/well on a Cell-Tak coated 96 well seahorse plate. Plate was gently centrifuged at 1200 rpm for 3 minutes with no brake to ensure no bubbles and the cells were adhered at the bottom of the well. The cell plate was kept at 37°C for 30 minutes in a non-CO_2incubator before insertion into the Seahorse analyser. During the incubation period, the water in the cartridge plate was substituted with pre-warmed calibration buffer (200 µl/well). Inhibitors were added to their designated ports of the seahorse cartridge plate prior to calibration. Inhibitor order and concentrations were as follows; Oligomycin (2 µM), Fluoro-Carbonyl Cyanide Phenylhdrazone (FCCP) (0.5 µM), Rotenone (100 µM) plus Antimycin –A (4 µM), and 2-deoxyglucose (2-DG) (30mM). After calibration, the cell plate was inserted for analysis. The Seahorse analyser sequentially measures ECAR and OCR of a monolayer of cells over time. Over the course of analysis, the inhibitors will be injected in that order to measure metabolic state of the cells.

Glycolytic measurements

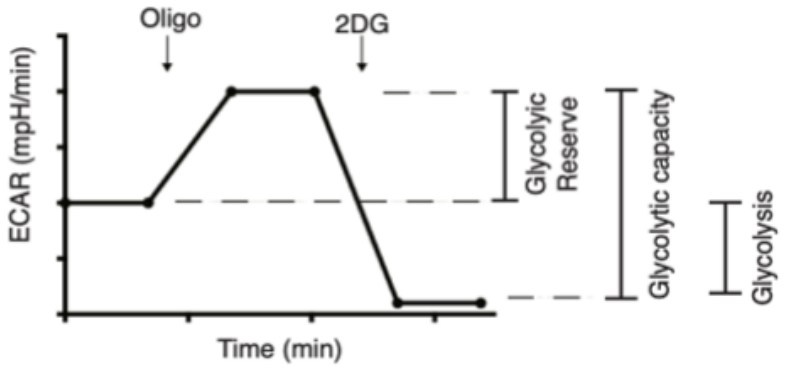

Figure 2.3: Determining Glycolytic rates using the Seahorse Metabolic Flux Analyser.

Basal Rates of glycolysis are determined by the change in extracellular acidification in the media over time, resulting from the release of protons during glycolysis (ECAR). Oligomycin inhibits ATP synthase, the enzyme that generates ATP from ADP at the end of the electron transport chain (ETC). In order to avoid energy crisis, the rate of glycolysis is maximally increased to the cells 'glycolytic capacity'. 2-DG is a direct glycolytic inhibitor, therefore in the presence of 2-DG, any change in acidification of the media can be attributed to processes other than glycolysis. This allows us to calculate the actual rate of glycolysis

Oxidative Phosphorylation Measurements

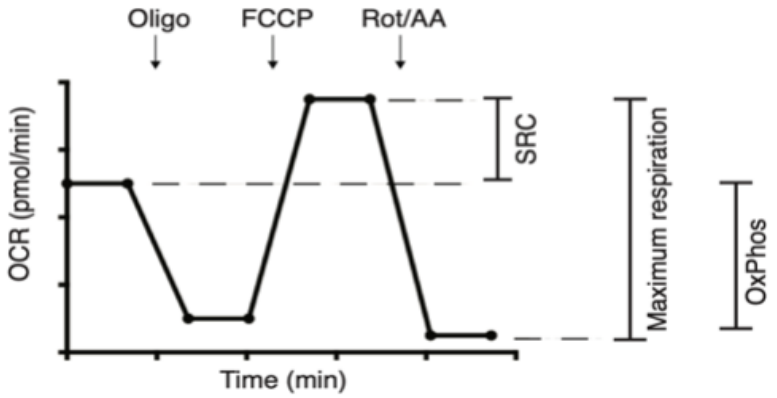

Figure 2.4: Determining the rates of OxPhos using Seahorse Metabolic Flux Analyser.

Basal rates of OxPhos can be determined by the amount of oxygen being consumed over time (OCR). Oligomycin (Oligo) inhibits ATP synthase, the enzyme that generates ATP from ADP at the end of the ETC. FCCP disrupts the proton gradient across the inner mitochondrial membrane, which is coupled to electron transport, thus allowing a free flow of protons through the inner mitochondrial membrane. In the presence of FCCP, the rate of OxPhos is maximally increased allowing the determination of Maximum Respiration. The Spare Respiratory Capacity (SRC) can be calculated by subtracting the basal rate of OxPhos from the MRC. Antimycin A and Rotenone inhibit complex III and I of the Electron transport chain respectively, therefore any residual oxygen consumption measured after the addition of these two compounds is not due to mitochondrial respiration. All these measurements together allow usto calculate the actual rate of OxPhos.

2.2.8 Calcein-release Cytotoxicity assay

For measurements of NK cell cytotoxicity, NK-92 cells were treated for 18 hours under various conditions prior to the assay. K562 target cells was stained with 10 µM Calcein-AM (BD Pharmingen) at 37°C for 30 minutes in DPBS and inverted 2-3 times at the 15 minutes. Calcein-AM stained cells were thoroughly washed three times to remove excess dye using wash buffer. Cells were resuspended at 0.3 x 10^6cells/ml in fresh RPMI and incubated at 37°C for 1 hr. After the incubation period cells were washed and resuspended in RPMI media. Cells were re-counted and adjusted to 0.3 x 10^6cells/ml and seeded at 100 µl per well in a 96 V-bottomed well plate to ensure 30,000 target cells per well. Treated NK-92 cells were washed thoroughly out of their conditioned media and were resuspended at 1.5 x 10^6cells/ml in fresh RPMI media. Cells were seeded at NK-92: Target ratio of 5:1, 2:1 and 1:1 to a total volume of 200 µl per well. Each sample and ratio were done in triplicates. Appropriate controls such as Spontaneous release and Maximum release was plated in triplicates. For spontaneous release, wells had Calcein-AM stained target cell only (100 µl of target plus 100 µl of media). For Maximum release, wells had calcein –AM stained target cells and lysed with 10 % Triton-X solution (100 µl of target cells plus 100 µl of media plus 8 µl of 10% Triton-X). The plate was incubated at in the dark at 37°C for 4 hours. After the 4hr incubation period, the plate was gently centrifuged at 200 x g for 5 minutes with no brake to ensure all cells were at the bottom of the well. 75 µl was carefully aspirated from the wells and placed into a black 96 well plate. It was ensured that there were no bubbles to prevent inaccurate readouts. Fluorescence was recorded using the FLUOstar OPTIMA Microplate Reader (BMG LABTECH). Fluorescence was read between 495 nm excitation and 515 nm emission, 6 flashes per read on automatic gain. Samples were measured in triplicates and the mean was used for analysis.Live cells take up the nonfluorescent Calcein-AM dye and is converted to a green-fluorescent calcein after acetoxymethyl ester hydrolysis by intracellular esterase. When NK-92 cells lysed target cells, the fluorescent dye is released into the supernatant.

Therefore, fluorescence is proportional to target cell killing and calculated as follows:

$$\frac{(X - \text{Spontaneous release}) \times 100}{(\text{Maximum release} - \text{Spontaneous release}}$$

2.2.9 Statistical Analysis

GraphPad Prism 9.5.1 (GraphPad Software) was used for statistical analysis. A one-way ANOVA test was used for the comparison of more than 2 groups throughout with a Tukey post-test for multiple comparisons. Analysis of data with 2 factors were analysed by a two-way ANOVA with Tukey post-test for multiple comparisons. A two-tailed Student's t-test was used when there were only 2 groups for analysis. For comparison of relative values, a one-sample t-test was used to calculated p values with a theoretical value set to 1 or 0. A p value <0.05 was considered as statistically significant. In all figures, *$p<0.05$, **$p<0.01$, ***$p<0.001$.

Chapter 3 – Metabolic characterization of an interleukin (IL) 2 dependent NK-92 cell line.

3.1 Introduction

NK-92 is an interleukin (IL) 2-dependent cell line ($CD56^{+}/CD3^{-}$) and once IL-2 is withdrawn, the cells are reported to die within 72hr. Several studies showed that IL-2 deprivation leads to the decline various of NK-92 effector functions, including cytotoxicity after 24hr and cell death within 72hr [114], [115]. Identifying the key signaling pathway that controls the anti-tumor activity of NK-92 cells such as cytotoxicity is valuable for developing novel therapeutic strategies [116], [117], It was therefore considered whether IL-2 is essential for NK-92 function and metabolism in my study.

Many previous studies demonstrated that murine and human NK cells strongly rely on metabolizing glucose by glycolysis to exert their effector functions like cytotoxicity [118]–[120]. In the tumor microenvironment (TME), the anti-tumor function of NK cells is disrupted in a diversity of ways, including metabolic modification through the consumption of most energy sources, and producing immunosuppressive factors that alter NK cell metabolism [121]–[123]. Accordingly, understanding how TME changes NK-92 cell metabolism is fundamental for optimal immunotherapies. I, therefore, investigated whether NK-92 cell glucose metabolism was required for optimal killing of tumor target cells to extend our insight into key metabolic regulators that sustain NK-92 cell cytotoxicity.

3.2 Characterizing the phenotype of NK-92 cells

Cell line phenotype changes over time, so I needed to characterize the phenotype of our NK-92 cell sub-clone. Additionally, identifying the NK-92 cell phenotype is essential for understanding NK cell functional fate. While the literature cites a given phenotype, we characterized our NK-92 cells which would be used for the project.

The cells were gated based on forward (FSC) and side scatter (SSC) profiles as shown in Method **(Figure 2.1)**. Viable cells were gated based on negative expression of viability stain (Zombie Near IR) and NK-92 cells were identified as $CD56^{+}CD3^{-}$. Comparing NK-92 cells with Human NK cells, shows that NK-92 cells express a higher level of CD56 ($CD56^{bright}$) in Method **(Figure 2.2)**

The literature suggested that this cell line is also positive for granzyme B, TRAIL, and activating receptors (NKp30, NKp46) and negative for CD3, CD16, NKp44, the majority of inhibitory receptors, and FasL [114], [124], [125] Our NK-92 cells express CD56, granzyme B, and NKp-44, while they are negative for CD16, CD3, FasL, TRIL, and, unexpectedly, NKp-46 **(Table 3.1)** and **(Figure 3.1)**. Overall, our NK-92 sub-clone cell line closely resembles the parental NK-92 cell line phenotype.

Table 3.1: The level of markers expressed in sub-clones of IL-2 dependent Nk-92 cells.

Summarizing the expression level of candidate markers in NK-92 cell lines that are involved in an immunophenotype and killing machinery; (+++) very high expression, (+) expressed, (-) not expressed.

.

Marker	Function	Based on literature review		Experimental data (Figure 3.1)
		Expression Level	Reference	Expression Level
Granzyme B	Cytotoxicity functional Molecules	++	[114], [124]	++
CD3	Lineage Markers	-	[114]	-
CD56		++	[114]	++
CD16		-	[124], [125]	-
FASL	Cell Death Ligand	-	[125]	-
TRAIL		+		-
NKp30	Activating receptors	++	[114], [124], [125]	-
NKp46		+		-
NKp44		-		+

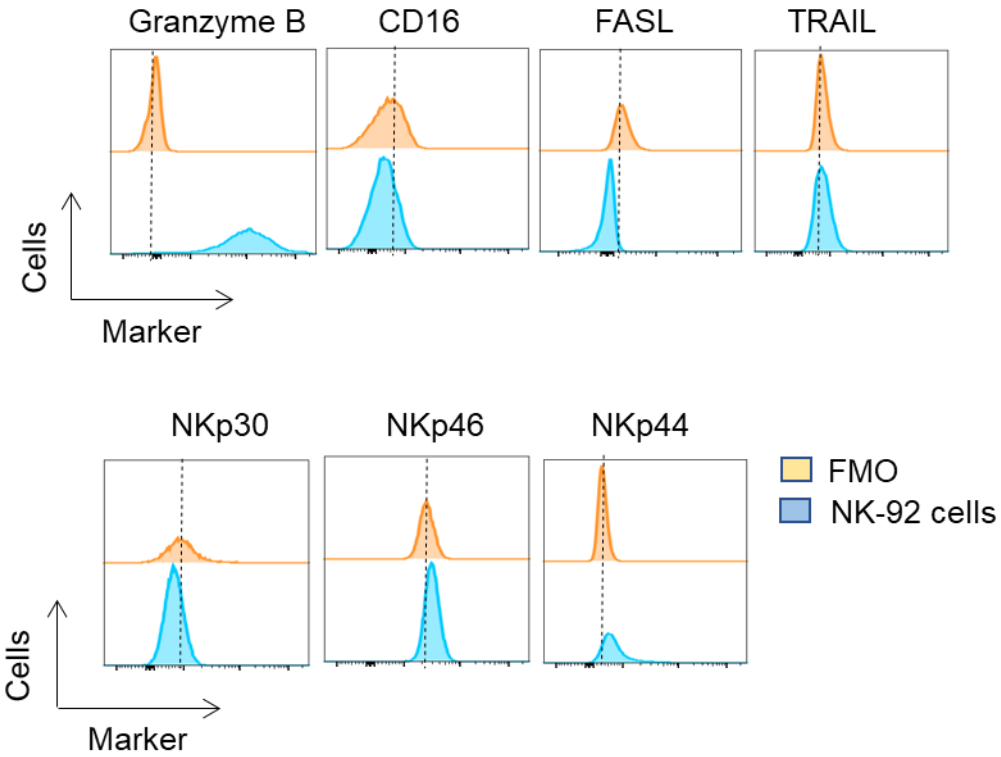

Figure 3.1: Phenotypic characterization of human NK-92 cell line.

NK-92 cells were stained with fluorochrome-conjugated antibodies specific to Granzyme B, CD16, FASL, TRAIL, NKp30, NKp46, and NKp44 and analysed by flow cytometry. Representative histogram graphs display the expression level of markers in NK-92 cells (in blue) and fluorescence minus one (FMO) (in orang). Data are representative of 3 independent experiments.

3.3 NK-92 cells are highly dependent on Interleukin (IL) 2 for sustaining their anti-tumor effector function.

To examine the importance of IL-2 for NK-92 metabolism and function, NK-92 cells were either left in presence or absence of IL-2 (100 UI/ml) for 0, 24, 48, and 72 hours and then stained with viability stain (Zombie NearIR) and their general characteristics examined. Also, NK-92 cells were stained with mouse anti-human CD71 (APC), also called Transferrin Receptor, which is required for iron import from transferrin into cells by endocytosis [121], [126] . The data shows that depriving NK92 cells of IL-2 for 72 hours did not impact on the viability **(Figure 3.2)** and cell size **(figure3.3).** The expression of CD71, which has been described as an IL2 regulated gene [127], [128], was decreased after 24 hours and further at 72 hours after IL-2 deprivation **(Figure 3.4).**

Based on the result, it was decided that overnight, which is 18 hours, was a suitable time to further study IL2 controlled NK92 cell metabolism. As expected, 18 hours IL-2 deprived-NK-92 cells were still viable and had the same cell size compared with IL-2 replete NK-92 cells (**Figure 3.5**). To investigate the consequences of withdrawing IL-2 on NK-92 cell metabolism, the Seahorse Metabolic flux analyzer was used to investigate metabolic flux through Oxidative phosphorylation (OxPhos) and glycolysis in NK-92 cells cultured in presence or absence of IL-2 (100 UI/ml) for 18 hours. The data show there was no significant change in glycolysis and OxPhos levels **(Fig 3.6)** and **(Figure 3.7),** respectively. However, it was

noted that there was substantial variability in the data.

Taking together this data shows IL-2 deprivation for 18 hours caused no changes in metabolic profile of NK-92 cells in term of seahorse extracellular flux analysis. The stability in the NK92 metabolic profile correlated with the fact that there was no reduction in NK-92 cytotoxicity towards K562 target cells **(Figure 3.8),** nor changes in granzyme B production **(Figure 3.9)** following 18 hours IL2 deprivation.

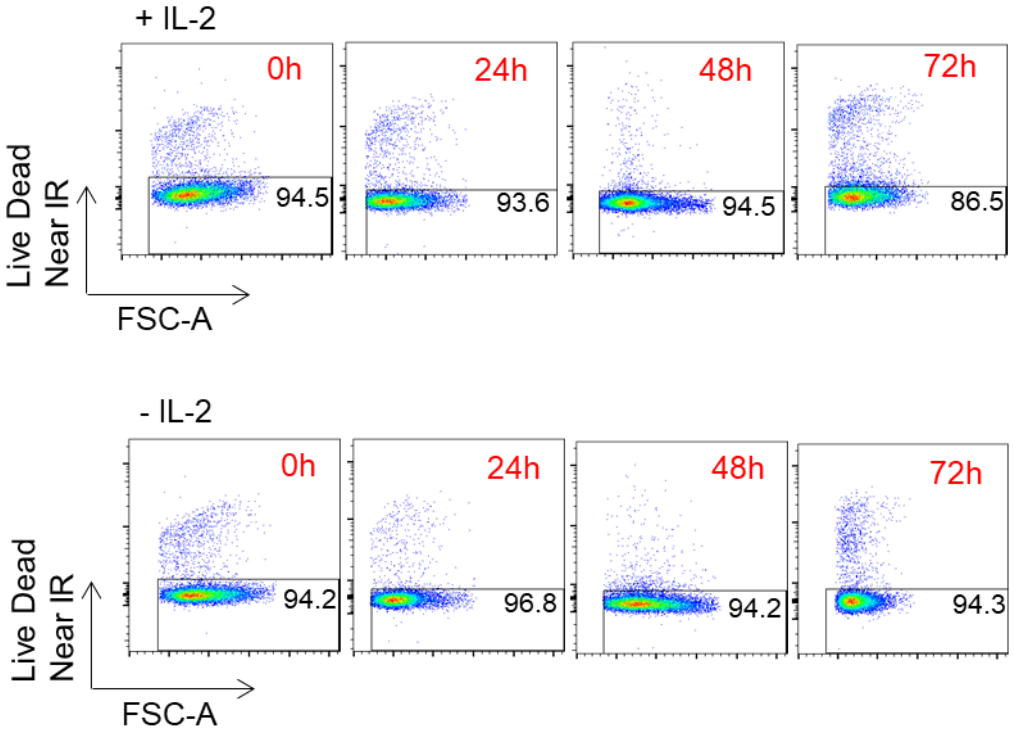

Figure 3.2: NK-92 viability is not compromised by 72 hours IL-2 deprivation. NK-92 cells were cultured with and without IL-2 (100 IU/ml) for 0, 24, 48, and 72 hours before analysis by flow cytometry. The viability of NK-92 cells was determined by staining the cells with Live Dead (Near IR). Data is dot plots of NK-92 cells that were culture with IL-2 (top) and without IL-2 (bottom) for the timepoints indicated and is representative of 3 independent experiments.

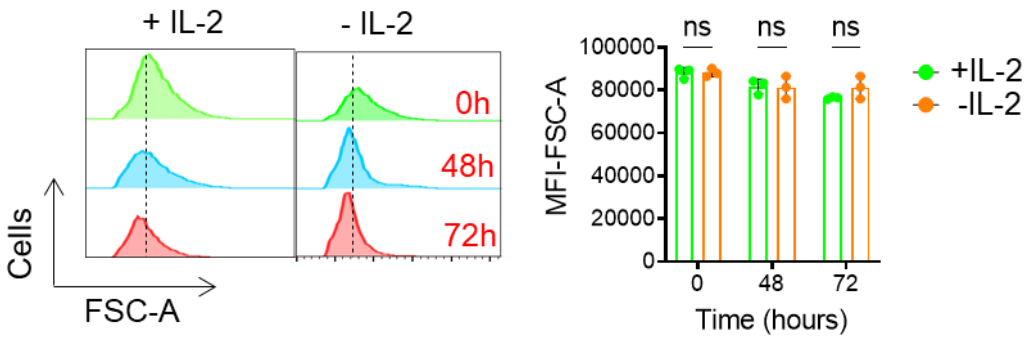

Figure 3.3: NK-92 cells size is not affected following 72 hours IL-2 deprivation.

NK-92 cells were cultured with and without IL-2 (100 IU/ml) for 0, 48, and 72 hours before analysis by flow cytometry for FSC-A, a measure of cell size. Data are representative (left) or mean+/-SEM (right) of 3 independent experiments. Data were analyzed using Two-way ANOVA test with a Sidak for multiple comparisons. ns, nonsignificant; MFI, mean fluorescence intensity.

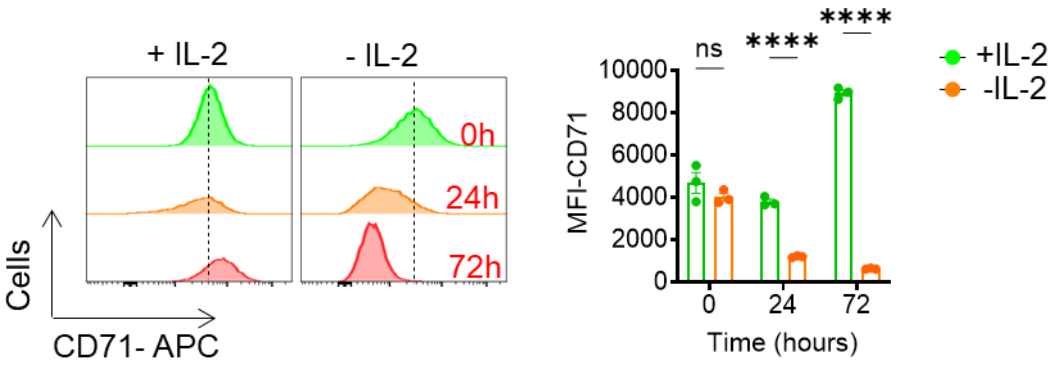

Figure 3.4: NK-92 cells have reduced CD71 expression following IL-2 deprivation.

NK-92 cells were cultured with and without IL-2 (100 IU/ml) for 0, 24, and 72 hours prior to analysis by flow cytometry for the expression of CD71, also called the transferrin receptor. Data are a representative histogram (left) or mean + /- SEM (right) of 3 independent experiments. Data were analyzed using Two-way ANOVA test with a Sidak post-test for multiple comparisons. ****p<0.0001; ns, nonsignificant; MFI, mean fluorescence intensity.

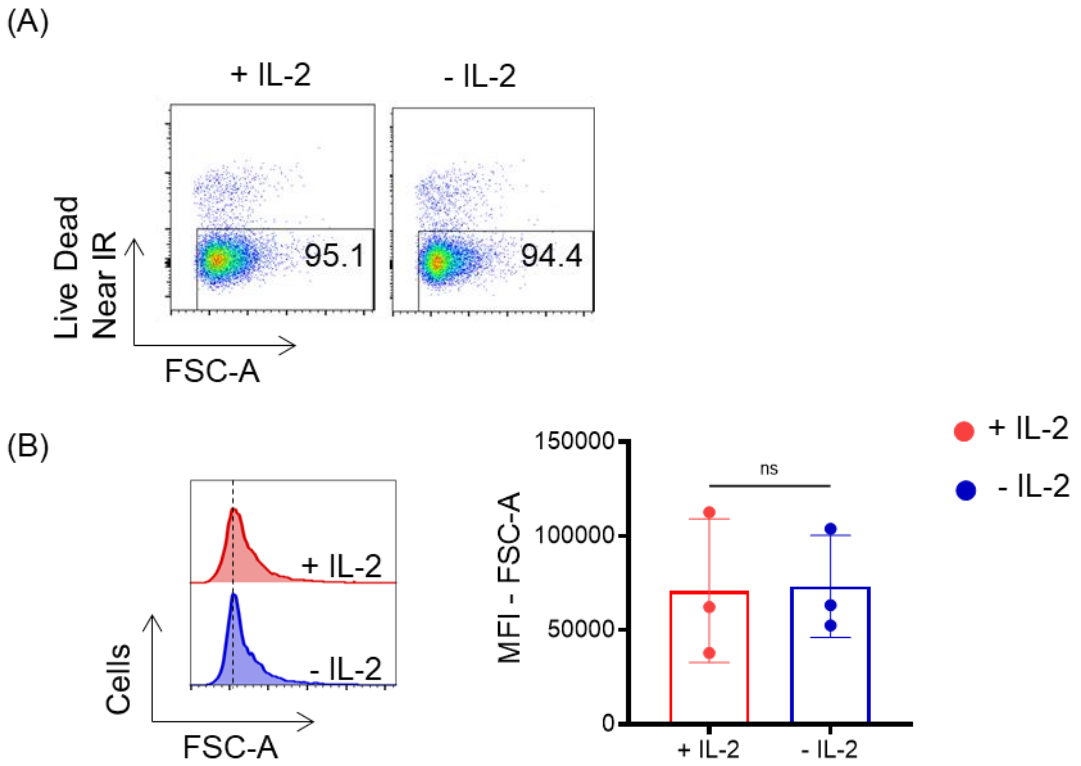

Figure 3.5: IL2 withdrawal for 18 hours does not affect NK-92 viability or cell size.

NK-92 cells were cultured with or without human recombinant IL-2 (100U/ml) for 18 hours before analysis by flow cytometry. (A) The viability of NK-92 cells was determined by staining the cells with Live Dead (Near IR Zombie) antibodies. (B) NK-92 cells were analyzed for FSC-A as a measure of cell size. Data are representative (A and B, left) or mean+/-SEM (B, right) of 3 independent experiments. Data were analyzed using an unpaired students t-test. ns, nonsignificant.

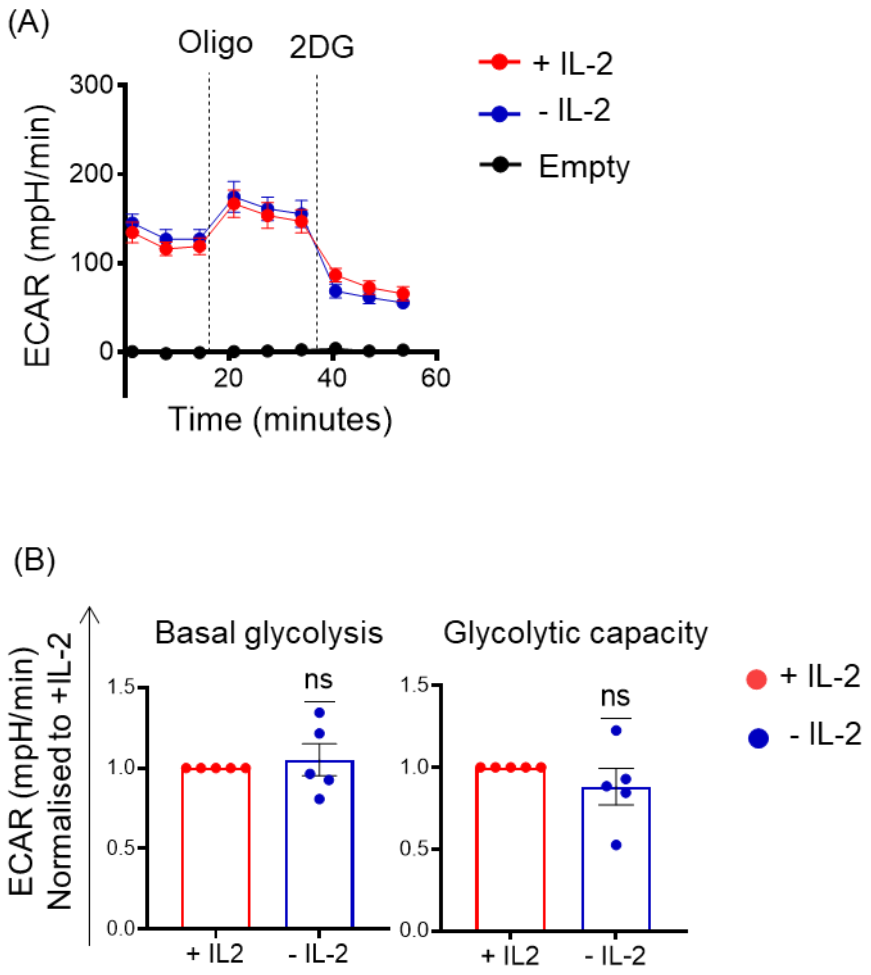

Figure 3.6: Glycolysis is unchanged in NK-92 deprived of IL2 for 18 hours.

NK-92 cells were cultured with or without IL-2 (100 IU/ml) for 18 hours. NK-92 cells were then plated at 150,000/well in fresh seahorse media and analyzed using the seahorse extracellular flux analyzer measuring basal extracellular acidification rate (ECAR) and rates after sequential injection of oligomycin (2 μM), and 2-deoxyglucose (30 mM). The data are presented as a representative ECAR trace (A) or mean +/- SEM (B) of 5 independent experiments. Statistical analysis was performed using a one sample t test against a hypothetical value of 1. ns, nonsignificant.

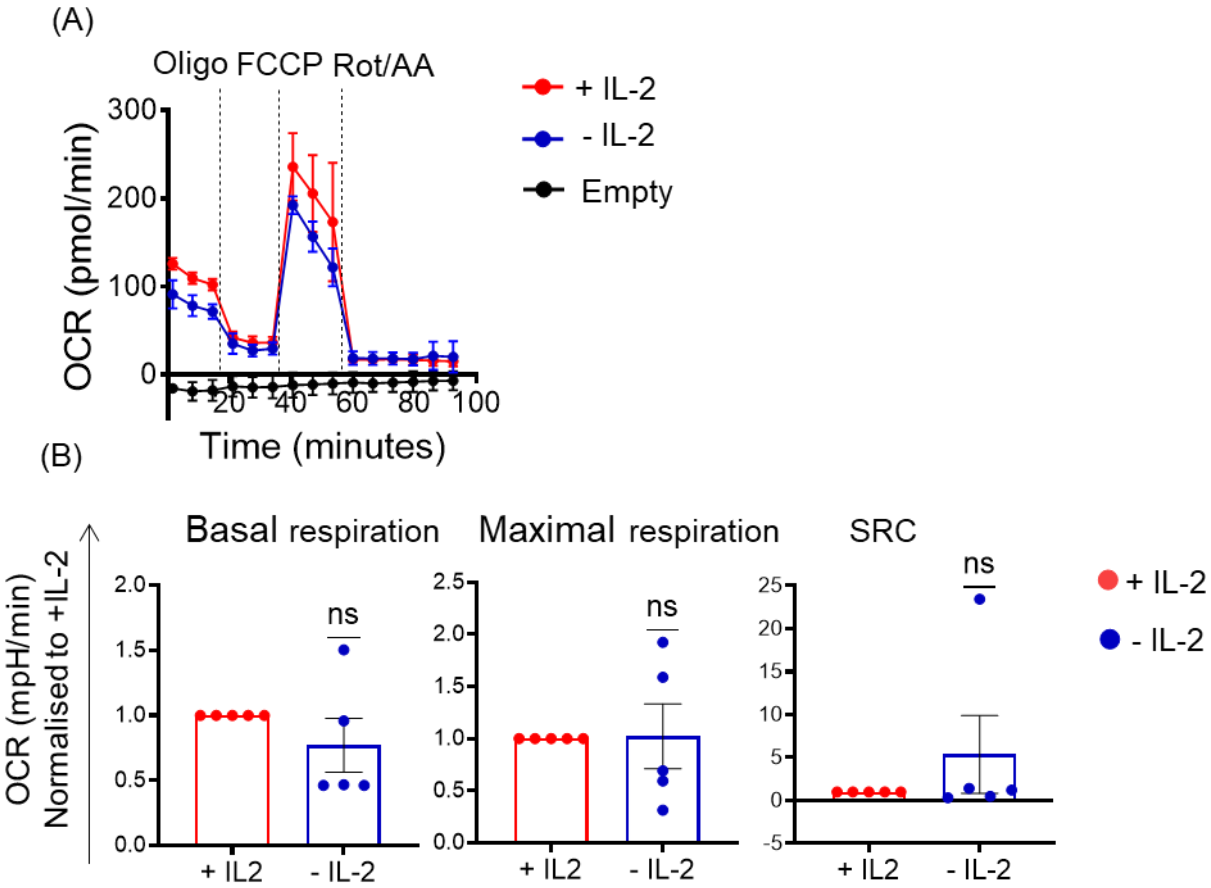

Figure 3.7: OxPhos rates in NK-92 cella is not affected by 18 hours IL2-deprivation.

NK-92 cells were cultured with or without IL-2 (100 IU/ml) for 18 hours. NK-92 cells were then plated at 150,000/well in seahorse media and analysed using the seahorse extracellular flux analyzer measuring basal oxygen consumption rate (OCR) and rates after sequential injection of oligomycin (2 μM), FCCP (0.5 μM) and Rotenone/Antimycin A (0.1μM / 4μM). The data are presented as a representative OCR trace (A) or mean +/- SEM (B) of 5 independent experiments. Statistical analysis was performed using a one sample t test against a hypothetical value of 1. ns, nonsignificant.

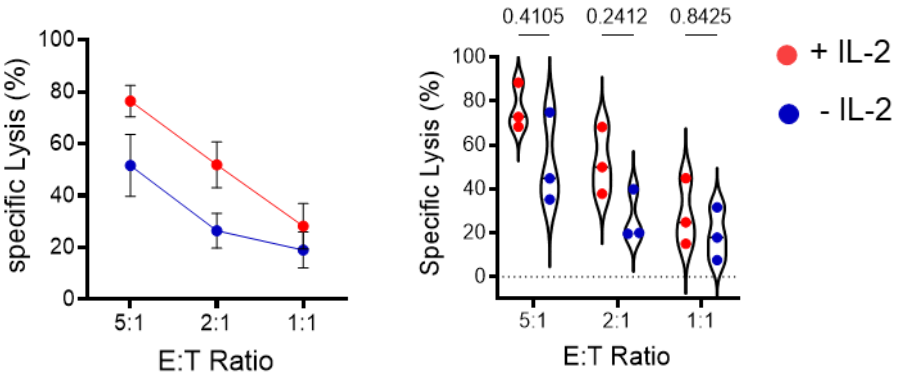

Figure 3.8: IL-2 deprivation for 18 hours does not affect NK-92 cytotoxicity.

NK-92 cell line were cultured with and without Il-2 (100 IU/ml) for 18 hours prior to assessing in *vitro* cytotoxicity against K562 tumour cells line. Cytotoxicity measured following co-incubation of NK-92 cell with K562 target cells for 4 hours at the ratio indicated, performed using technical triplicates. The data are presented as violin plot distributions (right) at the ratio indicated where each point represents an individual data points (right) of 3 independent experiments. Statistical analysis was performed using an unpaired t-tests (5:1) P value - 0.4105; (2:1) P value – 0.2412; (1:1) P value – 0.8425. This cytotoxicity assay was done by me and by Carrie Corkish (currently PhD student in Finlay's lab) who was completing her senior student project under the supervision of myself and Aisling McCrudden.

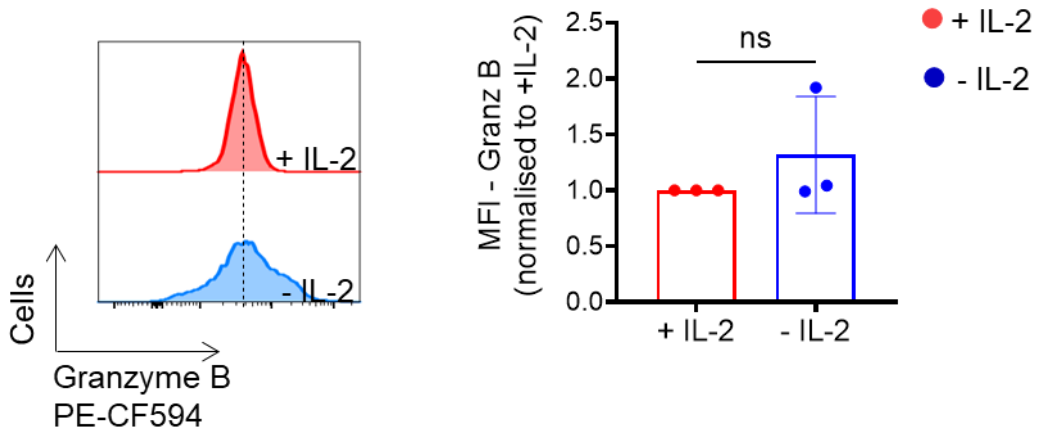

Figure 3.9: IL-2 deprivation for 18 hours does not affect granzyme B expression.

NK-92 cell line were cultured with and without IL-2 (100 UI/ml) for 18 hours prior to analysing by flow cytometry. The level of granzyme B was determined by staining the cells with PE-CF594. Data are a representative histogram (left) or mean + /- S.E.M (right) of 3 independent experiments. Data were analyzed using unpaired t-test. The level of granzyme B in – IL-2 is relative to + IL-2. MFI; mean fluorescence intensity ns, nonsignificant.

3.4 Decreased glycolytic rates inhibit NK-92 mediated cytotoxicity.

Next, I investigated whether NK-92 cell metabolism was required for optimal killing of tumor target cells. In **Figure 3.6** the seahorse extracellular flux analysis demonstrated that NK-92 cells have high levels of glycolysis. Therefore, I considered whether these increased rates of glycolysis would be crucial role in sustaining NK-92 cytotoxicity. I investigated the consequence of limiting the rate of glycolysis by using increasing concentrations of 2-Deoxyglucose (2-DG), which acts as an inhibitor of glycolysis.

To measure the importance of glucose as a fuel for NK-92 cells, the rates of OxPhos and glycolysis levels were measured by Seahorse Metabolic flux Analyzer. NK-92 cells (150,000/well) were prepared for seahorse extracellular flux analysis in either seahorse media in the presence or absence of glucose. Results show that NK-92 cells which were prepared with non-glucose seahorse media had significantly reduced levels of basal glycolysis compared to NK92 cells with glucose **(Figure 3. 10).** In the absence of glucose, NK92 cells had normal levels of basal OXPHOS but substantially higher maximal respiration in NK-92 were prepared with non-glucose seahorse media (**Figure 3. 11**). These data demonstrate that glucose is an important fuel for NK92 cells glycolysis but is not required to support rates of mitochondrial respiration. To investigate the importance of glycolysis for NK92 cell effector functions we used the glycolytic inhibitor 2-deoxyglucose (2-DG), which is known to inhibit

glycolysis due to the formation and accumulation of 2-deoxyglycose-6-phosphate (2-DG6P), which in return inhibits the function of hexokinase, one of the key enzymes in the glycolysis. I aimed to use 2-DG concentrations that reduce the rate of glycolysis in NK-92 cells but did not abolish glycolytic rates. To determine the impact of 2-DG on NK92 metabolism, the Seahorse Metabolic flux analyzer was used to investigate metabolic flux through OxPhos and glycolysis in NK-92 cells. Thus, NK-92 cell metabolism was measured while increasing the concentration of 2-DG concentration. NK-92 cells (150,000/well) were plated in seahorse media and then each injection pore was used to introduce 2-DG and increase the concentration (1mM, 2mM, 5mM, and 10mM), alongside NK-92 cells where seahorse media was injected as a control for the assay. With increasing 2-DG concentration, the glycolysis levels were decreased but not to the levels of NK92 cells cultured in the absence of glucose, indicating that NK-92 cells were still able to maintain some glycolytic flux **(Figure 3. 12)**. Therefore, we confirm that these concentrations of 2DG were not poisoning glycolysis in these cells.

In parallel, there was no change in OxPhos level in response to the injection of increasing doses of 2-DG **(Figure 3.13),** suggesting that NK-92 cells can maintain the basal levels of OxPhos even when they were limited in the ability to metabolize the glucose. These data suggest that NK-92 cells can use other fuel(s) to support OxPhos.

To examine the effect of long-term incubation of 2-DG on the metabolism

and function of NK-92 cells, the cells were cultured with different concentrations of 2-DG (0, 0.5, 1, 2 and 5 mM) for 18 hours and then cells were stained with viability stain (Zombie Near IR) and analyzed by flow cytometry. The result shows that 2-DG treatment did not impact on the basic cell biology of NK92 cells in terms of cell viability or cell size. NK-92 cells were still viable and were the same size as control NK-92 cells **(Figure 3.14).** To assess the consequence of this treatment on NK92 cell metabolism, the cells were analyzed for OxPhos and glycolysis levels by using Seahorse Metabolic flux Analyzer in media that did not contain any 2DG. The glycolysis levels were not affected by 18 hours treatment with increasing doses of 2DG **(Figure 3.15).** The trend in NK-92 OxPhos was towards increased rates of mitochondrial respiration at the lower doses of 2DG with inhibition of OXPHOS rates observed at the highest does or 10 mM 2DG **(Figure 3.16)**.

Crucially, pretreatment with dose of 2-DG as low as 1 mM for 18 hours showed a significant reduction in NK92 cytotoxicity towards K562 tumour target cells **(Figure 3. 17).** This decease in cytotoxicity was not associated with any decrease in granzyme B production **(Figure 3.18).** These results suggest that glucose metabolism through glycolysis is important for the ability of NK-92 cells to kill target cancer cells.

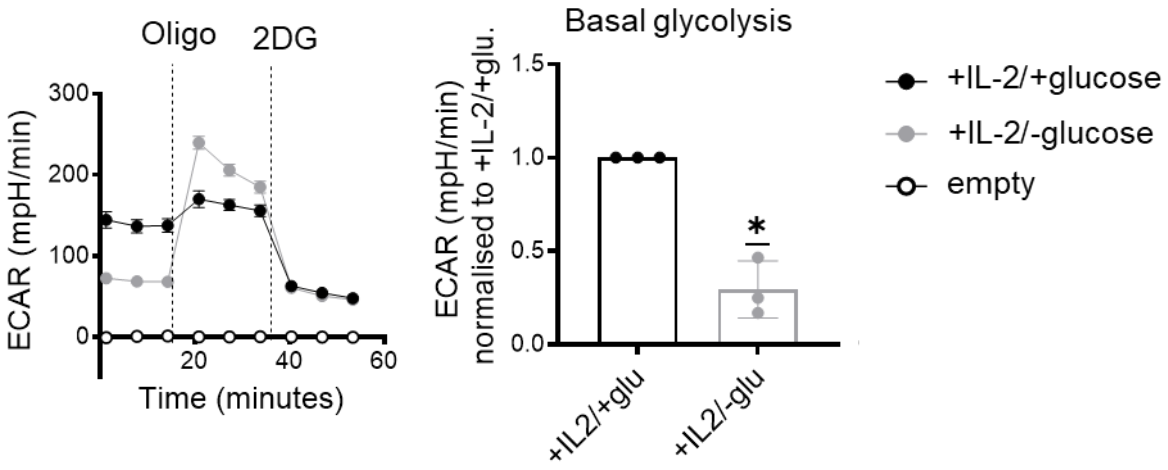

Figure 3.10: Glucose fuels glycolysis in NK92 cells.

NK-92 cells were cultured with human recombinant IL-2 (100 IU/ml) for 18 hours. NK-92 cells were then plated at 150,000/well in seahorse media in the presence or absence of glucose and analyzed using the seahorse extracellular flux analyzer measuring extracellular acidification rate (ECAR) and rates after sequential injection of oligomycin (2 μM), and 2-deoxyglucose (30 mM). The data are presented as a representative ECAR trace (right) or mean +/- SEM (left) of 3 independent experiments. Statistical analysis was performed using a one sample t test against a hypothetical value of 1. *$p<0.05$.

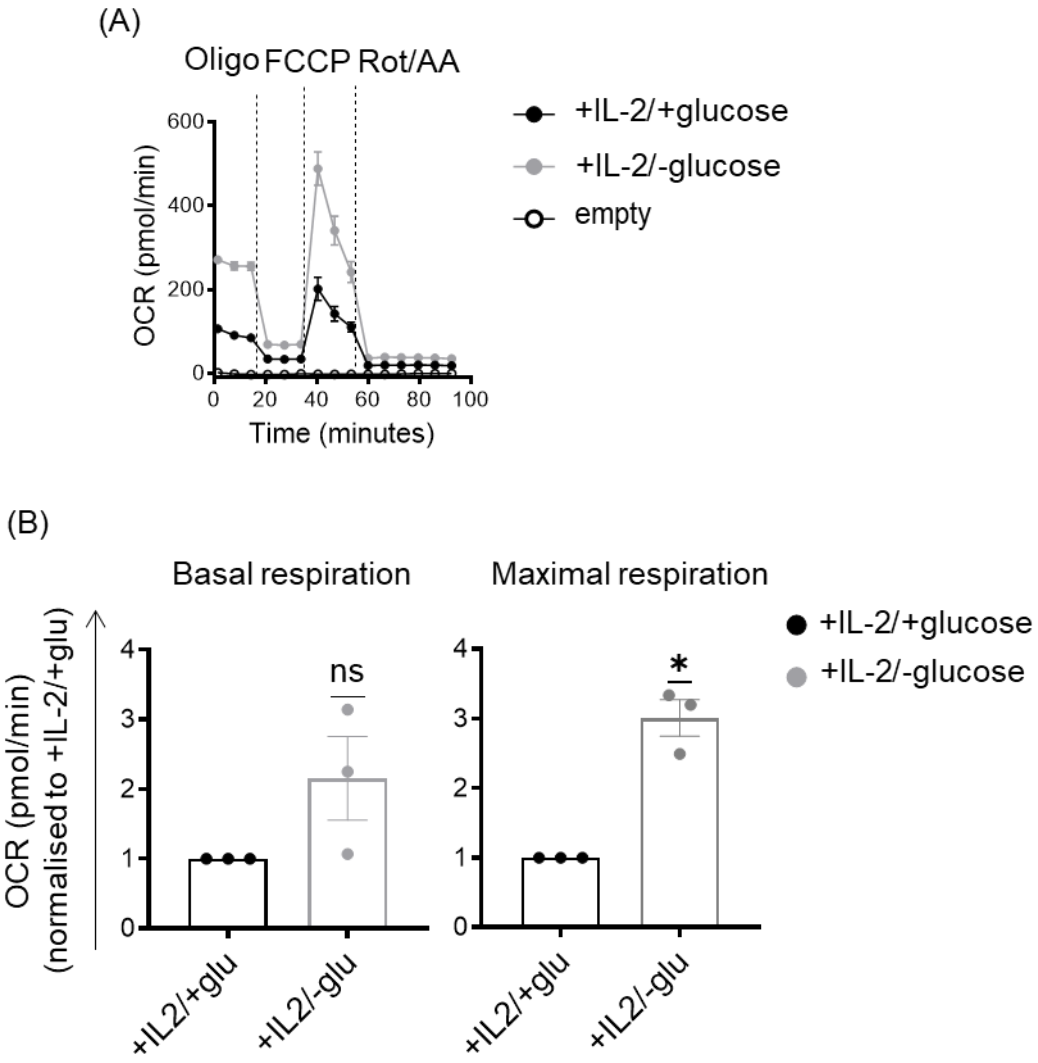

Figure 3.11: Glucose is not a key fuel for OxPhos in NK92 cells.

NK-92 cells were cultured with human recombinant IL-2 (100 IU/ml) for 18 hours. NK-92 cells were then plated at 150,000/well in seahorse media in the presence or absence of glucose and analysed using the seahorse extracellular flux analyzer measuring oxygen consumption rate (OCR) and rates after sequential injection of oligomycin (2 μM), FCCP (0.5 μM) and Rotenone/Antimycin A (0.1μM / 4μM). The data are presented as a representative OCR trace (A) or mean +/-SEM (B) of 3 independent experiments. Statistical analysis was performed using a one sample t test against a hypothetical value of 1. ns, nonsignificant; *p<0.05.

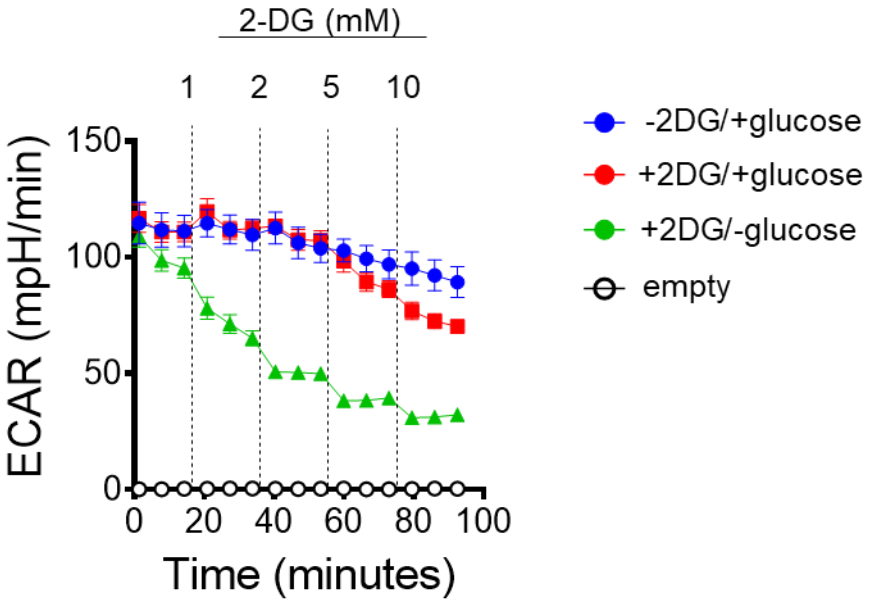
2-DG (mM)
1
2
5
10
ECAR (mpH/min)
150
100
50
0
0
20
40
60
80
100
Time (minutes)
-2DG/+glucose
+2DG/+glucose
+2DG/-glucose
empty

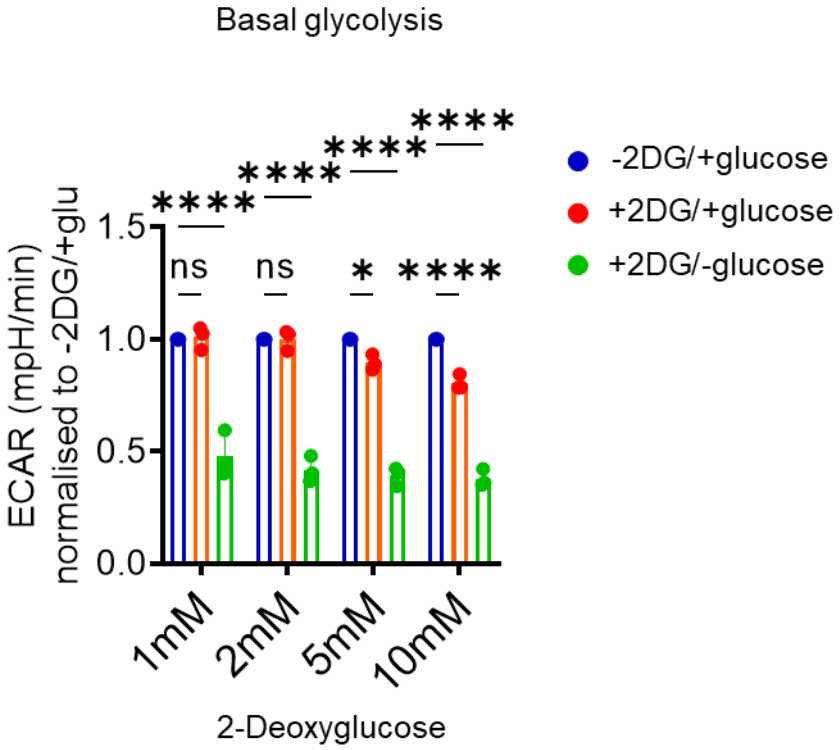
Basal glycolysis
ECAR (mpH/min)
normalised to -2DG/+glu
1.5
1.0
0.5
0.0
****
****
****
****
ns
ns
*
****
1mM
2mM
5mM
10mM
2-Deoxyglucose
-2DG/+glucose
+2DG/+glucose
+2DG/-glucose

Figure 3.12: Dose dependent inhibition of glycolysis by 2-DG in NK92 cells.

NK-92 cells were cultured with IL-2 (100 IU/ml) for 18 hours. NK-92 cells were then plated at 150,000/well in fresh seahorse media. Each pore injected with 2-DG increasing the overall concentration of 2-DG in the cell incrementally (Seahorse port A -1mM, Seahorse port B -2mM, Seahorse port C -5mM, Seahorse port D -10mM) and cells were analysed using the seahorse extracellular flux analyser measuring extracellular acidification rate (ECAR). The data are presented as a representative ECAR trace (above) of or mean +/- SEM (bottom) of 3 independent experiments. Statistical analysis was performed by two-way ANOVA with Dunnett's test for multiple comparison compared to 0 mM 2-DG. *$p<0.05$, ****$p<0.0001$; ns, nonsignificant.

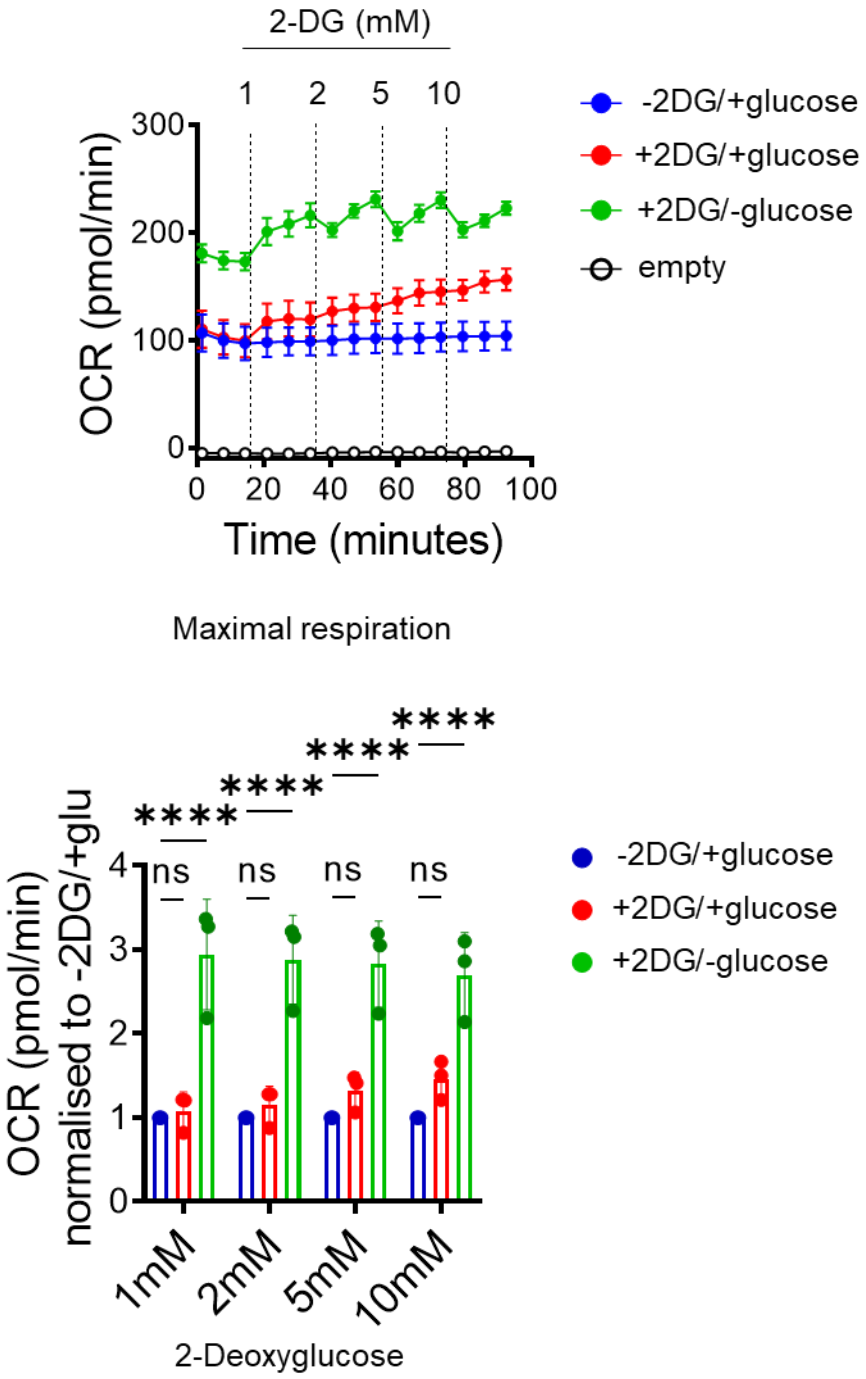
2-DG (mM)
1
2
5
10
300
200
100
0
OCR (pmol/min)
0
20
40
60
80
100
Time (minutes)
-2DG/+glucose
+2DG/+glucose
+2DG/-glucose
empty
Maximal respiration
****
****
****
****
ns
ns
ns
ns
4
3
2
1
0
OCR (pmol/min)
normalised to -2DG/+glu
1mM
2mM
5mM
10mM
2-Deoxyglucose
-2DG/+glucose
+2DG/+glucose
+2DG/-glucose

Figure 3.13: 2-DG does not inhibit OXPHOS in NK92 cells.

NK-92 cells were cultured with IL-2 (100 IU/ml) for 18 hours. NK-92 cells were then plated at 150,000/well in fresh seahorse media. Each pore injected with 2-DG increasing the overall concentration of 2-DG in the cell incrementally (Seahorse port A -1mM, Seahorse port B -2mM, Seahorse port C -5mM, Seahorse port D -10mM) and cells were analysed using the seahorse extracellular flux analyser measuring oxygen consumption rate (OCR). The data are presented as a representative OCR trace (above) of or mean +/- SEM (bottom) of 3 independent experiments. Statistical analysis was performed by two-way ANOVA with Dunnett's test for multiple comparison compared to 0 mM 2-DG. ****$p<0.0001$; ns, nonsignificant.

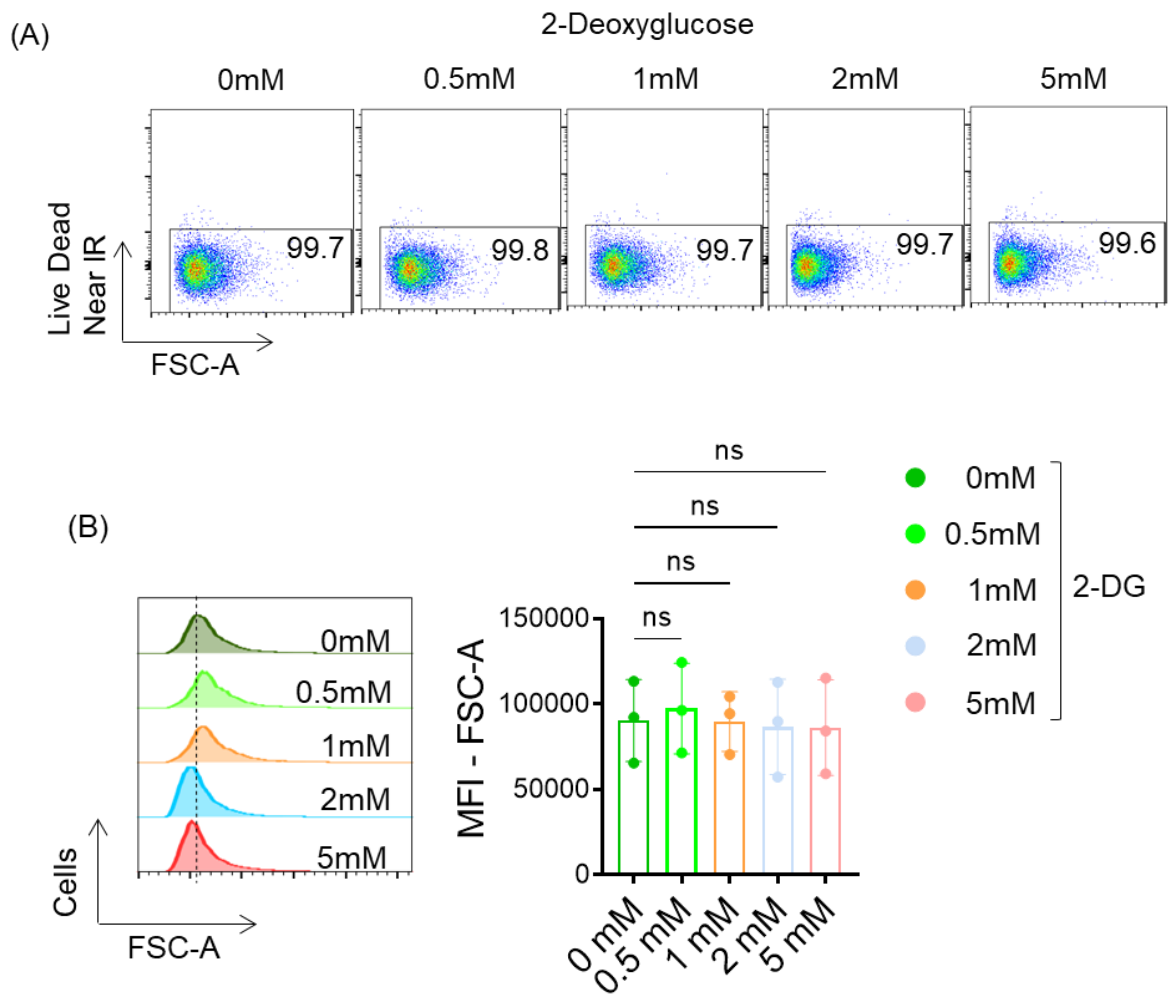

Figure 3.14: NK92 viability/size is not affected by 18 hours pre-treatment with 2-DG.

NK-92 cells were cultured with IL-2 (100 IU/ml) with different concentration of 2-DG (0, 0.5, 1, 2, 5 mM) for 18 hours before analyzing by flow cytometry. (A) The viability of NK-92 cells was determined by staining the cells with Live Dead (Near IR) (B) NK-92 cells were analyzed for FSC-A as a measure of cell size. Data are presented as representative (A and B, left) or mean +/- SEM (B, right) of 3 independent experiments. Data was analyzed using one-way ANOVA test with a Dunnett's post-test for multiple comparisons. ns, nonsignificant; MFI, mean fluorescence intensity.

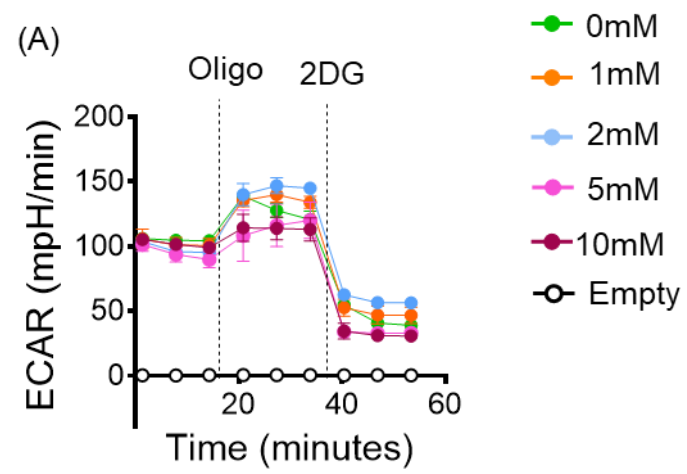
(A)
Oligo
2DG
ECAR (mpH/min)
200
150
100
50
0
20
40
60
Time (minutes)
0mM
1mM
2mM
5mM
10mM
Empty

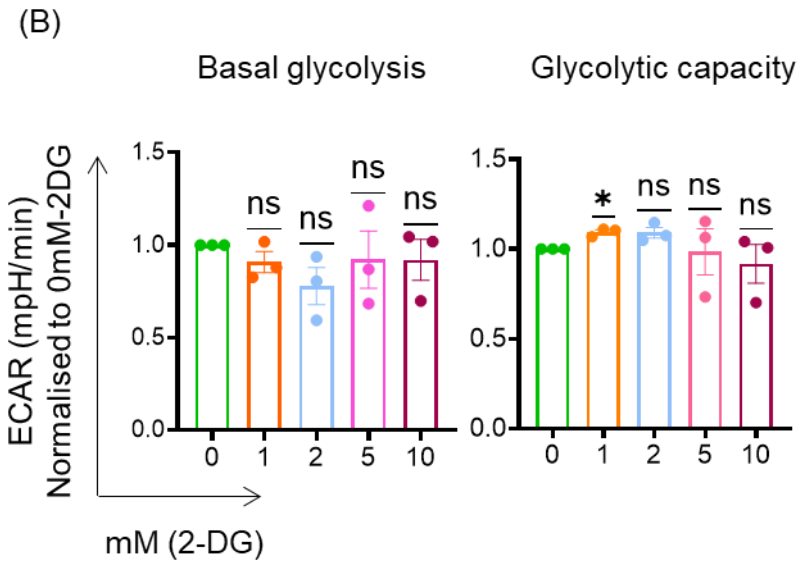
(B)
Basal glycolysis
Glycolytic capacity
ECAR (mpH/min)
Normalised to 0mM-2DG
1.5
1.0
0.5
0.0
ns
ns
ns
ns
*
ns
ns
0
1
2
5
10
mM (2-DG)

Figure 3.15: NK-92 glycolysis is not affected by 18 hours pre-treatment with 2-DG.

NK-92 cells were cultured with IL-2 (100 IU/ml) and pre-treatment with different concentration of 2-DG (0, 1, 2, 5, 10 mM) for 18 hours. The cells were then plated at 150K cells in fresh seahorse media (without any 2DG present) and analysed using the seahorse extracellular flux analyzer measuring extracellular acidification rate (ECAR) and rates after sequential injection of oligomycin (2 μM), and 2-deoxyglucose (30 mM). The data are presented as a representative ECAR trace (A) or mean +/-SEM (B) of 3 independent experiments. Statistical analysis was performed using a one sample t test against a hypothetical value of 1. *$p<0.05$; ns, nonsignificant; *$p<0.05$.

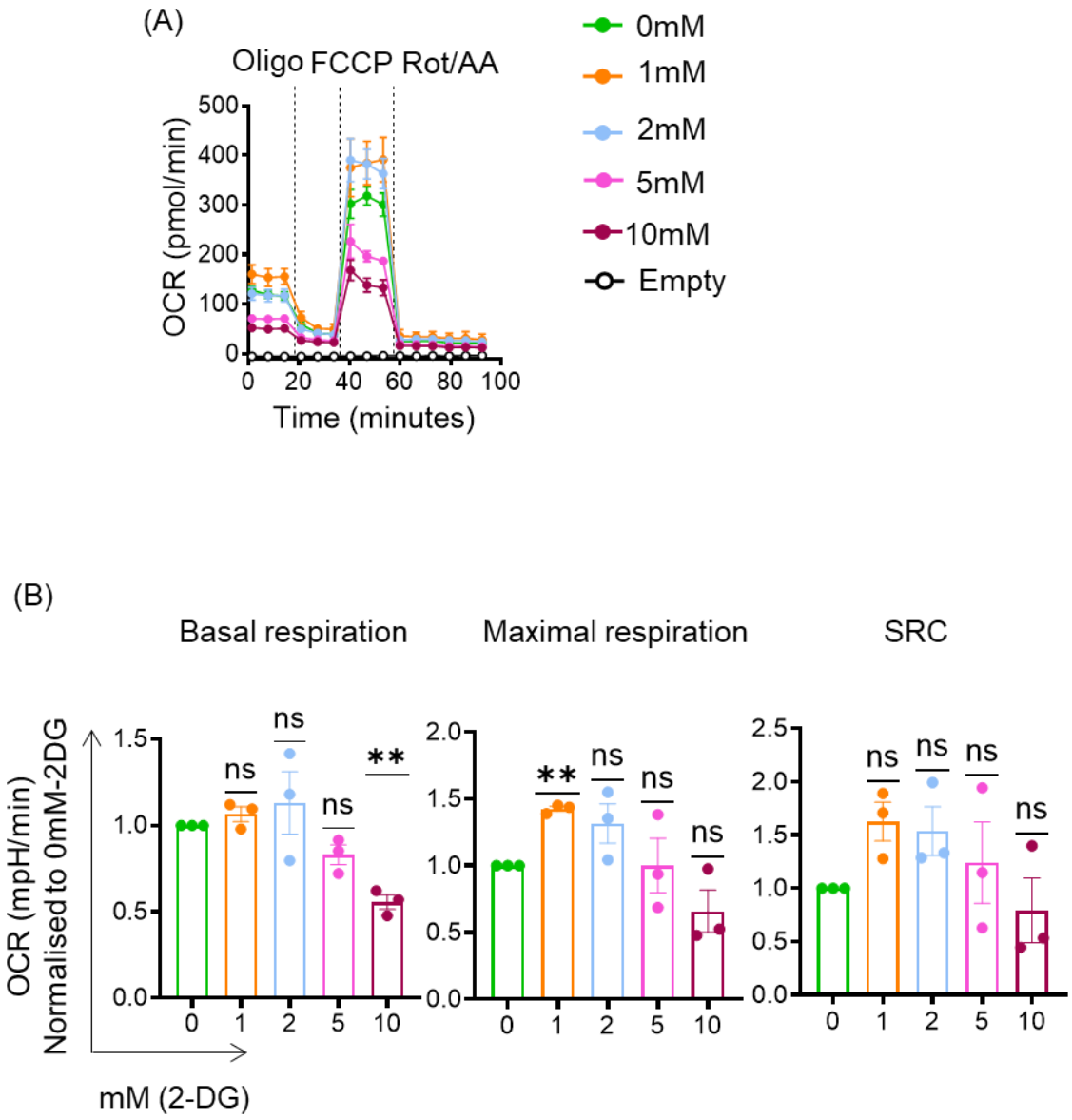
(A)
Oligo FCCP Rot/AA
OCR (pmol/min)
Time (minutes)
0mM
1mM
2mM
5mM
10mM
Empty
(B)
Basal respiration
Maximal respiration
SRC
OCR (mpH/min)
Normalised to 0mM-2DG
mM (2-DG)
ns
**

Figure 3.16: NK-92 OxPhos is inhibited by 18 hours pre-treatment with 2-DG

NK-92 cells were cultured with IL-2 (100 IU/ml) and pre-treatment with different concentration of 2-DG (1, 2, 5, 10 mM) for 18 hours. The cells were then plated at 150K cells in fresh seahorse media (without any 2DG present) and analyzed using the seahorse extracellular flux analyzer measuring oxygen consumption rate (OCR) and rates after sequential injection of oligomycin (2 μM), FCCP (0.5 μM) and Rotenone/Antimycin A (0.1μM / 4μM). The data are presented as a representative OCR trace (A) or mean +/- SEM (B) of 3 independent experiments. Statistical analysis was performed using a one sample t test against a hypothetical value of 1. **p<0.01; ns, nonsignificant.

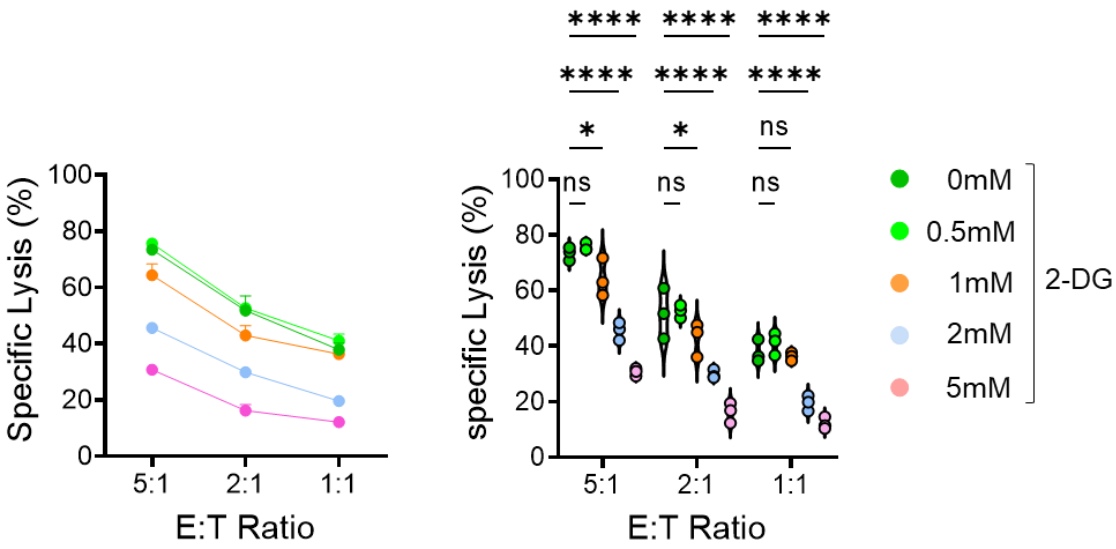

Figure 3.17: 2-DG pre-treatment for 18 hours inhibits NK-92 cell cytotoxicity.

NK-92 cell line were cultured with IL-2 (100 IU/ml) and treated with different concentration of 2-DG (0, 0.5, 1, 2, 5 mM) for 18 hours prior to assessing in *vitro* cytotoxicity against K562 tumor cells line. Cytotoxicity measured following co-incubation of NK-92 cell with K562 target cells for 4 hours (with no 2DG present) at the ratio indicated, performed using technical triplicates. The data are presented as violin plot distributions (right) at the ratio indicated where each point represents an individual data points (right) of 3 independent experiments. Statistical analysis was performed by two-way ANOVA with a Dunnett-test for multiple comparison compared to 0 mM 2-DG. ns, non-significant; *p<0.05, **p<0.01, ***p<0.001, ****p<0.0001.

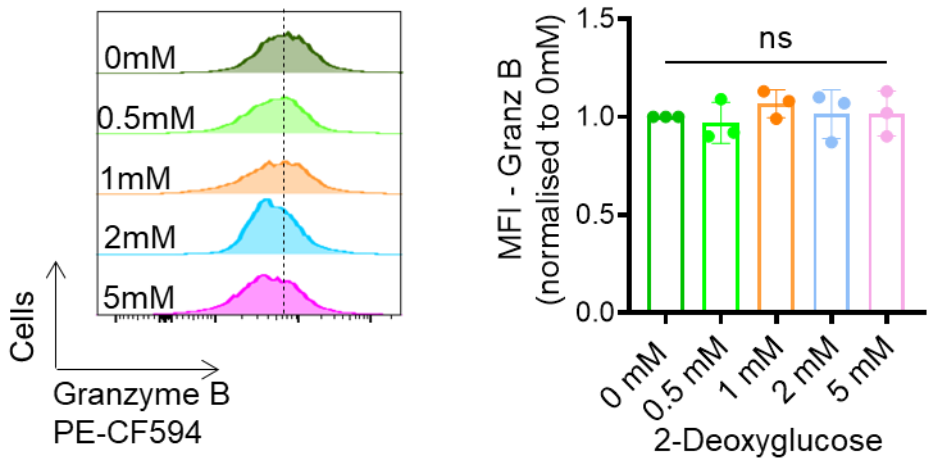

Figure 3.18: 2-DG pre-treatment for 18 hours does not affect had granzyme B expression in NK-92 cells.

NK-92 cell line were cultured with IL-2 (100 IU/ml) and treated with different concentration of 2-DG (0, 0.5, 1, 2, 5 mM) for 18 hours prior to analysing by flow cytometry. The level of granzyme B was determined by staining the cells with PE-CF594. Data are presented as a representative histogram (left) or mean + /- S.E.M (right) of 3 independent experiments. Data were analyzed using one-way ANOVA with Dunnett-test for multiple comparison compared to untreated cells. The level of granzyme B in 2DG-treated cells is relative to 0mM-2DG. MFI; mean fluorescence intensity ns, nonsignificant.

3.5 Discussion of Chapter 3

The IL2 dependent NK-92 Cell Line expressed a set of receptors on their surface that are important for the cytotoxic function of these cells [129]. As cell lines can change overtime it was important to characterize the phenotype of the cells to be used in this study. A review of the literature showed that the parental NK-92 cell line is described to have high expression for CD56, granzyme B, activating receptor such as NKp30 and NKp46 and TRAIL, but do not express CD3, CD16, FasL and NKp44. The NK-92 cells used herein are shown to express CD56, granzyme B and unexpectedly NKp44, while on the other hand they were negative for the rest of the indicating antigens surface. The NK-92 sub-clone cell line used in current study closely appears like the parental NK-92 cell line phenotype as both are identified as $CD56^{+}CD3^{-}$ subset and exerted their cytotoxic activity through producing cytolytic molecules like granzyme B. Additionally, they lack CD16 which means they are not able to exhibit their cytotoxicity through antibody-dependent cell-mediated cytotoxicity (ADCC) [114], [125], [127], [129]. Immunoglobulin superfamily receptors, NKp30, NKp46, and NKp44 known as natural cytotoxicity receptors are involved in identification and lysis of transformed cells, while NKp46 and NKp30 are expressed in all NK cells [130], and NKp44 is selectively induced by IL-2 activated NK cells [130], [131].

While NK92 cells require IL2 for proliferation, the results herein show that NK92 metabolism and cytotoxicity is relatively resistant to acute IL2 withdrawal. Withdrawal of IL2 did not affect the viability of NK92 cells over 72 hours, nor did if affect the cytotoxicity of NK92 cells over 18 hours. The withdrawal of IL2 also did not affect the rates of glycolysis or OXPHOS in NK92 cells. This is in contrast to other IL2 dependent cytotoxic lymphocytes, such as murine CTL, which show substantial metabolic deficits after just 18 hours IL2 withdrawal, including reduced glycolysis

[132]. One indicator that IL2 had been successfully withdrawn from NK92 cels was the decrease in the expression of CD71, a known IL2 regulated protein [133]. CD71 functions to regulate transferrin-iron uptake into the cells, which is a crucial nutrient for survival, function, and determine the metabolic state of lymphocytes. Thus, expression of cell surface transferrin receptor CD71 has been used as a marker for the proliferative capacity of T and NK cells [133]–[135] . This is in line with several previously published studies on T and NK cells. For instance, unstimulated NK cells from tissue and peripheral blood had similar CD71 expression level, but after being stimulated by cytokines, a significantly higher level of CD71 on peripheral blood and tissue-derived $CD56^{bright}$ NK cells to facilitate the metabolic requirement of proliferation was observed [21], [134]. Nevertheless, IL-2 deprivation has no impact on NK-92 killing capacity against K562 and the metabolic profile reflecting the sustainability of this cell line and their reliability on supporting their killing machinery through district metabolic configuration. In 1996, Klingemann H. G. *et al* showed that with IL-2 deprivation, NK-92 cytotoxicity declined after 24 hours, however, the substantial cytotoxicity of NK-92 was maintained up to 48 hours in vitro [136]. .

Metabolism has been shown to alter both human and murine NK cell functions [121], [137]. Glucose is not only a fuel to generate energy but also as a source for the biosynthetic precursors [138], [139]. Therefore, cells engaging in robust proliferation and growth are adapted to aerobic glycolysis as it provides precursors feeds into many of biosynthetic pathways [138]. The results showed the introduction of oligomycin results in a higher ECAR rates (Figure 3.10) compared to what was observed in the presence of glucose alone, and this effect is suppressed by 2DG (Figure 3.12) suggesting that the glucose is present in NK-92 cells even after washing out the culture medium. However, the basal OxPhos level

was normal in the absence of glucose (Figure 3.11), indicating glucose was not a key fuel to support rate of mitochondrial respiration as the data in Figure 3.10 suggest the glucose must present in the cells. Interestingly, although the short-term incubation with 2-DG affect the glycolysis rate, the 18 hours incubation with 2-DG does not affect NK-92 glycolysis (Figure 3.15). In contrast, short term incubation with 2-DG does not affect the NK-92 OxPhos level, but long-term incubation does affect OxPhos level of NK-92 cell. To sum, the data suggest the inhibition of NK-92 glycolysis by 2-DG is reversible.

The seahorse extracellular flux analysis indicated that NK-92 cells have high levels of basal glycolysis. In this regard, it was observed that highly activated lymphocytes were highly glycolytic producing high amount of lactate [140], and this metabolic configuration was adapted by cells engaging in robust proliferation and growth as it provides precursors that are involved in biosynthetic pathways [138], [140], [141]. Many of the intermediates in the glycolysis can act as a source of carbon that feeds into a variety of pathways involved in the synthesis of effector molecules [138]. For instance, the first step in glycolysis produces glucose-6-phosphate that can be utilizing by pentose phosphate pathway (PPP) to generate ribose-5-phosphate which can further be used for nucleotides synthesis. Thus, for activated lymphocytes that adapted to this aerobic glycolysis, the main function of glucose was shifted from energy generation to be a source of carbon that can be further utilized for biosynthesis purposes [139], [140].

The findings from this study indicate that 2DG inhibit NK OxPhos levels, leading to a decrease in cytotoxicity without affecting the glycolytic rate. Consequently, the evaluation of cytotoxicity was carried out in the absence of 2-DG, thus the direct impact of 2-DG on cytotoxicity was not explored in this report. Therefore, based on the data available, it remains uncertain whether glycolysis is essential for NK-92 cytotoxicity. It is

important to explore the direct influence of 2-DG on the cytotoxicity assay to further investigate this matter. The indication also implies that the reduced cytotoxicity (Figure3.17) could be attributed to the inhibition of OxPhos, although the situation might be more intricate.

2-DG could affect NK-92 cytotoxicity and that may be through inhibition of glucose-dependent processes not only through simply inhibition of energy. Even though 2-DG is well-known to inhibit glycolysis, it has a huge metabolic effect and involvement with different biological processes including cellular energy depletion, interference with N-linked glycosylation, enhancement of autophagy, and reinforcement of oxidative stress [141]. As a result of this interference, various signaling pathways are activated such as AMP-activated protein kinase (AMPK), beta actin, mitogen-activated protein kinase (MAPK), and phosphoinositide-3-kinase (PI3K) and somewhat all these events are related and integrated [142], [143]. Therefore, the toxicity of 2-DG on different cell types is caused by more than one potential mechanism. 2-DG is transported in the cell by GLUTs and thus competitively inhibits glucose uptake. After entering the cells, 2-DG will be phosphorylated by Hexokinase (HK) to form 2-Deoxy-D-glucose-6-phosphate (2DG-6-P), which cannot further metabolize through glycolysis, as a result, the accumulation of 2DG-6-P inhibit HK, a critical first step in glycolysis, leading to completely inhibit glycolysis [144], [145]. Reducing ATP levels elevates the AMP/ATP ratio, leading to AMPK activation. This, in turn, enhances catabolic metabolism by phosphorylating downstream targets like mTOR [146]. Additionally, decreased ATP levels prompt cells towards extrinsic apoptosis by causing the binding of TRIL to their respective death receptors [147], [148]. Nevertheless, 2-DG treatment, imitating glucose deprivation, does not affect the effector function because of energy deprivation as the cells can maintain OxPhos function and use alternative carbon sources like amino

acid, and fatty acid to build up ATP under well-oxygenated conditions [149], [150].

In addition, the treatment of 2-DG on T and B lymphoma cell lines shows a clear effect on energy metabolism, however treatments of mannose and anti-apoptotic protein BcI-2 overexpression rescue the cells from 2-DG-induced cell death, but not reverse the ATP depletion [151]. Elevated glucose metabolism reduces oxidative stress by clearing ROS and maintaining redox homeostasis through the generation of NADP and ribose-5phosphate (R5P) from PPP and pyruvate formation from glycolysis [152], [153]. The PPP is one of the main pathways of glucose metabolism that does not provide ATP to meet the energy need, instead, it generates NADPH and R5P for proliferation and survival purposes [154], [155]. NADPH is a reducing equivalent used for fatty acid, nucleotides, and sterols synthesis. Additionally, NADPH is essential for cellular antioxidant defenses as it is required for the conversion of oxidized glutathione (GSSG) to reduced form (GSH) through glutathione reductase [154], [155]. On the other hand, R5P is required for nucleic acid synthesis [155]. Pyruvate is important for maintaining the intracellular redox state by maintaining the reduced form level of glutathione, which provides the production of superoxide and thus scavenging hydrogen peroxide [156]. 2-DG treatment, which mimics glucose deprivation, enhances the mitochondrial stress as 2DG-6-P cannot be further metabolized through glycolysis and PPP to produce pyruvate, NADPH, and R5P. Therefore, these treatment leads to NADPH and R5P deficiencies which damage the antioxidant defense of the cells and could make them more vulnerable to oxidative stress [157], [158].

Protein glycosylation is the enzymatic process that plays a significant role in modifying proteins and therefore determines the protein structure, function, and stability [159]. N-linked glycosylation occurs when glycan is attached to nitrogen of arginine or asparagine side chain of protein in ER.

Mannose-guanosine diphosphate (GDP) acts as a precursor for N-linked glycosylation of proteins [160]. Glucose is involved in the N-linked glycosylation of proteins as it is converted to G-6-P, which is then converted to mannose-6-phosphate by phospho-mannose isomerase (PMI) and then further metabolized to mannose-GDP, which forming the oligosaccharide chains of proteins [161]. Because 2-DG has a similar structure to mannose and can be metabolized to 2DG-GDP, 2-DG interferes and disrupts the formation of the oligosaccharide chain of proteins [161]. As a result, the inhibition of N-linked glycosylation prevents normal protein folding and thus enhances the retention of unfolded proteins in ER, which activates unfolded protein response (UPR) [162].

Numerous studies show that 2-DG-induced cell death under aerobic conditions is responsible for the inhibition of glycosylation rather than glycolysis [151], [163]. Adding mannose can rescue various cells from 2-DG-induced cell death, however, cannot reverse the decrease in production of ATP [164], [165]. Therefore, ER stress induced by 2DG can also be an autophagic trigger as the addition of exogenous mannose, can reduce ER stress, leading to abolish autophagy [166], [167]. The result in this report shows that 2-DG inhibited NK-92 OxPhos level and that was associated with a reduction in the cytotoxicity without impacting on glycolytic rate, meaning 2-DG could affect NK-92 in multiple ways. Many already published studies demonstrated that mTORC1-dependent glycolytic metabolism is essential for activated cytokine NK cells function and development [138], [140], [142].

The glycolytic reprogramming of NK cells is dependent on mTORC1 signaling and is inhibited by the mTORC1 specific inhibitors known as rapamycin [142]. On the other hand, upon cytokine activation mTORC1 is not required for increasing the OxPhos rates in NK cells [142]. In early NK cells progenitors, deletion of mTORC1 inhibit the NK cells maturation and peripheral homeostasis [143]. Additionally, manipulating the mTORC1

activity in iNKT progenitors results in a significant inhibition in iNKT cell development which is associated with a downregulation of nutrient receptors, proliferation and cell growth [144], [145]. Thus, it is worth further investigating whether inhibition of mTORC1 has a consequence for the metabolism and effector function of NK92 cells using a highly specific mTORC1 inhibitor called rapamycin.

Chapter 4 - Oxysterols inhibit NK-92 cells metabolism and function.

4.1 Introduction

The IL-2 receptor can drive signaling through multiple signaling pathways including the mammalian target of rapamycin complex 1 (mTORC1) pathway which is important in metabolic regulation [146], [147]. The mTORC1 is a key regulator of cellular metabolism and controlling immune responses for many immune cells including NK cells [147]. The evidence provides that metabolism plays a crucial role in dominating immune cells' function and proliferation. [148]–[150]. Indeed, it was found in activated murine NK cells, that mTORC1 activity is fundamental for glycolytic reprograming and that this metabolic profile is required for sustaining normal effector function in NK cells [146]. mTORC1 activation is induced by IL-2 and leads to enhanced NK cell proliferation and effector function [146], [151]. To determine whether mTORC1 signaling is required for IL-2-induced metabolic reprogramming and supported effector functions of NK-92 cells, the activity of of mTORC1 was blocked using a highly specific mTORC1 inhibitor, rapamycin, and the consequences for NK92 cell metabolism and function investigated.

Another IL-2-induced metabolic regulator is the Sterol regulatory element binding protein (SREBP), transcription factor. The Finlay lab previously has shown that SREBP activation is important for the metabolic phenotype of cells that respond to IL-2 in murine and human NK cells [152]. Moreover, inhibiting the activation of SREBP using pharmacological inhibitors leads to significantly reduced NK cell effector functions [152]. SREBP activation and process can be disrupted by oxysterols, oxidized derivatives of cholesterol such as 25-hydroxycholesterol (25-HC) and 27-hydroxycholesterol (27-HC). Although oxysterols are intermediate compounds, different oxysterols could have different actions based on their concentration and the type of cells, which can contribute to the development of many diseases [153]–[156]. Indeed, our lab found that

25-HC and 27-HC are potent inhibitors of murine and human NK cells' effector function such as cytotoxicity at the concentration found systemically during infection and other immune contexts [157]–[159]. Therefore, we hypothesize that 25-H and 27-HC can inhibit NK-92 metabolism and thus impair the effector function through Srebp activation.

4.2 mTORC1 is not required for maintaining the NK-92 cell cytotoxicity.

The highly specific mTORc1 inhibitor rapamycin was used to investigate a role for mTORC1 in the regulation of IL-2-induced metabolism and function of NK-92 cells. Firstly, I confirmed the specificity of rapamycin in NK92 cells by analyzing the levels of phosphorylated S6 ribosomal protein on serine 235/6 (pS6), total S6, and b-actin using Western Blot analysis. S6 ribosomal protein is phosphorylated on serine 235/6 by the p70/p85 S6 kinase1 (S6K1) and p54/p56 S6 kinase2 (S6K2) [160] that are activated downstream of mTORC1. This phosphorylated residue is a robust readout of mTORC1 activity, and the phosphorylation is lost rapidly when mTORC1 activity is inhibited (within minutes). NK-92 cells were cultured with IL-2 and either treated with or without rapamycin (20 nM) for 18 hours before analyzing them by wet transfer western blot. The immunoblotting result shows that mTORC1 signaling was inhibited in rapamycin-treated NK-92 cells as the loss of phospho-S6 ribosomal protein **(Figure 4.1).**

Next, I examined the effect of rapamycin treatment on NK-92 cell viability and size. NK92 cells were cultured with IL-2 +/- rapamycin for 18 hours and then stained with viability stain (Zombie Near IR) before analysis by flow cytometry. Rapamycin treatment did not affect the viability and size of NK92 cells. Rapamycin-treated cells were still viable and equivalent in cell size compared to NK92 cells not treated with rapamycin (**Figure 4.2).**

To investigate the effect of rapamycin treatment on NK-92 cell

metabolism, the Seahorse Metabolic flux analyzer was used to investigate metabolic flux via OxPhos and glycolysis in NK-92 cells cultured with IL-2 in the presence or absence of rapamycin for 18 hours. The data showed that there was no change in basal glycolysis levels or the glycolytic capacity of the NK92 cells (**Figure 4.3).** However, there was significant decrease in OxPhos levels in rapamycin-treated NK-92 cells (**Figure 4.4).** These inhibition on basal and maximum respiration does not affect NK-92 cytotoxicity **(Figure 4.5).**

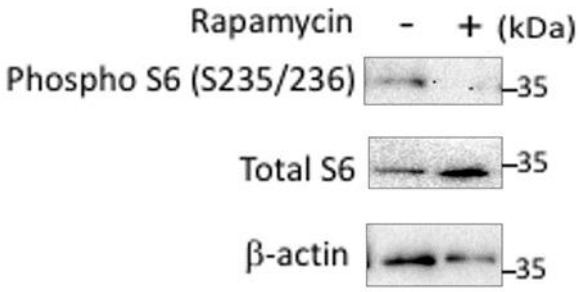

Figure 4.1: Phosphorylation of S6 was lost following rapamycin treatment in NK-92 cells.

NK-92 cells were cultures in IL-2 (100 IU/ml) in the presence or absence of rapamycin for 18 hours. NK-92 cells were harvested for immunoblotting analysis of phosphorylated S6 ribosomal protein on serine 235/6 (pS6), total ribosomal protein (S6) and b-actin. Data are representative blot of 3 independent experiments.

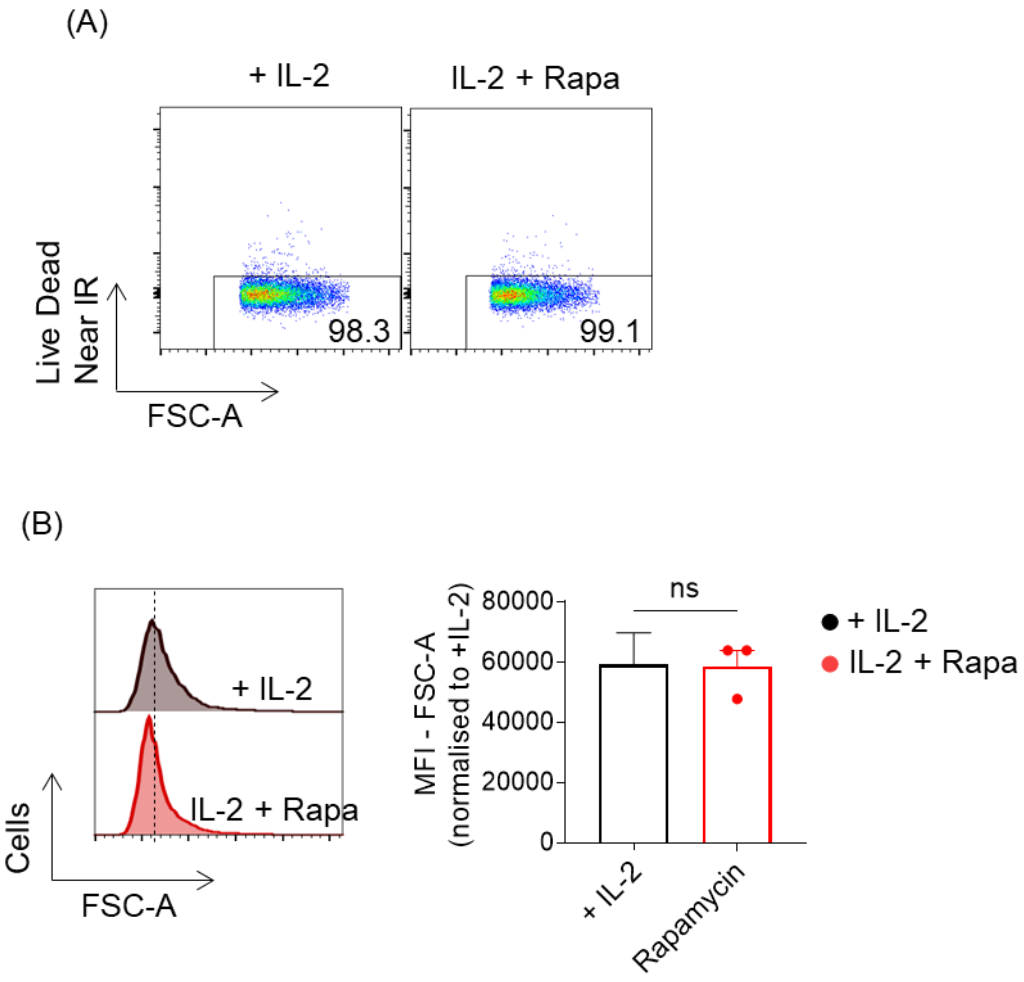

Figure 4.2: Rapamycin treatment does not affect on NK-92 viability and cell size. NK-92 cells were cultured with human recombinant IL-2 (100U/ml) and treated with and without rapamycin (Rapa) (20nM) for 18 hours before analysis by flow cytometry. (A) The viability of NK-92 cells was determined by staining the cells with Live Dead (Near IR) (B) NK-92 cells were analyzed for FSC-A as a measure of cell size. The data are presented as a representative (A and B, left) or mean+/-SEM (B, right) of 3 independent experiments. Statistical analysis (B, right) was performed by unpaired t-test compared to +IL-2. ns, nonsignificant; MFI, mean fluorescence intensity.

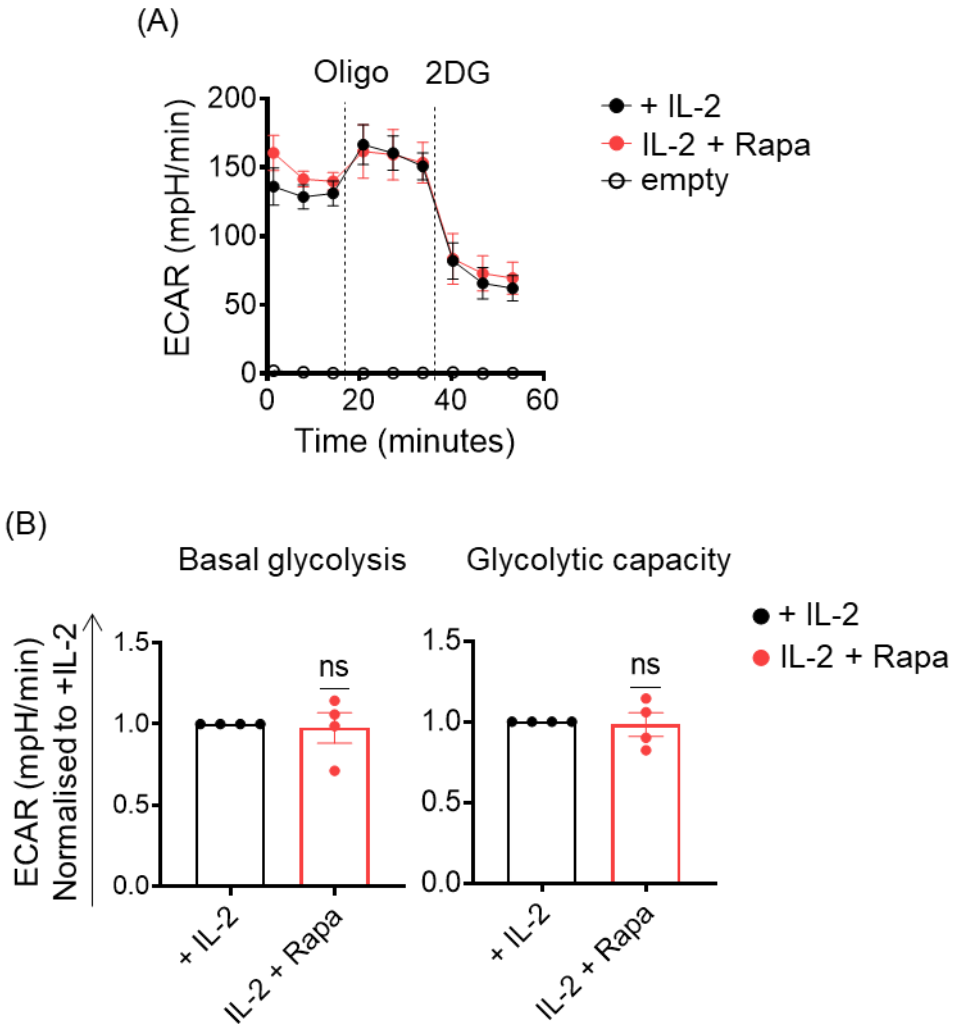

Figure 4.3: Glycolysis is unchanged in rapamycin-treated NK-92 cells 18 hours.

NK-92 cells were cultured with IL-2 (100 IU/ml) and then were treated with or without rapamycin (20nM). NK-92 cells were then plated at 150000/well in seahorse media and analysed using the seahorse extracellular flux analyzer measuring extracellular acidification rate (ECAR) and rates after sequential injection of oligomycin (2 μM), and 2-deoxyglucose (30 mM). The data are presented as a representative OCR trace (A) or mean +/- SEM (B) of 4 independent experiments. Statistical analysis was performed using a one sample t test against a hypothetical value of 1. ns, nonsignificant.

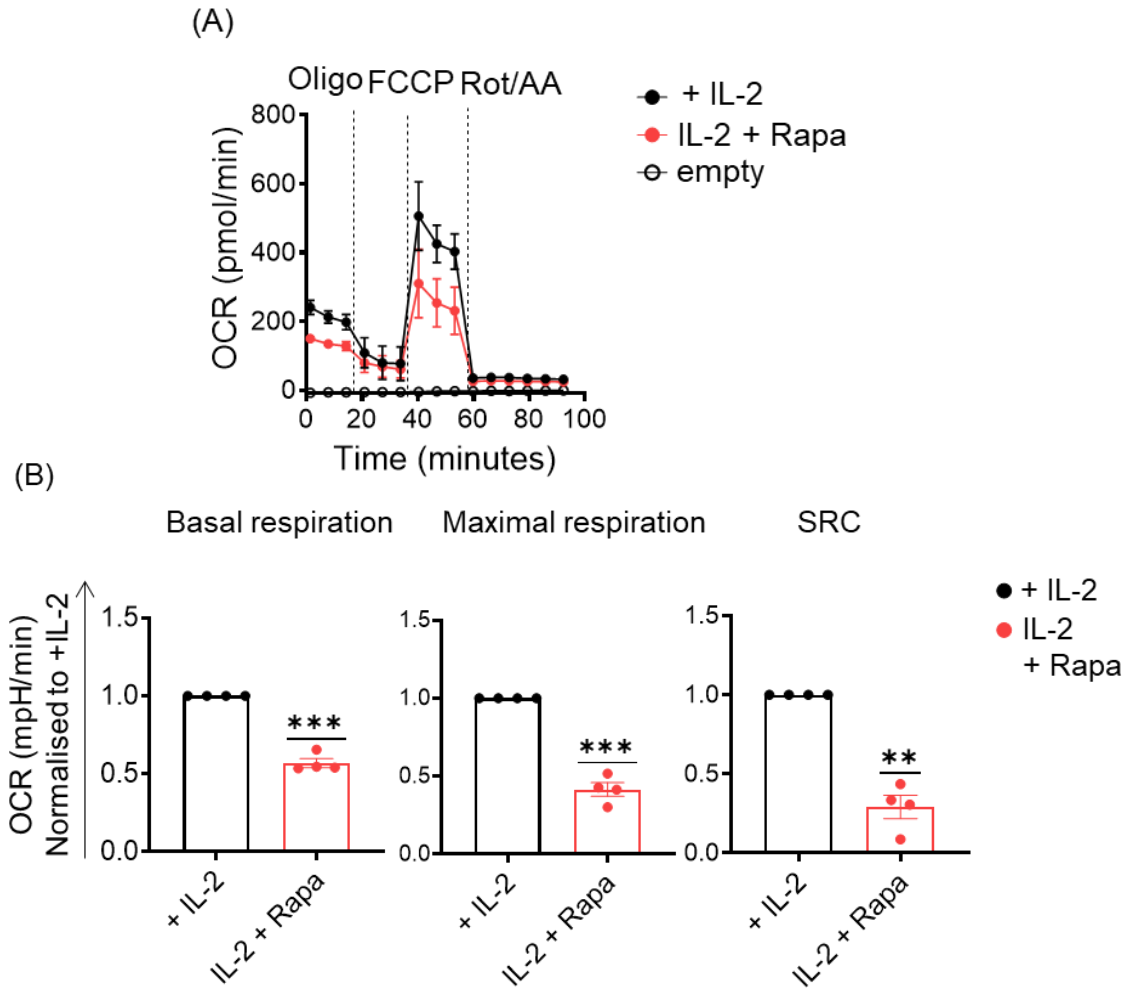

Figure 4.4: NK-92 OxPhos is inhibited by 18 hours pre-treatment with rapamycin.

NK-92 cells were cultured with IL-2 (100 IU/ml) and then were treated with or without rapamycin (20nM) for 18 hours. NK-92 cells were then plated at 150000/well in seahorse media and analysed using the seahorse extracellular flux analyzer measuring oxygen consumption rate (OCR) and rates after sequential injection of oligomycin (2 μM), FCCP (0.5 μM) and Rotenone/Antimycin A (0.1μM / 4μM). The data are presented as a representative (above) or mean +/- SEM (bottom) of 4 independent experiments. Statistical analysis was performed using a one sample t test against a hypothetical value of 1. ns; nonsignificant, **p<0.01, ***p<0.001.

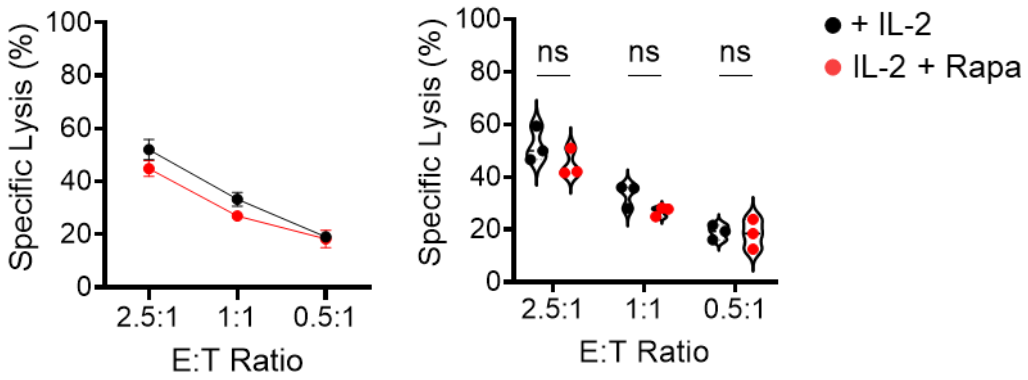

Figure 4.5: Rapamycin treatment for 18 hours does not affect NK-92 Cytotoxicity.

NK-92 cell line were cultured with IL-2 (100 UI/ml) and treated with or without rapamycin (20 nM) for 18 hours prior to assessing *in vitro* cytotoxicity against K562 tumor cells line. Cytotoxicity measured following co-incubation of NK-92 cell with K562 target cells for 4 hours at the ratio indicated, performed using technical triplicates. The data are presented as a representative of violin-plot distribution (right) at the ratio indicated where each point represents an individual data points (right) of 3 independent experiments. Statistical analysis was performed by Unpaired student t-tests. ns, nonsignificant.

4.3 25-HC and 27-HC inhibits the metabolism and cytotoxicity of NK-92 cells

Next, I continued to investigate the mechanism by which IL-2-induced metabolic regulation and augmented effector functions of NK-92 cells. As mentioned above, our research has shown that 25-HC and 27-HC are a potent inhibitor for NK metabolism and function in primary murine and human NK cells. Therefore, experiments were designed to investigate the impact of oxysterols on metabolic profile and effector function of NK92 cells.

NK-92 cell were cultured in IL-2 (100 IU/ml) and in the presence or absence of 25-HC (2 μM) or 27-HC (5 μM) for 18 hours and then stained with viability stain (Zombie Near IR) to examine whether NK-92 cell viability and size is affected.

The data shows that oxysterol treatment did not impact on the basic cell biology of NK92 cells, in term of the viability and cell size. The cells treated with oxysterols remained viable and exhibited a similar cell size compared to the control NK-92 cells. **(Figure 4.6).** To investigate the consequences of 25-HC and 27-HC treatment in NK-92 cell metabolism, the Seahorse Metabolic flux analyzer was used to investigate metabolic flux through OxPhos and glycolysis in NK-92 cells cultured in the presence or absence of 25-HC or 27-HC and plated at 150,000/well for 18 hours. The result shows there were no changes in the glycolytic level for either oxysterol (**Figure 4.7),** but NK-92 OxPhos was strongly inhibited in presence of either 25HC or 27HC **(Figure 4.8)**. Pre-treatment of NK92 cellls with either 25-HC or 27-HC significantly inhibited NK-92 cytotoxicity **(Figure 4.9)** in the absence of any changes in granzyme B expression **(Figure 4.10).**

Importantly, these changes in metabolic profile corresponded to a clear

reduction in NK-92 cytotoxicity towards K562 target cells. However, it was clear that 25-HC exhibited greater effect in inhibiting NK-92 cytotoxicity capacity and OxPhos level than 27-HC.

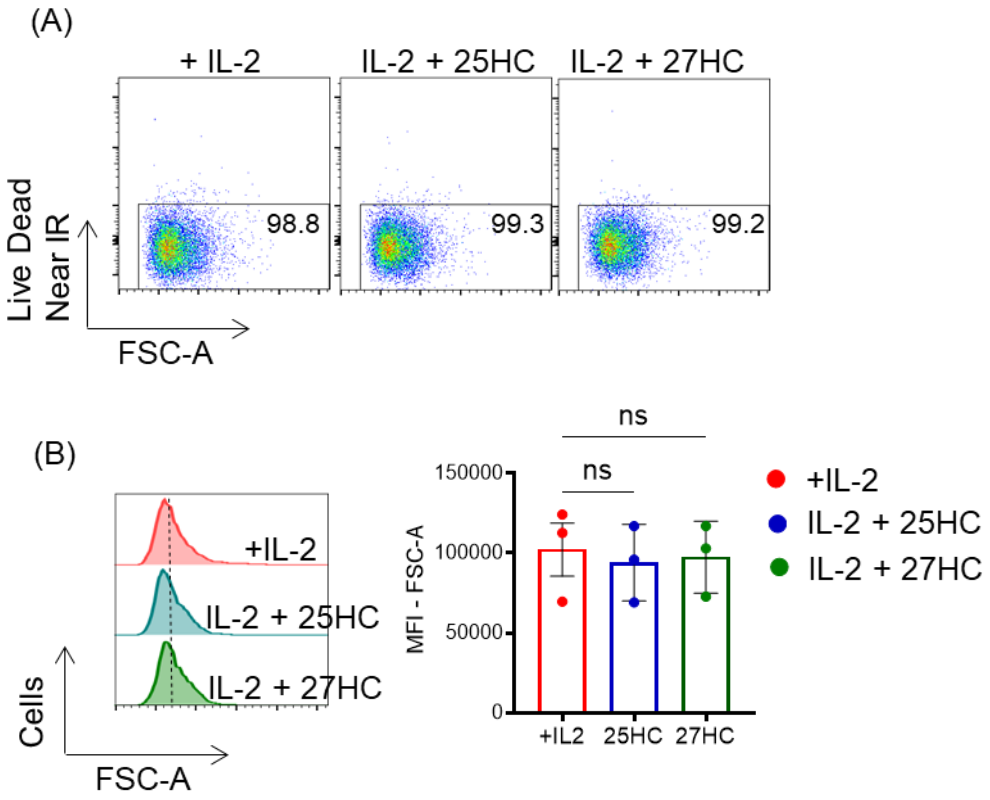

Figure 4.6: Pre-treatment with 25-HC or 27-HC does not affect NK-92 viability or cell size.

NK-92 cells were cultured with human recombinant IL-2 (100 IU/ml) in the presence or absence of 25-HC (2 μM) or 27-HC (5 μM) for 18 hours before analysis by flow cytometry. (A) The viability of NK-92 cells was determined by staining the cells with Live Dead (Near IR). (B) NK-92 cells were analyzed for FSC-A as a measure of cell size. Data shown are represented as representative (A and B, left) or mean +/- SEM (B, right) of 3 independent experiments. Data were analyzed using one-way ANOVA with a Dunnett-test for multiple comparisons compared to +IL-2. ns, nonsignificant.

(A)

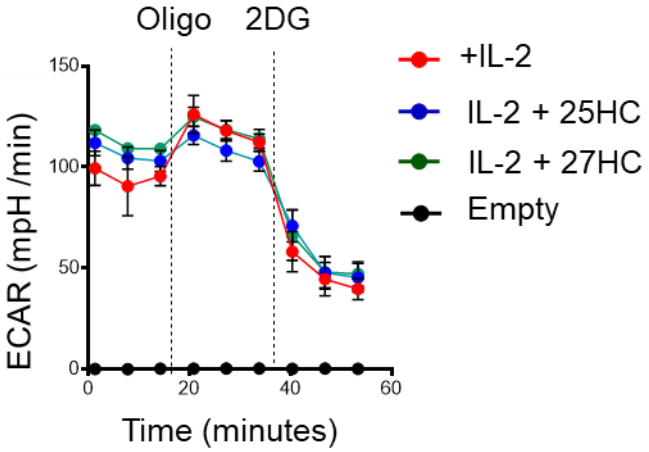
Oligo
2DG
+IL-2
IL-2 + 25HC
IL-2 + 27HC
Empty
ECAR (mpH /min)
150
100
50
0
0
20
40
60
Time (minutes)

(B)

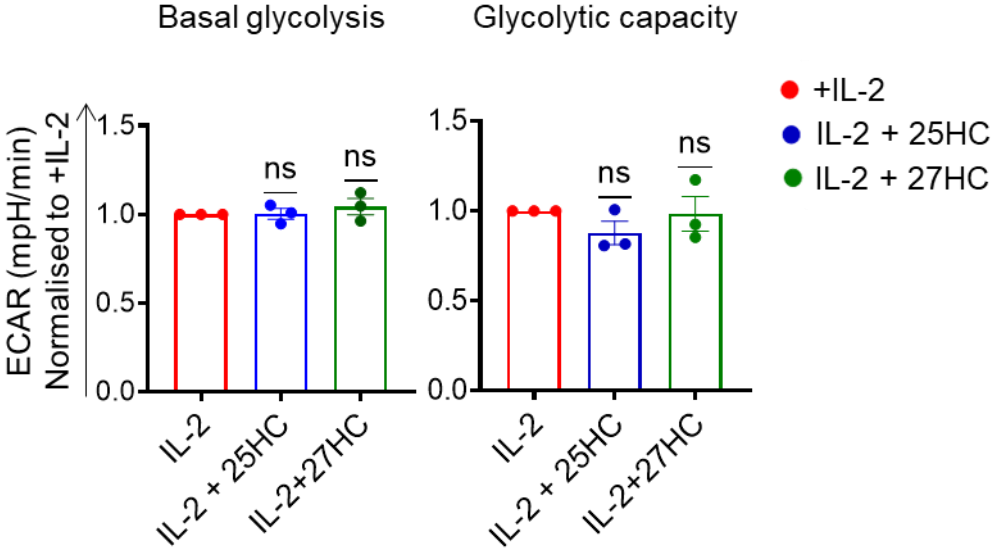
Basal glycolysis
Glycolytic capacity
+IL-2
IL-2 + 25HC
IL-2 + 27HC
ECAR (mpH/min)
Normalised to +IL-2
1.5
1.0
0.5
0.0
ns
ns
ns
ns
IL-2
IL-2 + 25HC
IL-2+27HC
IL-2
IL-2 + 25HC
IL-2+27HC

Figure 4.7: Pre-treatment with 25-HC and 27-HC for 18 hours does not affect glycolysis level in NK-92 cells.

NK-92 cells were cultured with IL-2 (100 IU/ml) and then were treated with or without 25-HC (2 μ) or 27-HC (5μM) for 18 hours. NK-92 cells were then plated at 150,000/well in seahorse media and analyzed using the seahorse extracellular flux analyzer measuring basal extracellular acidification rate (ECAR) and rates after sequential injection of oligomycin (2μM), and 2-deoxyglucose (30mM). The data are presented as a representative ECAR trace (A) or mean +/- SEM (B) of 4 independent experiments. Statistical analysis was performed using a one sample t test against a hypothetical value of 1. ns, nonsignificant.

(A)

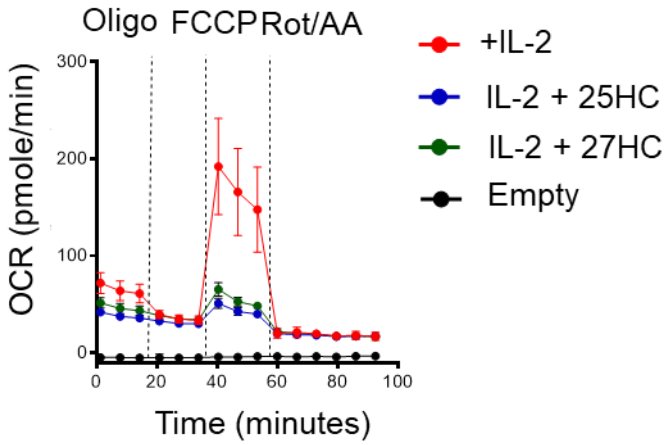
Oligo
FCCP
Rot/AA
OCR (pmole/min)
300
200
100
0
0
20
40
60
80
100
Time (minutes)
+IL-2
IL-2 + 25HC
IL-2 + 27HC
Empty

(B)

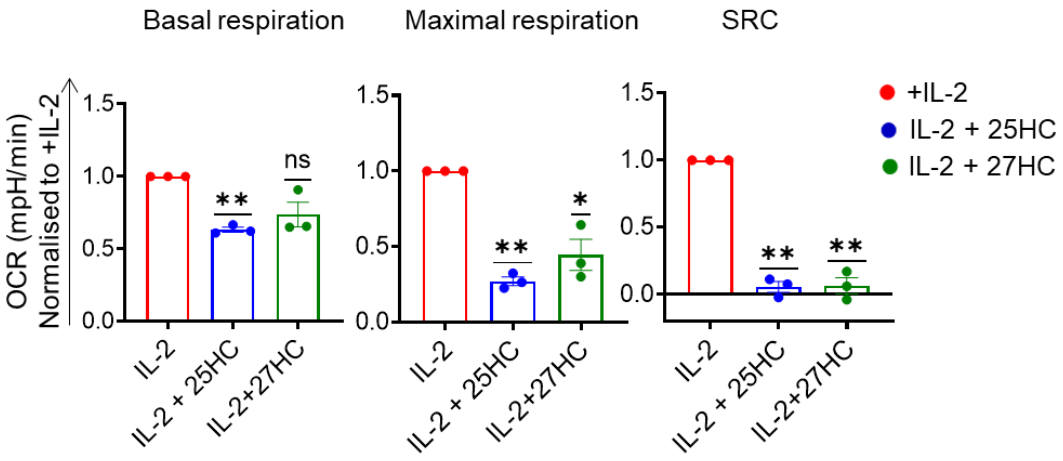
Basal respiration
Maximal respiration
SRC
OCR (mpH/min)
Normalised to +IL-2
1.5
1.0
0.5
0.0
**
ns
*
**
**
**
IL-2
IL-2 + 25HC
IL-2+27HC
+IL-2
IL-2 + 25HC
IL-2 + 27HC

Figure 4.8: NK-92 OxPhos is inhibited by 18 hours pre-treatment with 25-HC and 27-HC.

NK-92 cells were cultured with IL-2 (100 IU/ml) and then were treated with or without 25-HC (2 μ) or 27-HC (5μM) for 18 hours. NK-92 cells were then plated at 150,000/well in seahorse media and analysed using the seahorse extracellular flux analyzer measuring basal oxygen consumption rate (OCR) and rates after sequential injection of oligomycin (2μM), FCCP (0.5μM) and Rotenone/Antimycin A (0.1 /4μM). The data are presented as a representative OCR trace (A) or mean +/- SEM (B) of 4 independent experiments. Statistical analysis were performed using a one sample t test against a hypothetical value of 1. ns, nonsignificant.

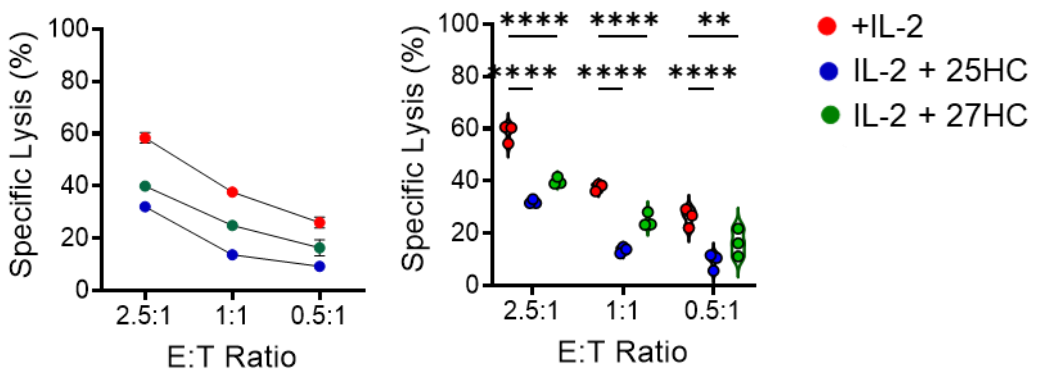

Figure 4.9: 25-HC and 27-HC pre-treatment for 18 hours inhibits NK-92 cell cytotoxicity.

NK-92 cells were cultured with and without 25-HC (2 μM) or 27-HC (5 μM) for 18 hours prior to assessing *in vitro* cytotoxicity against K562 tumour cells and. Cytotoxicity measured following co-incubation of NK-92 cell with K562 target cells for 4 hours (with no 25-HC or 27-HC present) at the ratios indicated, performed using technical triplicates. The data are presented as violin plot distributions (right) at the ratio indicated where each point represents an individual data points (right) of 3 independent experiments. Data were analyzed using a two-way ANOVA with Dunnett-test for multiple comparison compared to +IL-2. ns, nonsignificant; **p<0.01, ****p<0.0001.

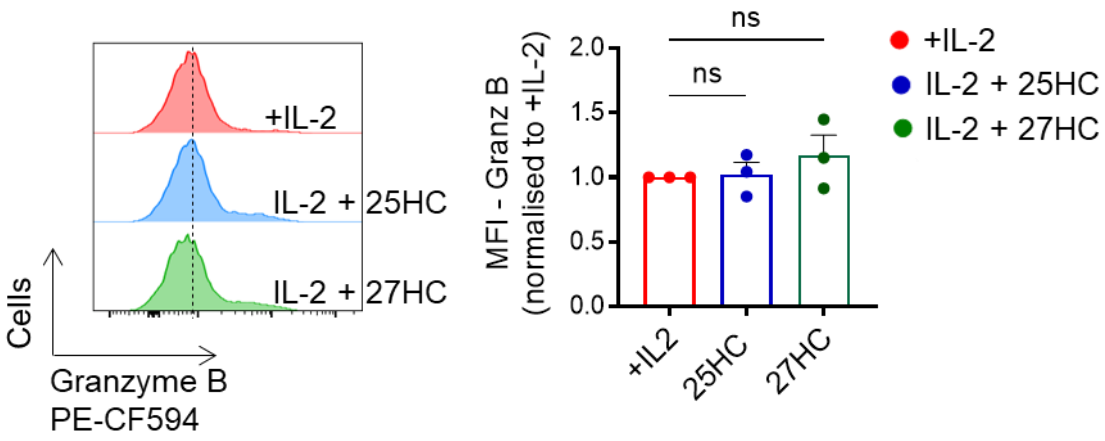

Figure 4.10: 25-HC and 27-HC pre-treatment for 18 hours does not affect granzyme B expression in NK-92 cells.

NK-92 cells were cultured with and without 25-HC (2 μM) or 27-HC (5 μM) for 18 hours prior to analysing by flow cytometry. The level of granzyme B was determined by staining the cells with PE-CF594. Data are presented as a representative histogram or mean + /- S.E.M of 3 independent experiments. Data were analyzed using one-way ANOVA with Dunnett-test for multiple comparison compared to +IL-2. The level of granzyme B in treated cells is relative to + IL-2. MFI; mean fluorescence intensity; ns, nonsignificant.

4.4 Pharmacological inhibition of SREBP activation does not phenocopy oxysterol treatment of NK92 cells.

The transcriptional factor SREBP activation is important for the metabolic reprogramming of cells that respond to IL-2 in murine and human NK cells. I next investigated whether the observed effects of oxysterols on NK92 metabolism and function are likely to be due to the inhibition of SREBP activation. First, I investigated whether NK92 express Srebp1 and/or Srebp2 isoforms. NK92 cells were analyzed for mRNA expression by qRT-PCR to quantify the expression of established SREBP 1 and SREBP 2. The data shows that both SREBP 1 and SREBP 2 were expressed in NK-92 cells, however, SREBP 1 level is expressed at a higher level than SREBP 2 (**Figure 4.11).** To confirm that oxysterols do in fact inhibit SREBP activation in NK92 cells I made use of a quantitative proteomics dataset that was generated comparing NK92 cells +/- 18 hours 25HC treatment. This Quantitative proteomic data **(Figure 4.12)** showed that 25-HC treated NK92 cells have significant decreases in the expression proteins that are known Srebp target genes, including 3-hydroxy-3-methylglutaryl-CoA synthase 1 *(HMGCS)*, stearoyl-CoA desaturase *(SCD),* and 3-hydroxy-3-methylglutaryl-CoA reductase *(HMGCR).* Interestingly, 25HC treatment does not lead to widespread changes in protein expression levels as might be the case if 25HC had triggered an ER stress response for instance [161]. In fact, the data show that only 7 proteins were significantly increased in expression and only 45 proteins significantly decreased in expression **(Figure 4.12)**. When the differentially regulated proteins were submitted to the Reactome pathway analysis program, the top pathway identified was the activation of Srebp control genes. **(Figure 4.13)**.

Next, I disrupted the SREBP processing and activation in a different way by using the pharmacological inhibitors PF429242, which is a potent inhibitor of Site-1-Protease (S1P) and so prevents the cleavage and release of N-terminal DNA binding fragment of SREBP **(Figure 4.14).** I confirmed that PF429242 treatment led to decreased expression of the SREBP target genes HMGCS1 and SCD1 **(Figure 4.15)**. The outcomes of these manipulations on NK-92 cells' metabolism and function were then measured.

NK-92 cells were cultured in IL-2 (100UI/ml) and in the presence or absence of 25-HC (2 μM) or PF49242 (10 mM) for 18 hours and then stained with viability stain (Zombie Near IR) to examine whether NK-92 cell viability and size is affected. The result shows that the treatment of 25-HC and PF49242 did not impact basic cell biology in terms of viability and cell size. Treated cells are still viable and have the same cell size compared with control NK-92 **(Figure 4.16).**

The impact of PF49242 treatment on NK-92 cell metabolism, was assessed using the Seahorse Metabolic flux analyzer to measure metabolic flux through OxPhos and glycolysis. NK-92 cells were cultured in the presence or absence of 25-HC or PF49242 and plated at 150,000/well for 18 hours. The data show that PF49242 treatment did not affect rates of glycolysis nor that of OXPHOS **(Figure 4.17 and 4.18)** in NK 92 cells. While the impact of 25HC on OXPHOS in this set of experiment was not as strong as seen previously (Figure 4.9), there was a clear and significant decrease observed for the spare respiratory capacity of the NK92 cells **(Figure 4.19).** Overall, the data argue that PF429242-treatment does not affect the metabolism of NK92 cells.

The next important experiment was to ascertain if inhibition of SREBP using PF429242 would be sufficient to repress the cytotoxicity of NK92 cells. While 25HC treatment significantly inhibited NK 92 killing of K562 target cells the NK92 cells treated with PF429242 were able to kill these target cells as efficiently as untreated NK92 cells (Figure 4.20). Neither 25HC nor PF429242 treatment affected the expression of granzyme B expression **(Figure 4.20).** To summarize, this data argues that oxysterol inhibit NK-92 cytotoxicity through mechanism independent of SREBP, because inhibition of SREBP activation through a distinct mechanism, through the use of PF429242, did not affect NK92 cytotoxicity.

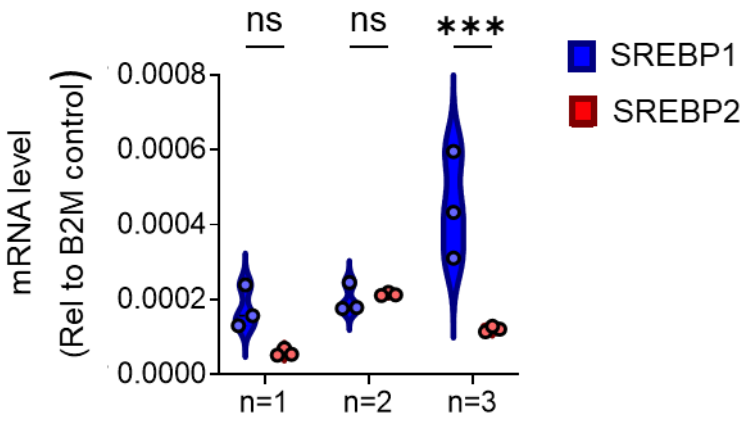

Figure 4.11: SREBP1 level is expressed at a higher level than SREBP2 level in NK92 cells.

NK-92 cells were cultured with IL-2 (100 IU/ml) for 18 hours. Cells were lysed and analysed for qRT-PCR for Sterol regulatory element binding protein 1 and 2 (SREBP1 and SREBP2) mRNA level. Data is normalized to the level of the control gene B2M and presented relative to mRNA level in B2M. The data are presented as violin plot distributions at 3 independent experiments indicated where each point represents a technical replicate. Statistical analysis was performed by Two -way ANOVA with a Sidak for multiple comparison. ns, nonsignificant; ***p<0.001.

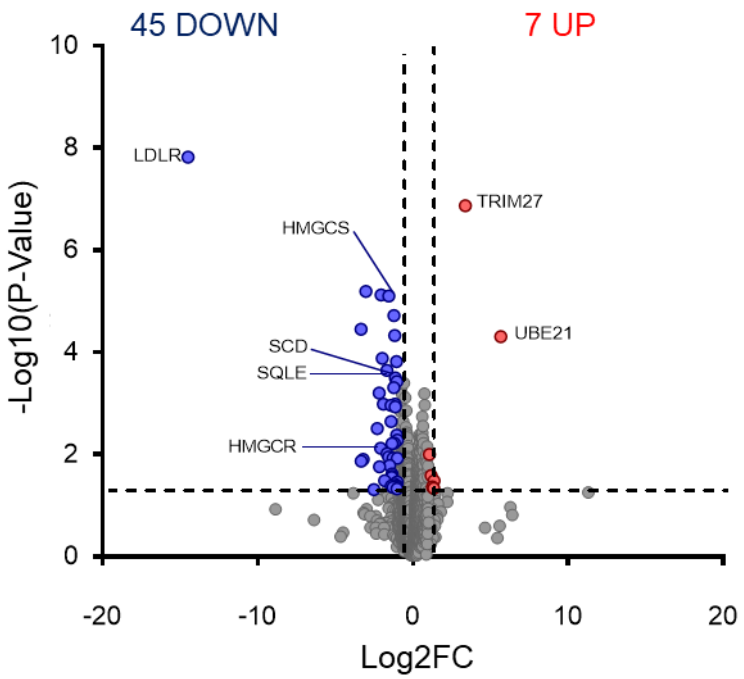

Figure 4.12: Pre-treatment with 25-HC decreased the protein expression of SREP target genes in NK-92 cells.

NK-92 cells were cultured with and without 25-HC (2 μM) for 18 hours before preparing the cells for proteomic analysis. Data are volcano plot from proteomic data and these points indicates different proteins that display both large magnitude fold-change (x-axis) and high statistical significance (-log10 of p value, y axis). Dashed horizontal line shows the p values cutoff, the two vertical dashed lines indicate down (blue)/up (red) regulated proteins.

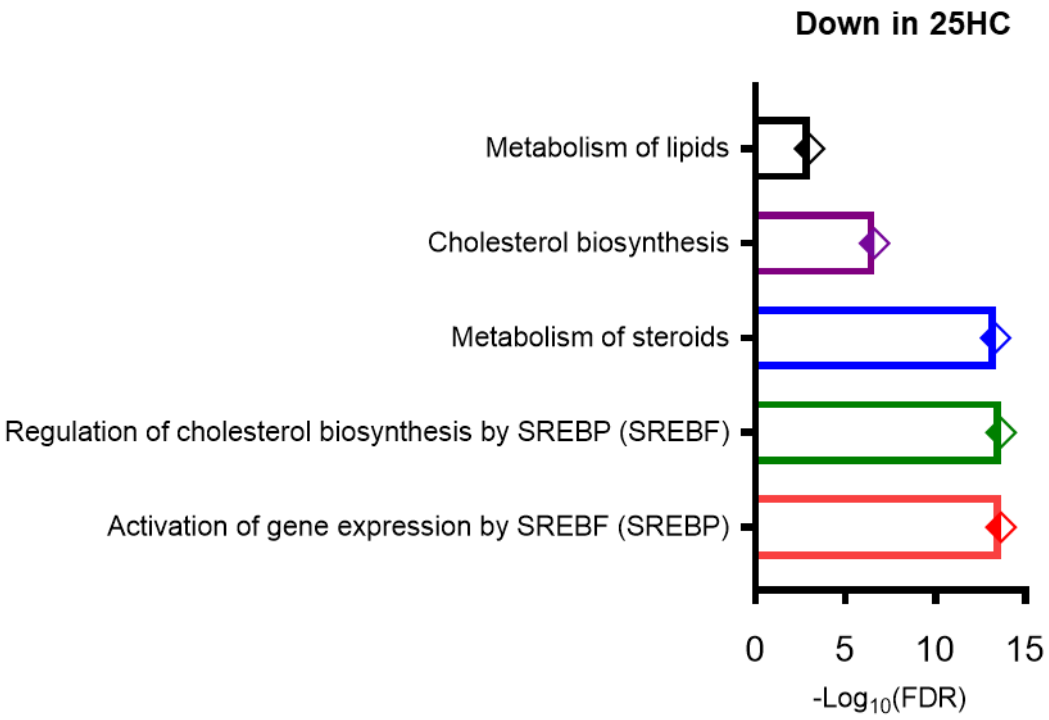

Figure 4.13: The SREBP control genes was the top pathway significantly enriched in 25-HC-treated NK-92 cells.

Bar plot of differentially regulated proteins from quantitative proteomic data submitted to Reactome pathway analysis program. The names of the pathways are shown on the vertical axis, and the bars on the horizontal axis represent the – the p-value adjusted by FDR (false discovery rate).

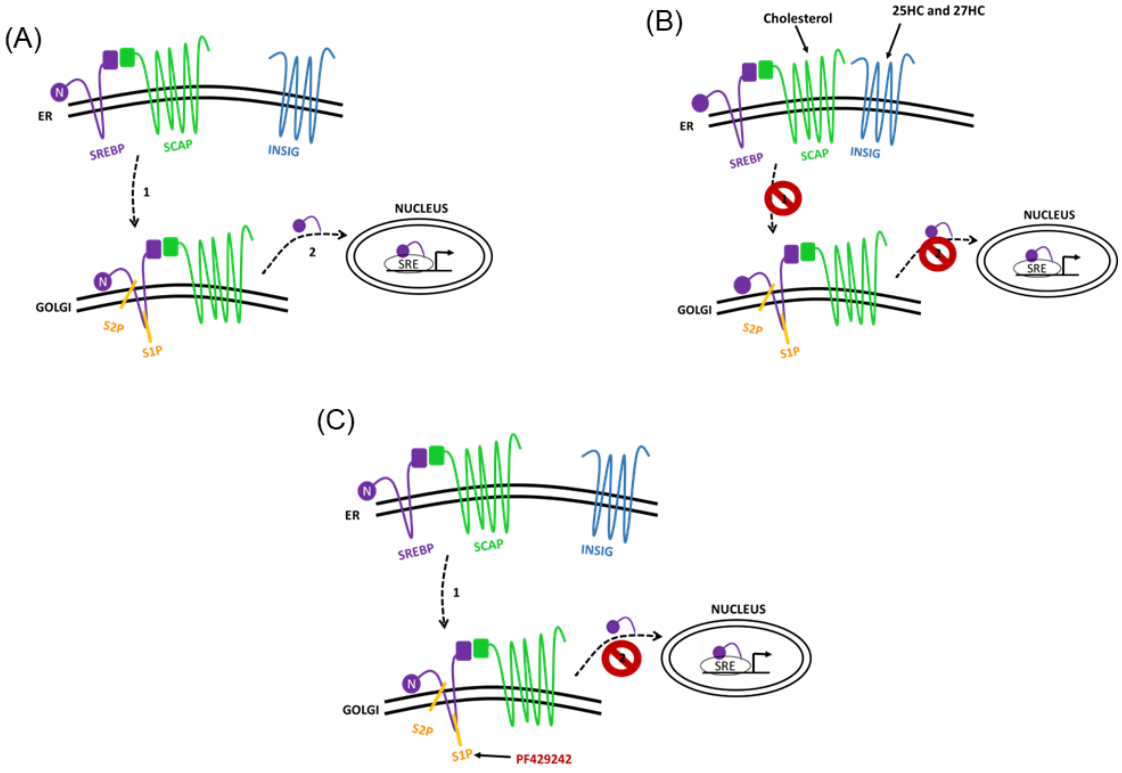
(A)
ER
SREBP
SCAP
INSIG
1
GOLGI
S2P
S1P
2
NUCLEUS
SRE
(B)
Cholesterol
25HC and 27HC
ER
SREBP
SCAP
INSIG
GOLGI
S2P
S1P
NUCLEUS
SRE
(C)
ER
SREBP
SCAP
INSIG
1
GOLGI
S2P
S1P
PF429242
NUCLEUS
SRE

Figure 4.14: Schematic illustration the mechanism of SREBP activation and inhibition.

(A) When sterol is depleted in the cells, Sterol regulatory element-binding protein (SREBP) is transported by SREBP cleavage activating protein (SCAP) to Golgi apparatus, where two proteases, Site-1 protease (S1P) and Site-2 protease (S2P), act sequentially to release the N-terminal, transcriptionally active domine, to allow nuclear translation. (B) High level of cholesterol or its derivations (25HC and 27HC) will influence the interaction between SREBP, SCAP and Insulin induce gene (INSIG) in the ER membrane and thereby preventing SREBP processing and activation. (C) PF-429242 is potent inhibitor of S1P and prevent release of N-terminal of SREBP leading to reduce level of SREBP target genes.

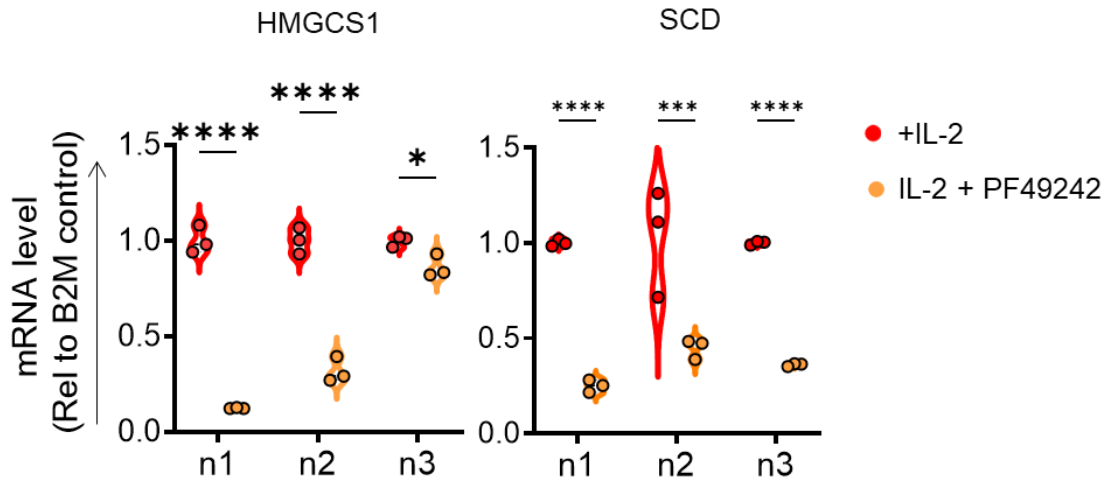

Figure 4.15: PF49242-treated cells reduce expression of SREBP target genes.

NK-92 cells line were cultured with IL-2 (100 UI/ml in the presence or absence of PF49242 (10 mM) (SREBP inhibitors) for 18 hours. Cells were lysed and analysed for qRT-PCR for mRNA level of Hydroxymethylglutaryl-CoA Synthase 1 (HMGCS1), and stearoyl-CoA desaturase (SCD). The data are normalized to the level of the B2M control gene and presented relative to mRNA level in IL-2-replete cells. Data are violin-plot distribution at 3 independent experiments indicated where each point represents a technical replicate. Statistical analysis was performed by Two -way ANOVA with a Sidak for multiple comparison. ns, nonsignificant; *p<0.01, ***p<0.001, ****p<0.0001.

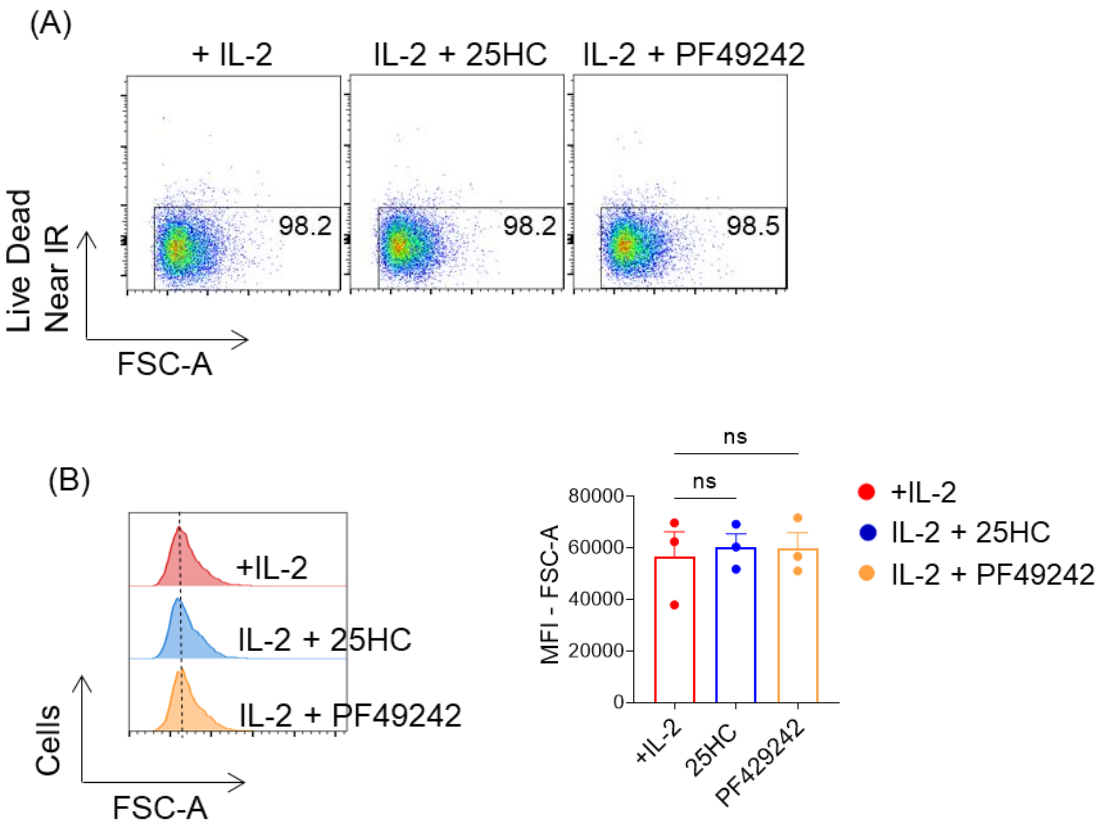

Figure 4.16: Pre-treatment with PF49242 does not affect NK-92 viability or cell size.

NK-92 cells were cultured with human recombinant IL-2 (100 U/ml) in the presence or absence of 25-HC (2 μM) or PF49242 (10 mM) for 18 hours before analysis by flow cytometry. (A) The viability of NK-92 cells was determined by staining the cells with Live Dead (Near IR). (B) NK-92 cells were analyzed for FSC-A as a measure of cell size. The data shown are presented as representative (A and B, left) or mean +/- SEM (B, right) of 3 independent experiments. Data were analyzed using one-way ANOVA with a Dunnett-test for multiple comparisons compared to +IL-2. ns, nonsignificant.

(A)

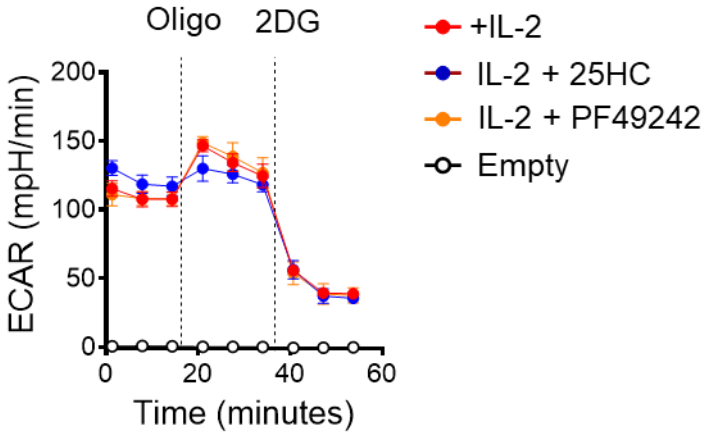
Oligo
2DG
+IL-2
IL-2 + 25HC
IL-2 + PF49242
Empty
ECAR (mpH/min)
200
150
100
50
0
0
20
40
60
Time (minutes)

(B)

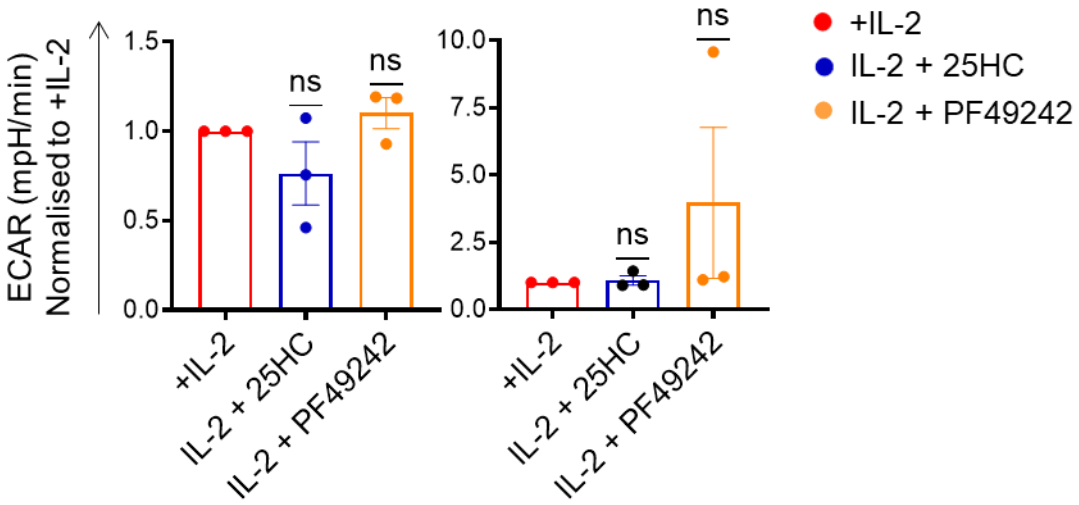
Basal glycolysis
Glycolytic capacity
ECAR (mpH/min)
Normalised to +IL-2
1.5
1.0
0.5
0.0
ns
ns
10.0
7.5
5.0
2.5
0.0
ns
+IL-2
IL-2 + 25HC
IL-2 + PF49242
+IL-2
IL-2 + 25HC
IL-2 + PF49242

Figure 4.17: Pre-treatment with PF49242 does not change the rate of glycolysis in NK92 cells.

NK-92 cells were cultured with IL-2 (100 IU/ml) and then were treated with or without of 25-HC (2 μM) or PF49242 (10 mM) for 18 hours. NK-92 cells were then plated at 150,000/well in seahorse media and analyzed using the seahorse extracellular flux analyzer measuring basal extracellular acidification rate (ECAR) and rates after sequential injection of oligomycin (2μM), and 2-deoxyglucose (30mM). The data shown are presented as a representative ECAR trace (A) or mean +/- SEM (B) of 3 independent experiments. Statistical analysis was performed using a one sample t test against a hypothetical value of 1. ns, nonsignificant.

(A)

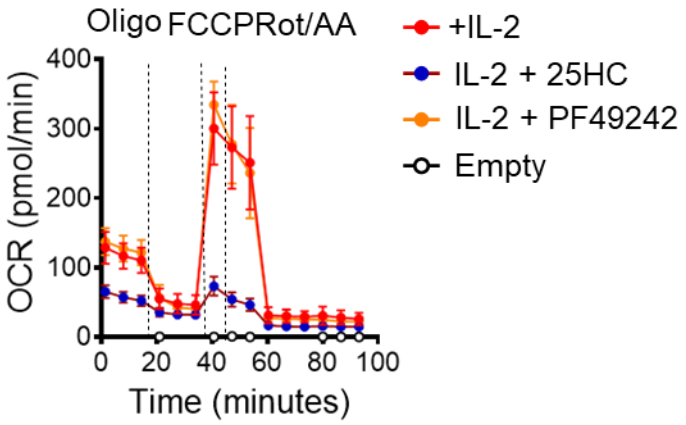
Oligo
FCCP
Rot/AA
+IL-2
IL-2 + 25HC
IL-2 + PF49242
Empty
OCR (pmol/min)
400
300
200
100
0
0
20
40
60
80
100
Time (minutes)

(B)

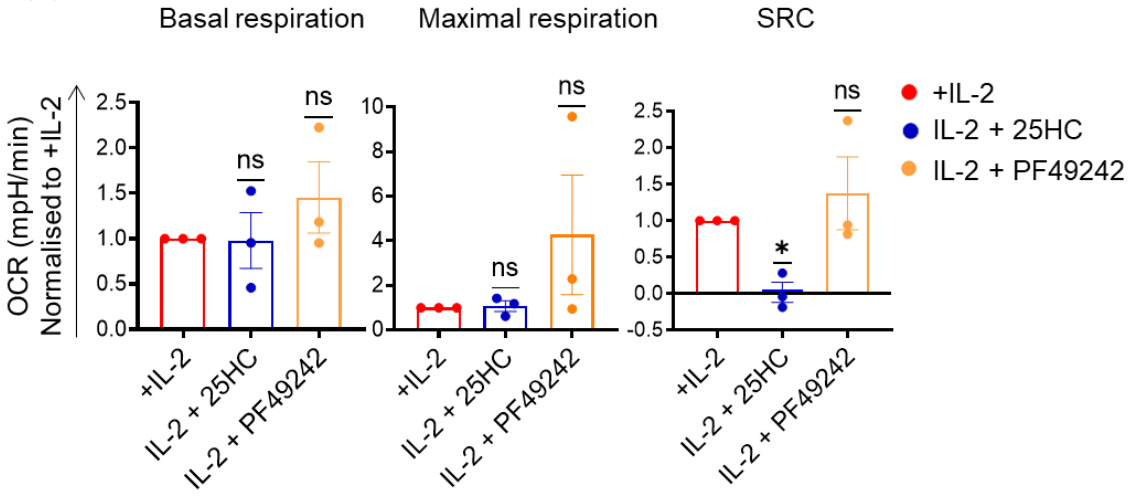
Basal respiration
Maximal respiration
SRC
OCR (mpH/min)
Normalised to +IL-2
ns
ns
ns
ns
ns
*
+IL-2
IL-2 + 25HC
IL-2 + PF49242

Figure 4.18: NK-92 OxPhos is not inhibited by 18 hours pre-treatment with PF49242.

NK-92 cells were cultured with IL-2 (100 IU/ml) and then were treated with or without 25-HC (2 μM) or PF49242 (10 mM) for 18 hours. NK-92 cells were then plated at 150,000/well in seahorse media and analysed using the seahorse extracellular flux analyzer measuring basal oxygen consumption rate (OCR) and rates after sequential injection of oligomycin (2μM), FCCP (0.5μM) and Rotenone/Antimycin A (0.1 /4μM). The data shown are presented as a representative OCR trace (A) or mean +/- SEM (B) of 3 independent experiments. Statistical analysis were performed using a one sample t test against a hypothetical value of 1. ns, nonsignificant. *$p<0.05$.

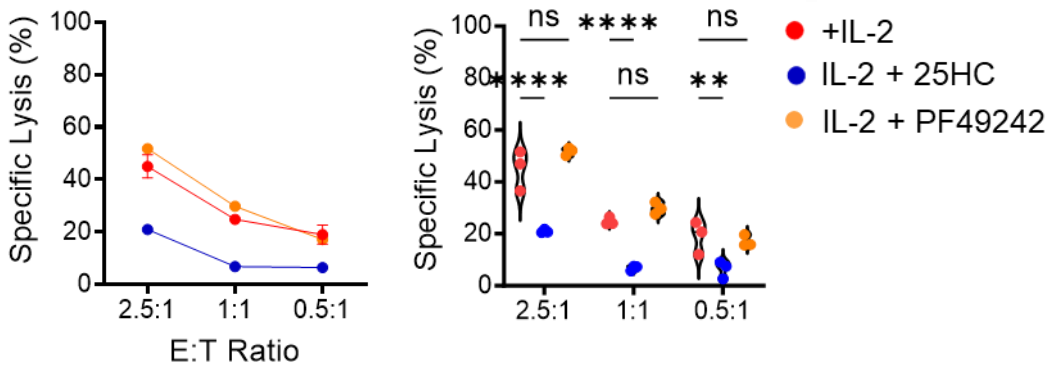

Figure 4.19: PF49242 pre-treatment for 18 hours does not inhibit NK-92 cell cytotoxicity.

NK-92 cells were cultured with and without 25-HC (2 μM) or PF49242 (10 μM) for 18 hours prior to assessing *in vitro* cytotoxicity against K562 tumour cells and. Cytotoxicity measured following co-incubation of NK-92 cell with K562 target cells for 4 hours (with no PF49242 present) at the ratios indicated, performed using technical triplicates. The data are presented as a representative (left) of violin-plot distribution at the ratio indicated where each point represents an individual data points (right) of 3 independent experiments. Data were analyzed using a two-way ANOVA with Dunnett-test for multiple comparison compared to +IL-2. ns, nonsignificant; **p<0.01, ****p<0.0001.

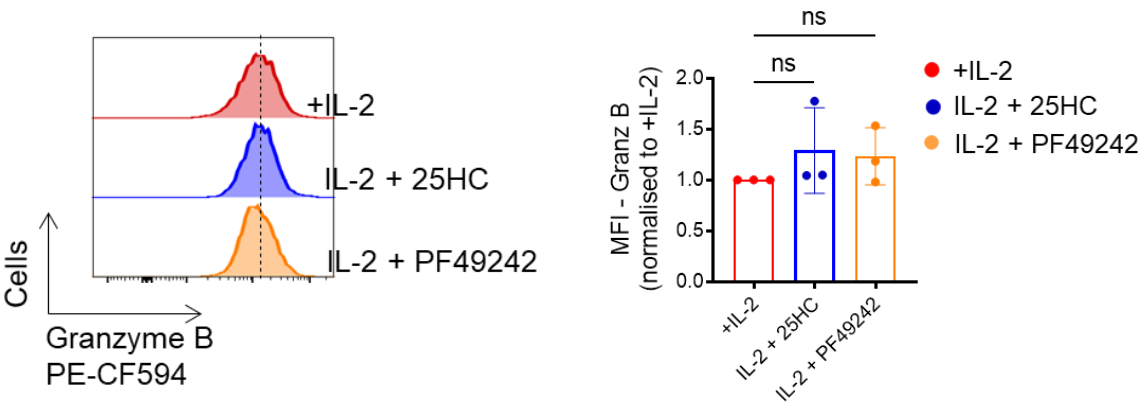

Figure 4.20: PF49242 pre-treatment for 18 hours does not affect granzyme B expression in NK-92 cells.

NK-92 cells were cultured with and without 25-HC (2 μM) or PF49242 (10 mM) for 18 hours prior to analysing by flow cytometry. The level of granzyme B was determined by staining the cells with anti-granzyme B PE-CF594. Data are a representative histogram or mean + /- S.E.M of 3 independent experiments. Data were analyzed using one-way ANOVA with Dunnett-test for multiple comparison compared to +IL-2. The level of granzyme B in treated cells is relative to + IL-2. MFI; mean fluorescence intensity; ns, nonsignificant.

4.5 Ligation of LXR does not affect NK-92 metabolism or cytotoxicity.

In addition to acting to inhibit the activation of SREBP transcription factors, 25HC and 27HC can also act as agonists for LXR nuclear receptors **(Figure 4.21)** [154], [156]. Therefore, I questioned whether oxysterols binding and activation of LXR mediated gene expression is responsible for the observed changes in metabolism and function of NK92 cells. To test this a LXR agonist GW3965, which does not inhibit SREBP activation but activates LXR, was used. The outcomes of these manipulation on NK-92 cells metabolism and function were then measured.

NK-92 cells were cultured in IL-2 (100UI/ml) and in the presence or absence of 25-HC (2 μM) or GW3965 (2 μM) for 18 hours and then stained with viability stain (Zombie Near IR) to examine whether NK-92 cell viability and size is affected. The result shows that the treatment of 25-HC and GW3965 had no impact upon NK92 viability and cell size. Treated cells are still viable and have the same cell size compared with control NK-92 **(Figure 4.22).** To confirm that LXR agonist GW3965 does promote the expression of LXR target genes, NK-92 cells were cultured with IL-2 (100UI/ml) in the presence or absence of GW3965 (2 μM) and cells were lysed to measure the level of mRNA expression by using RT-qPCR analysis. The expression of established LXR target genes were measured; ATP binding cassette subfamily G member 1 (*ABCG1*) and fatty acid synthase (*FASN*). While there was some variability in the data acquired, overall, it supported a finding that in NK-92 cells cultured in the presence of GW3965 (2 μM) for 18 hours there was increased the expression of *ABCG1* and *FASN* **(Figure 4.23).**

To investigate the consequences of 25-HC and GW3965 treatment in NK-92 cell metabolism, the Seahorse Metabolic flux analyzer was used to investigate metabolic flux through OxPhos and glycolysis in NK-92 cells cultured in the presence or absence of 25-HC or GW3965 and plated at

150,000/well for 18 hours. The data shows that GW3965 treatment did not affect rates of glycolysis **(Figure 4.24)** and OxPhos in NK 92 cells, but the previously observed reduction in OXPHOS in response to this 25-HC treatment was clearly evident **(Figure 4.25).**

The next important question was whether GW3965 treatment affects NK-92 cytotoxicity. The data clearly shows that when NK92 cells were treated with this LXR agonist there was no effect on NK92 cytotoxicity **(Figure 4.26)** nor the expression of granzyme B compared with the control of NK-92 cells **(Figure 4.27).** To summarize, this data strongly argues that effects of oxysterols on NK92 metabolism and function are not due to LXR activation.

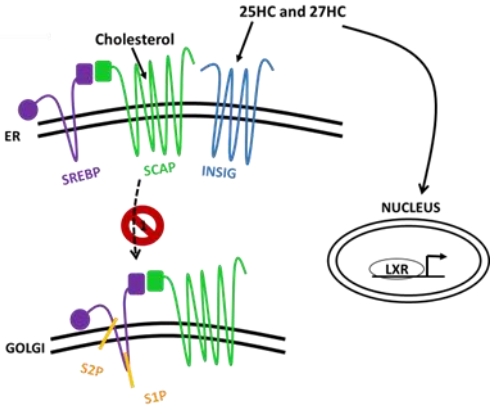

Figure 4.21: Schematic illustration the mechanism of oxysterols act as endogenous ligand for LXR nuclear receptor.

25HC and 27HC are naturally endogenous ligands for Live X Receptor (LXR). This binding activates LXR and induces gene expression that controlling lipid homeostasis. This function of these oxysterols is separate to their actions to inhibit the translocation of SREBP/SCAP to Golgi apparatus, an essential step for SREBP activation.

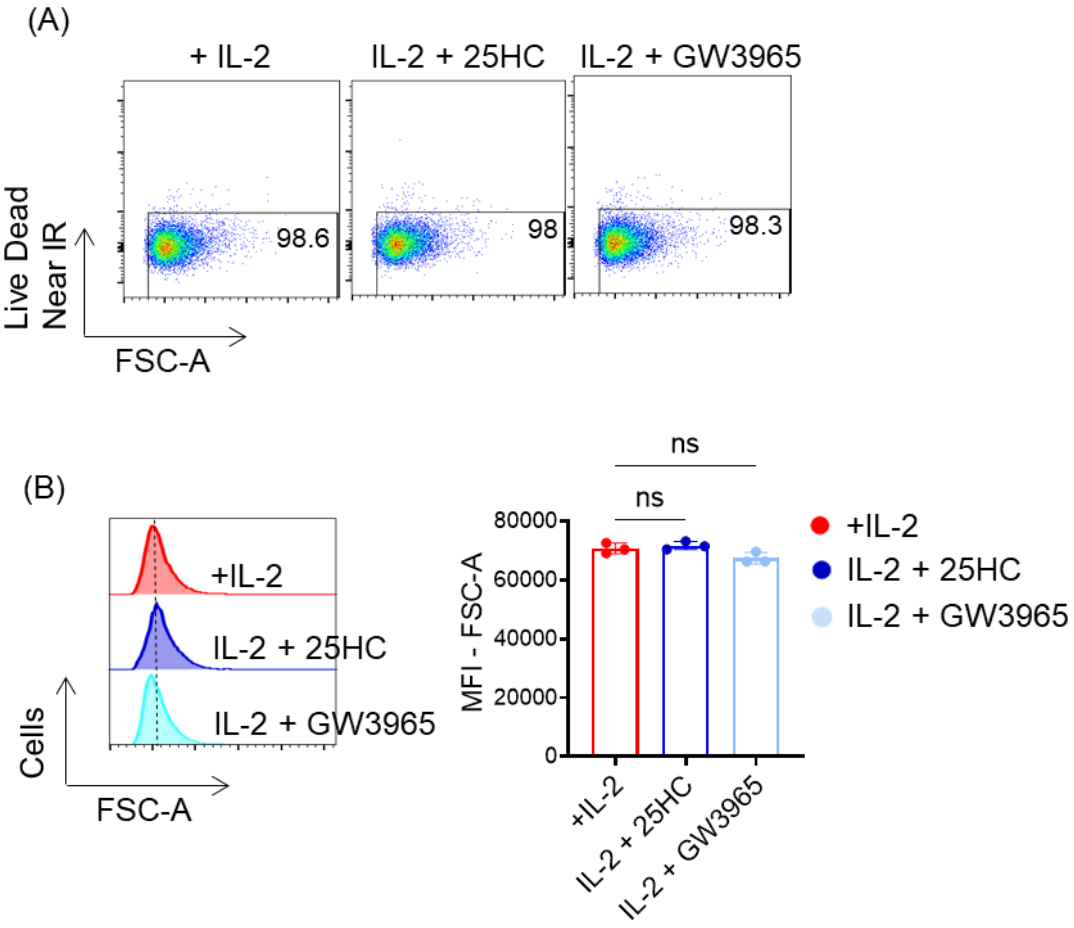

Figure 4.22: NK92 viability and size is not affected by 18 hours pre-treatment with GW3965.

NK-92 cells were cultured with human recombinant IL-2 (100 U/ml) in the presence or absence of 25-HC (2 μM) or GW3965 (2 μM) for 18 hours before analysis by flow cytometry. (A) The viability of NK-92 cells was determined by staining the cells with Live Dead (Near IR). (B) NK-92 cells were analyzed for FSC-A as a measure of cell size. Data shown are representative (A and B, left) or mean +/- SEM (B, right) of 3 independent experiments. Data was analyzed using one-way ANOVA with a Dunnett-test for multiple comparisons compared to +IL-2. ns, nonsignificant.

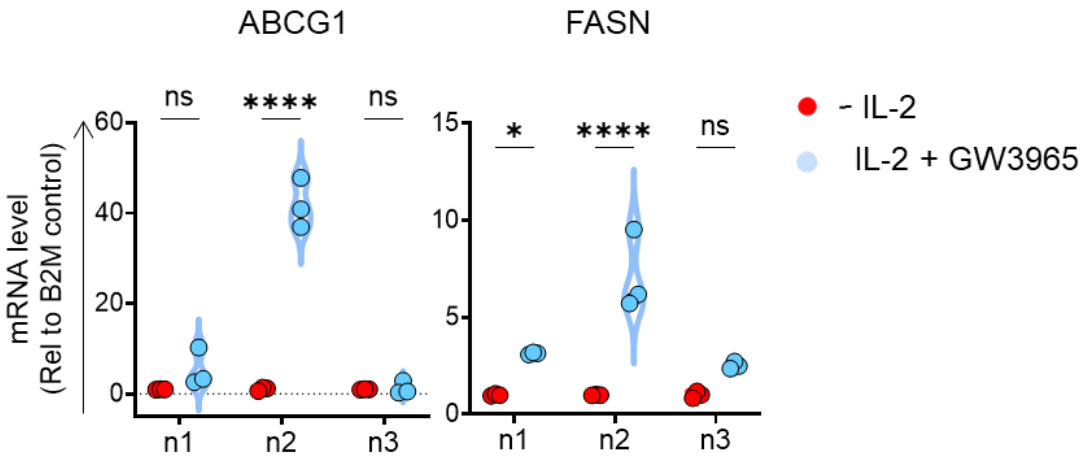

Figure 4.23: GW3965-treated cells induce expression of LXR target genes.

NK-92 cells line was cultured with IL-2 (100 UI/ml in the presence or absence of GW3965 (2 μM) (LXR agonist) for 18 hours. Cells were lysed and analysed for qRT-PCR for mRNA level of ATP binding cassette subfamily G member 1 (ABCG1) mRNA levels, and Fatty acid synthase (FASN. Data is normalized to the level of the B2M control gene and presented relative to mRNA level in IL-2-replete cells. Data are violin-plot distribution at 3 independent experiments indicated where each point represents a technical replicate. Statistical analysis was performed by Two -way ANOVA with a Sidak for multiple comparison. ns, nonsignificant; *p<0.01, ***p<0.001, ****p<0.0001.

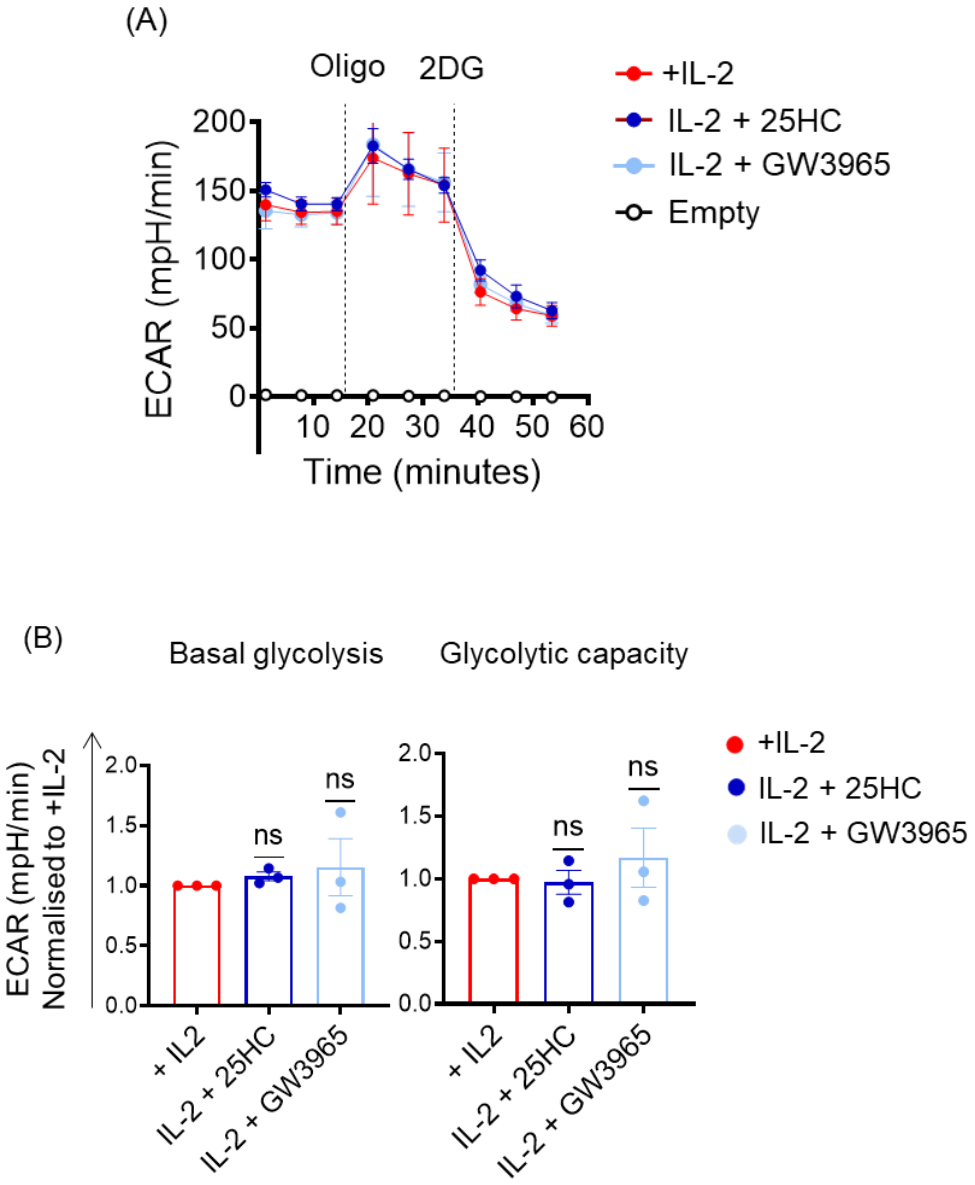
(A)
Oligo
2DG
+IL-2
IL-2 + 25HC
IL-2 + GW3965
Empty
ECAR (mpH/min)
200
150
100
50
0
10 20 30 40 50 60
Time (minutes)
(B)
Basal glycolysis
Glycolytic capacity
ECAR (mpH/min)
Normalised to +IL-2
2.0
1.5
1.0
0.5
0.0
ns
ns
ns
ns
+ IL2
IL-2 + 25HC
IL-2 + GW3965
+IL-2
IL-2 + 25HC
IL-2 + GW3965

Figure 4.24: NK-92 glycolysis is not affected by 18 hours pre-treatment with GW3965.

NK-92 cells were cultured with IL-2 (100 IU/ml) and then were treated with or without of 25-HC (2 μM) or GW3965 (2 μM) for 18 hours. NK-92 cells were then plated at 150,000/well in seahorse media and analyzed using the seahorse extracellular flux analyzer measuring basal extracellular acidification rate (ECAR) and rates after sequential injection of oligomycin (2μM), and 2-deoxyglucose (30mM). Data shown are a representative ECAR trace (A) or mean +/- SEM (B) of 3 independent experiments. Statistical analysis was performed using a one sample t test against a hypothetical value of 1. ns, nonsignificant.

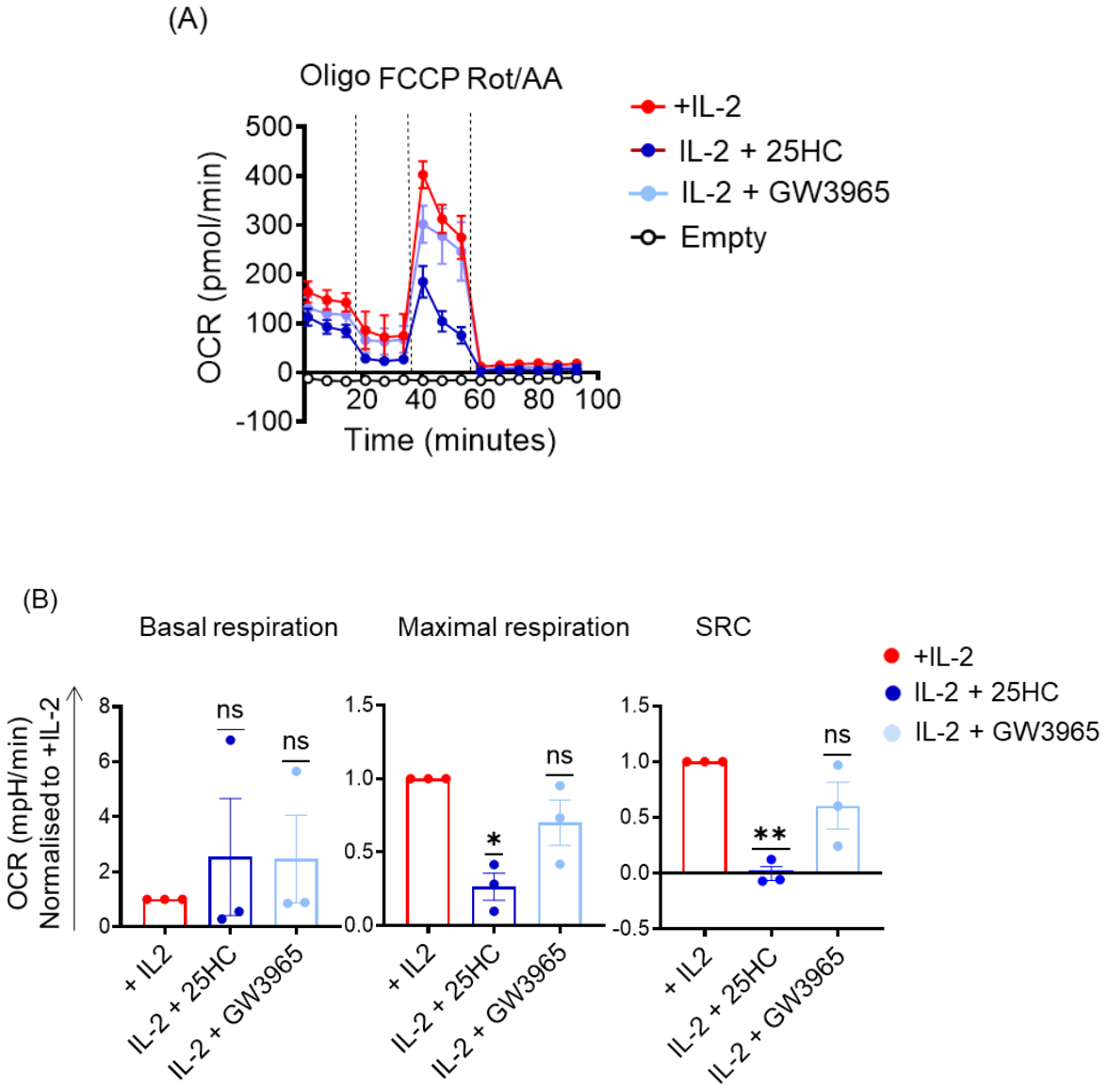
(A)
Oligo FCCP Rot/AA
OCR (pmol/min)
500
400
300
200
100
0
-100
20
40
60
80
100
Time (minutes)
+IL-2
IL-2 + 25HC
IL-2 + GW3965
Empty
(B)
Basal respiration
Maximal respiration
SRC
OCR (mpH/min)
Normalised to +IL-2
ns
ns
*
ns
**
ns
+IL2
IL-2 + 25HC
IL-2 + GW3965

Figure 4.25: NK-92 OxPhos is not inhibited by 18 hours pre-treatment with GW3965.

NK-92 cells were cultured with IL-2 (100 IU/ml) and then were treated with or without 25-HC (2 μM) or GW3965 (2 μM) for 18 hours. NK-92 cells were then plated at 150,000/well in seahorse media and analysed using the seahorse extracellular flux analyzer measuring basal oxygen consumption rate (OCR) and rates after sequential injection of oligomycin (2μM), FCCP (0.5μM) and Rotenone/Antimycin A (0.1 /4μM). Data shown are a representative OCR trace (A) or mean +/- SEM (B) of 3 independent experiments. Statistical analysis was performed using a one sample t test against a hypothetical value of 1. ns, nonsignificant.

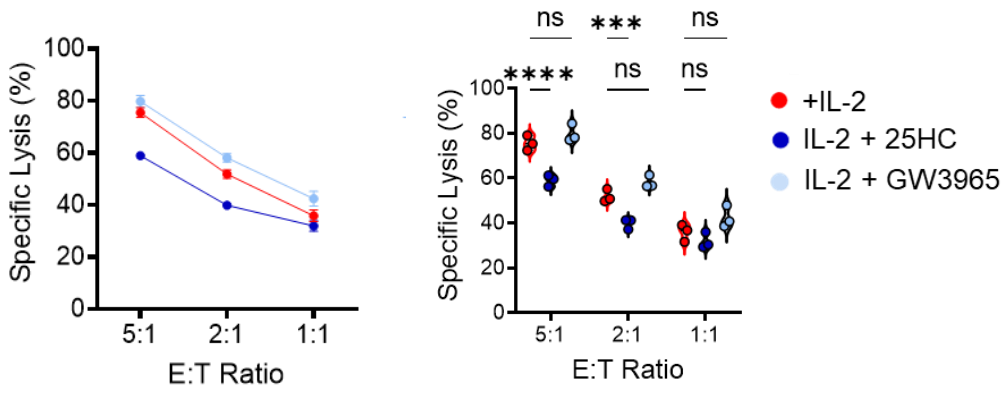

Figure 4.26: GW3965 pre-treatment for 18 hours does not inhibit NK-92 cell cytotoxicity.

NK-92 cells were cultured with and without 25-HC (2 μM) or GW3965 (2 μM) for 18 hours prior to assessing in vitro cytotoxicity against K562 tumour cells and. Cytotoxicity measured following co-incubation of NK-92 cell with K562 target cells for 4 hours (with no GW3965 present) at the ratios indicated, performed using technical triplicates. The data are presented as violin plot distributions (right) at the ratio indicated where each point represents an individual data points (right) of 3 independent experiments. Data were analyzed using a two-way ANOVA with Dunnett-test for multiple comparison compared to +IL-2. ns, nonsignificant; ***p<0.001, ****p<0.0001.

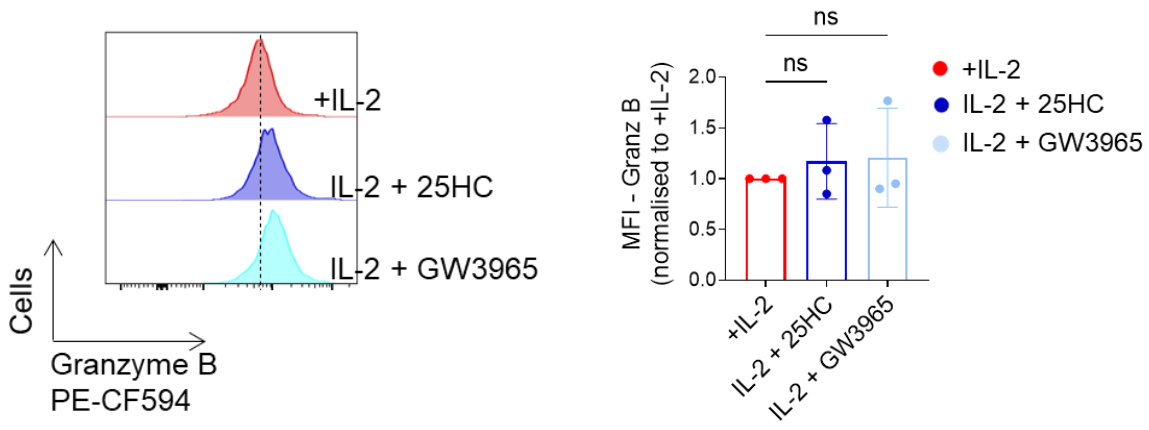

Figure 4.27: GW3965 pre-treatment for 18 hours does not affect granzyme B expression in NK-92 cells.

NK-92 cells were cultured with and without 25-HC (2 μM) or GW3965 (2 μM) for 18 hours prior to analysing by flow cytometry. The level of granzyme B was determined by staining the cells with anti-granzyme B PE-CF594. Data is a representative histogram or mean + /- S.E.M of 3 independent experiments. Data were analyzed using one-way ANOVA with Dunnett-test for multiple comparison compared to +IL-2. The level of granzyme B in rapamycin-treated cells is relative to + IL-2. MFI; mean fluorescence intensity; ns, nonsignificant.

4.6 Discussion of Chapter 4

Numerous studies have established that the mammalian target of rapamycin complex1 (mTORC1) coordinates cell growth and metabolism with environmental resources, including nutrients, and growth factors [162]. As many previous studies demonstrated cellular metabolism is integrally linked to immune cell function. Now, emerging evidence proposed that mTORC1 regulating cellular metabolism is fundamental for immunoregulatory function in immune cells [142]. In CTLs, the maintenance of high rates of glycolysis is required by glycolysis to support normal migratory patterns and effector functions [132], [144]. Previous research from the Finlay group revealed upon NK cell activation, glucose uptake, and glycolysis were elevated and that mTORC1 is essential to attaining this elevated glycolysis.I Also, directly limiting glycolytic rate is inhibited IFN-γ production and expression of granzyme B [142]. The group showed that mTORC1-mediated metabolism supports normal NK cell proinflammatory function in murin NK cells [142]. On other hand, we have found that rapamycin treatment of human NK cells from PBMC does not have a significant effect on metabolism and function [151]. This is in contrast to what we have seen in murine NK cells. Herein, we aimed to investigate whether signaling through mTORC1 is required for regulating NK-92 metabolism and cytotoxicity. The data presented in this chapter demonstrates that the use of rapamycin, a selective inhibitor for mTORC1, significantly inhibited OxPhos levels without affecting glycolytic rate. Consequently, this inhibition led to impaired NK-92 cytotoxicity. In the preceding chapter, inhibition of NK-92 cytotoxicity was observed when OxPhos was inhibited, yet glycolysis remained unaffected. However, similar metabolic conditions were observed with rapamycin treatment, which did not correlate with a decline in cytotoxicity. Considering these findings collectively, it is suggested that the inhibition of OxPhos alone

may not be solely responsible for the effect on NK-92 cytotoxicity; other underlying factors may be at play. [163], [164]. A similar pattern of results was obtained in human NK cell from PBMC in our lab, human NK stimulated by cytokines causes metabolic changes leading to increase glycolytic rates and OxPhos level. Nevertheless, Il-2-induced glycolysis is dependent on mTORC1, but OxPhos level is not inhibited by rapamycin. $CD56^{brigh}$ NK cells induce robust expression of CD69, activating receptor NKp44 and death ligand TRAIL in response to cytokines. However, all these responses were not inhibited by rapamycin. Additionally, rapamycin does not affect on granzyme B upregulation in $CD56^{brigh}$ NK cells [151]. In the context of the metabolic demands for cytotoxicity, there is a need for a more nuanced or balanced examination of whether glycolysis, OxPhos (or possibly both) are essential.

Even though IL-2 signaling is fundamental for expansion, development, and NK-92 cytotoxicity, the signaling pathways mediated by IL-2 are fully understood [163]. IL-2 could induce the expression of various genes, and these genes are triggered by multiple signaling pathways, one of them is Janus - activated kinase (Jak) - signal transducers and activators of transcription (STAT) signal pathway in T and NK cells [24], [166]. A recent study presented a liquid chromatography-mass spectrometry (LC-MS) phospho-proteomic characterization of IL-2 signaling in the NK-92 cell line [163]. In the early signaling kinetics, the quantitative analysis shows that IL-2 active intracellular signaling in NK-92 cells, including both known (JAK/STAT) [165], [167] and novel (p90 ribosomal S6 kinase, RSK) family signaling pathways [163] are required for NK-92 cell proliferation. IL-2-mediated proliferation of NK-92 was demonstrated by using pharmacological inhibitors. Signaling through IL-2 does seem to depend on multiple pathways in NK-92 cells and this may be the reason why we did not affect NK-92 cytotoxicity as a consequence of mTORC1 inhibition.

Another significant metabolic regulator that is emerging to be discovered is the Sterol regulatory binding protein (SREBP) which regulates OxPhos and effector function in murine NK cells [168]. Our group previously demonstrated the important role of SREBP transcription factors in cytokine-mediated metabolic reprogramming of NK cells and this role was independent of their conventional role in promoting the genes involved in fatty acid and cholesterol synthesis [168]. 25HC has been shown previously to inhibit murine and human NK cell effector responses [168]. More recently, work by others in the lab have shown that 27HC is also a potent inhibitor of SREBP activation in murine NK cells and of NK cell cytotoxicity (unpublished data). 27HC has also been shown to inhibit SREBP activation in hepatic cells previously [169]. The result of this chapter is show that 25-HC and 27-HC inhibit OxPhos rates in NK92 cells and significantly reduce NK-92 cytotoxicity capacity. However, the impact of 25-HC on cytotoxicity and OxPhos levels was greater than that of 27-HC. Interestingly, the data show that oxysterols inhibit NK-92 cytotoxicity through a mechanism independent of SREBP, because inhibition of SREBP activation through a distinct mechanism, using PF429242, did not affect NK92 cytotoxicity. This is a novel finding that highlights that oxysterols can inhibit NK cells cytotoxicity through multiple mechanisms.

The quantitative proteomic data in this report shows a successful decrease in SREBP target gene protein expression. Further analysis was done using the Reactome pathway analysis program which showed the activation of SREBP control genes is the top pathway identified. Considering that 25HC and 27HC can have multiple effects on a cell an alternative approach was used to inhibit the activation of SREBP in NK92 cells using the pharmacological inhibitor of site-1-protease (S1P) called PF429242. The activity of S1P is required for the cleavage of membrane

bound SREBP to generate the active transcription factor. This data argues that inhibition of SREBP is not sufficient to inhibit NK 92 cell metabolism or indeed NK92 cytotoxicity. Remarkably, the proteomic analysis revealed a noteworthy alteration in the level of the Low-density lipoprotein receptor (LDLR) due to 25-HC treatment, a change directly linked to cholesterol uptake [170]. Numerous studies have demonstrated that LXR not only facilitates cholesterol elimination but also regulates LDL uptake to maintain cholesterol homeostasis. LXR achieves this by impeding the LDLR pathway through the transcriptional activation of Idol (inducible degrader of the LDLR), an E3 ubiquitin ligase that initiates the ubiquitination of the LDLR's cytoplasmic domain, thereby marking it for degradation. [170]. As previously stated, 25-HC functions as an agonist for LXR, suggesting that it may exert control over cholesterol uptake by decreasing LDLR levels.

Common properties between 25-HC, 27-HC, and other oxysterols is that they can act as Liver X receptor (LXR) agonists [171]. Numerous studies show that signaling through LXR leads to regulating immune cell functions. For instance, in primary human $CD4^+$ T cells, it was demonstrated the role of LXR-regulated metabolic processes in controlling plasma membrane lipids (cholesterol and glycosphingolipids), which significantly influence T cell immune signaling and function [172]. The evidence indicates that LXR activity primes macrophages for an induced response. However, when the cell encounters a bacterial challenge, the activation of LXR produces anti-inflammatory effects. [173]. A similar pattern of result was obtained in Monocyte-derived dendritic cells (MDDCs) [174]. LXR activation has been shown to induce and inhibit cytokine release by dendritic cells. MDDCs are differentiated in the presence of LXR agonists before stimulation with TLR ligands releases more chemokines and cytokines and reveals enhanced capacity to elicit CD4+ T cell proliferation [174]. Therefore, it was considered if LXR ligation

could contribute to the inhibitory effects of 25-HC and 27-HC that were observed in NK-92 cells. To this end, NK-92 cells were treated with GW3965, a pharmacological LXR agonist that does affect SREBP activation, GW3965 induced known LXR target genes including FASN [175]. The data clearly shows that GW3965 did not affect NK-92 metabolism or cytotoxicity. Therefore, while SREBP and LXR signaling can have clear roles in controlling the metabolism and function of immune cells, the data herein show that this is not the case in NK92 cells. Taken together, the data in chapter 4 argues that oxysterols are potent inhibitors of NK92 cytotoxicity through a mechanism independent of inhibition of SREBP or activation of LXR.

Chapter 5 - A potential mechanism by which Oxysterols inhibit NK cell cytotoxicity.

5.1 Introduction

While NK-92 cells can sustain their cytotoxicity for a certain duration after IL-2 deprivation, extended clinical applications necessitate prolonged treatment with fully activated NK-92 cells to maximize disease eradication efficacy. [176], [177]. The ability to sustain the cytotoxic activity of NK-92 with exogenously administrated IL-2 is limited by accompanied toxicity [177], [178]. To overcome obstacles, IL-2-dependent NK-92 cells (NK-92CRL) were transfected with human IL-2 cDNA by particle-mediated gene transfer to generate IL-2-independent NK cell (NK-92MI), a cell line that was able to produce its IL-2 [177], [179]. Since NK-92MI were extensively studied in both *in vivo* and *in vitro* assays, additionally growing numbers of published trials used genetically chimeric antigen receptor (CAR)-transfected to NK-92MI cells in tumor immunotherapy, we decided to shift to use NK-92MI to perform further investigations about the potential mechanisms that oxysterols-mediated cytotoxicity inhibition.

5.2 Phenotypic, metabolic, and functional characterization of IL-2-independent NK-92 cell (NK-92MI)

Initial experiments were performed to confirm whether the IL-2-independent NK-92 cell (NK-92MI) has a similar phenotype as the parental NK-92 cell (NK-92CRL). Moreover, comparative studies were performed to investigate the impact of oxysterols on NK-92MI cells versus NK-92CRL with respect to metabolism and cytotoxicity. The data show NK-92MI and NK-92CRL cell lines have a similar expression profile of the majority of surface receptors and markers analysed (Table 5.1. Figure 5.1). Both cell lines are defined as $CD56^{+}CD3^{-}$ cells with high expression of granzyme B. NK-92MI express NKp44 at a higher level than NK-92CRL and did not express NKp46 **(Table 5.1, Figure 5.1)**. Other surface markers analyzed, including CD16, NKp30, FasL, and TRAIL, were not expressed in either NK-92CRL or NK-92MI cell

lines, as was expected based on the published literature [88]–[90], [114], [180]–[182] .

Next, the metabolic profile and the cytotoxicity of NK-92MI and the NK-92CRL cells were investigated and, in the presence, and absence of oxysterol 25HC and 27HC. In all experiments NK-92CRL cells were provided with recombinant IL-2 (100UI/ml) but NK-92MI cells were not given IL-2 cytokine as they are engineered to make the IL2 they require for growth, proliferation and function. NK-92CRL cells and NK-92MI cells were cultured in the presence or absence of 25-HC (2 μM) or 27-HC (5 μM) for 18 hours and then stained with viability stain (Zombie Near IR) to examine cell viability and cells size. The data shows NK-92MI cell viability **(Figure 5.2),** and cell size **(Figure 5.3)** are not affected as we treated the cells with 25-HC and 27-HC, as was the case for NK-92CRL cells cultured with IL-2 (100mUI/ml). To investigate the consequences of 25-HC and 27-HC treatment in NK-92MI cell metabolism, the Seahorse Metabolic flux analyzer was used to investigate metabolic flux through OxPhos and glycolysis in NK-92MI cells and of NK-92CRL cells (plus IL-2) were cultured in the presence or absence of 25-HC or 27-HC and plated at 150,000/well for 18 hours. The data shows no changes in the glycolytic level for either cell type cultured with 25HC or 27HC oxysterol (**Figure 5.4 and 5.6).** However, the rates of maximum respiration was strongly inhibited in the presence of either 25HC **(Figure 5.5)** or 27HC **(Figure 5.7)** and is inhibition was equivalent in NK-92MI cells and NK-92CRL (plus IL-2) cells. Next the impact of 25HC and 27HC on cytotoxicity was measured. NK92MI cells and NK-92CRL (plus IL-2) cells were pre-treated with either 25-HC (2 μM) or 27-HC (5 μM) **(Figure 5.8)** and then co-cultured with K652 target cells. Both oxysterols significantly inhibited NK92MI cell and NK-92CRL (plus IL-2) cell cytotoxicity without affecting the expression of granzyme B **(Figure 5.8-5.9).** However, the magnitude of inhibition was much greater for NK-92CRL (+IL2) cells.

Table 5.1: The level of markers expressed in both sub-clones of IL-2 dependent Nk-92 cells and IL-2 independent NK-92 cells.

Summarizing the expression level of candidate markers in NK-92 cell lines; IL-2 dependent NK-92 cells (CRL) and IL-2 independent cell lines (MI) that are involved in an immunophenotype and killing machinery; (+++) very high expression, (+) expressed, (-) not expressed.

Marker	Function	Experimental data (Figure 5.1)	
		IL-2 dependent NK-92 cells (CRL)	IL-2 independent NK-92 cells (MI)
Granzyme B	Cytotoxicity functional Molecules	+++	+++
CD3	Lineage Markers	-	-
CD56		+++	+++
CD16		-	-
FASL	Cell Death Ligand	-	-
TRAIL		-	-
NKp30	Activating receptors	-	-
NKp46		+	-
NKp44		+	+

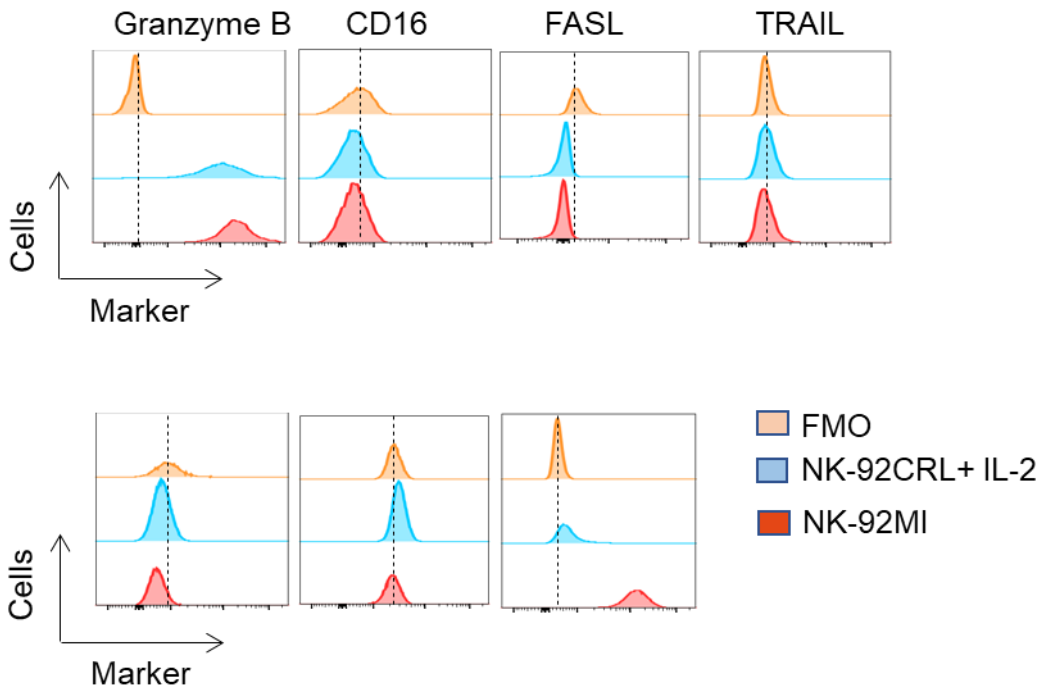

Figure 5.1: Phenotypic comparison of both sub-clones of human NK-92 cell line.

IL-2 dependent NK-92 cells (NK-92CRL) and IL-2 independent NK-92 cells (NK-92MI) were stained with fluorochrome-conjugated antibodies specific to Granzyme B, CD16, FASL, TRAIL, NKp30, NKp46, and NKp44 and analysed by flow cytometry. Representative histogram graphs display the expression level of markers in CRL cell lines (in blue), in MI cell lines (in red), and fluorescence minus one (FMO) (in orang). Data are representative of 3 independent experiments.

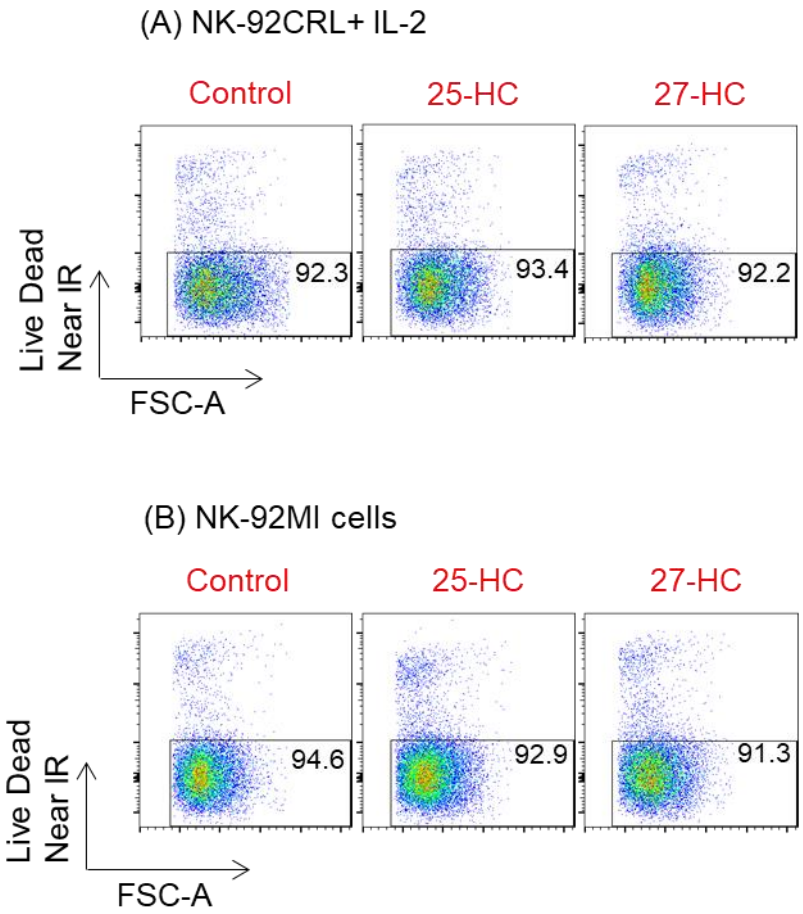

Figure 5.2: Pre-treatment with 25-HC or 27-HC does not affect the viability in NK-92MI cells.

NK-92 cell lines were cultured with (CRL cells, A) and without (MI cells, B) human recombinant IL-2 (100 U/ml) in the presence or absence of 25-HC (2 μM) or 27-HC (5 μM) for 18 hours and analysis by flow cytometry. The viability of NK-92 cell lines was determined by staining the cells with Live Dead (Near IR). Data are dot plots of IL-2 dependent NK-92 cells CRL (A) and IL-2 independent NK-92 cells MI (B) and is representative of 3 independent experiments. Data in (A) is the same as that shown in Figure 4.6.

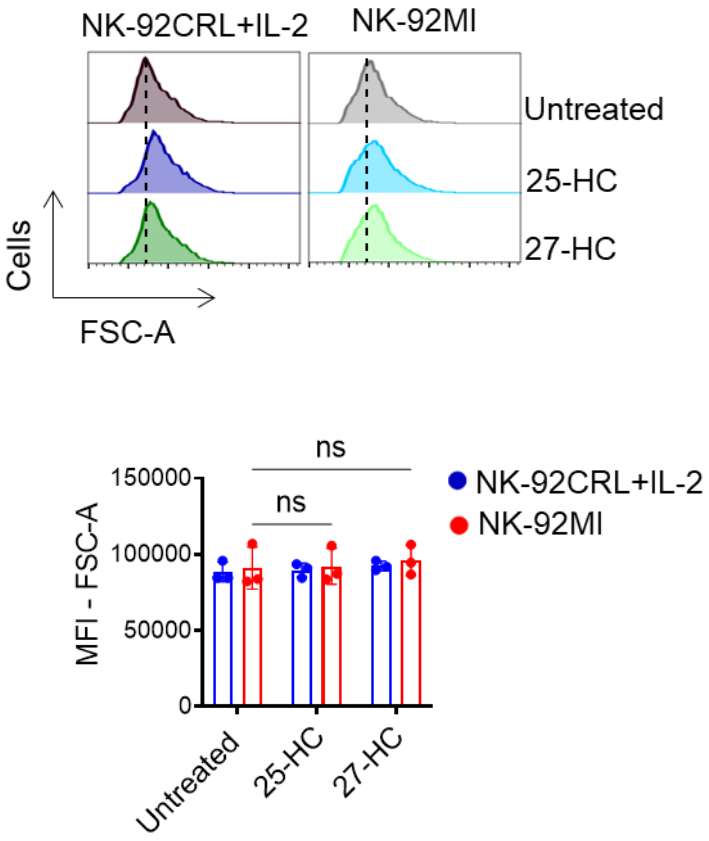

Figure 5.3: 25-HC or 27-HC pre-treatment does not affect the cell size in NK-92MI cells.

NK-92 cell lines were cultured with (CRL cells) and without (MI cells) human recombinant IL-2 (100 U/ml) in the presence or absence of 25-HC (2 μM) or 27-HC (5 μM) for 18 hours prior to analysis by flow cytometry. NK-92 cells were analyzed for FSC-A as a measure of cell size. Data shown are representative (above) or mean +/- SEM (below) of 3 independent experiments. Data was analyzed using Two-way ANOVA with a Dunnett-test for multiple comparisons compared to untreated NK-92 cells. ns, nonsignificant.

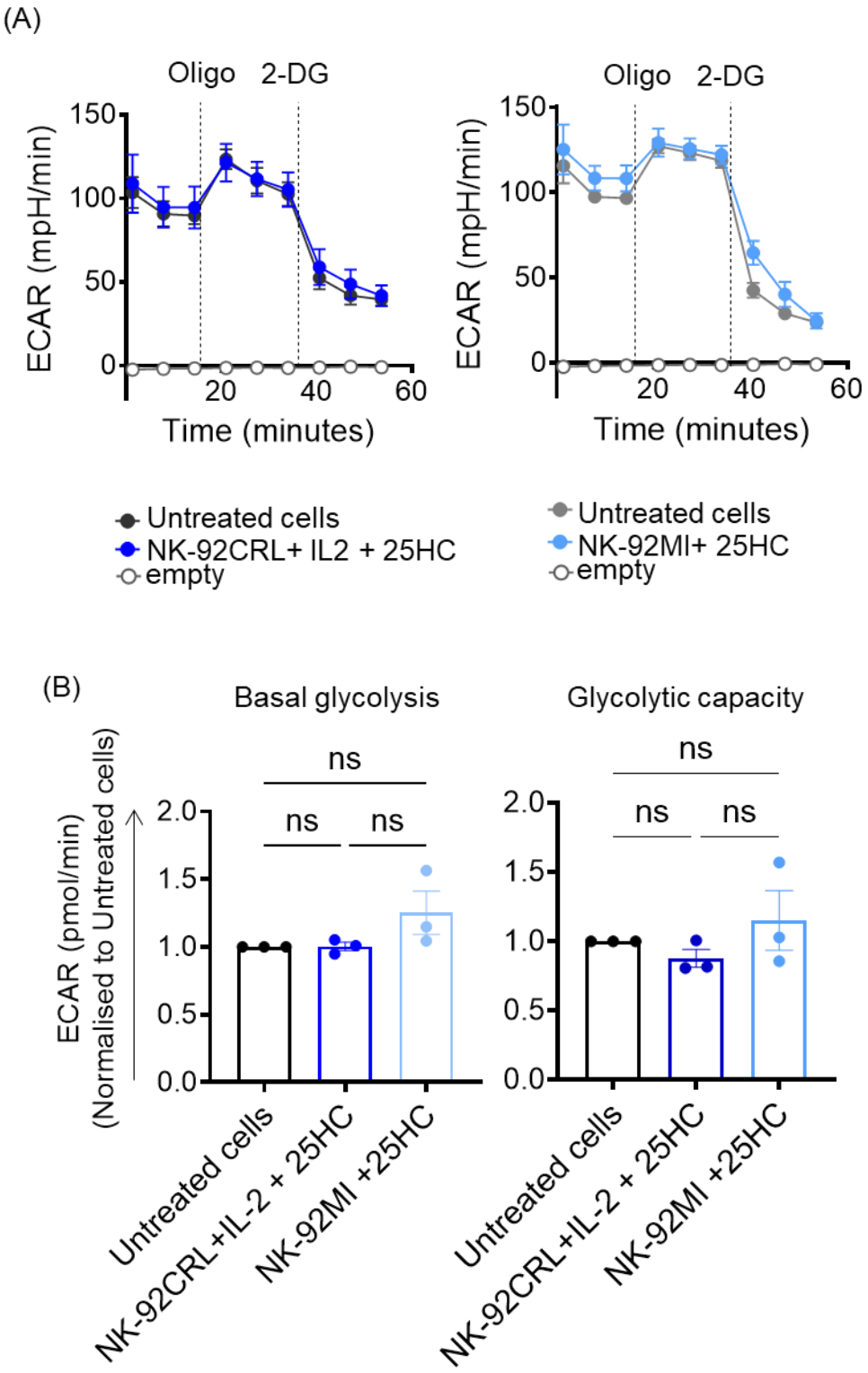
(A)
Oligo
2-DG
ECAR (mpH/min)
150
100
50
0
20
40
60
Time (minutes)
Untreated cells
NK-92CRL+ IL2 + 25HC
empty
Untreated cells
NK-92MI+ 25HC
empty
(B)
Basal glycolysis
Glycolytic capacity
ECAR (pmol/min)
(Normalised to Untreated cells)
ns
2.0
1.5
1.0
0.5
0.0
Untreated cells
NK-92CRL+IL-2 + 25HC
NK-92MI +25HC

Figure 5.4: Glycolysis is unchanged by 18 hours pre-treatment with 25-HC in NK-92MI cells like NK-92CRL cells.

NK-92 cell lines were cultured with (CRL cells) and without (MI cells) human recombinant IL-2 (100 U/ml) in the presence or absence of 25-HC (2 μM) for 18 hours. NK-92 cells were then plated at 150,000/well in seahorse media (without any 25-HC) and analyzed using the seahorse extracellular flux analyzer measuring basal extracellular acidification rate (ECAR) and rates after sequential injection of oligomycin (2μM), and 2-deoxyglucose (30mM). The data are presented as a representative ECAR trace (A) or (B) mean +/- SEM (B) of 3 independent experiments. Statistical analysis was performed using a one-way ANOVA with a Tukey-test for multiple comparisons compared to untreated NK-92 cells. ns, nonsignificant.

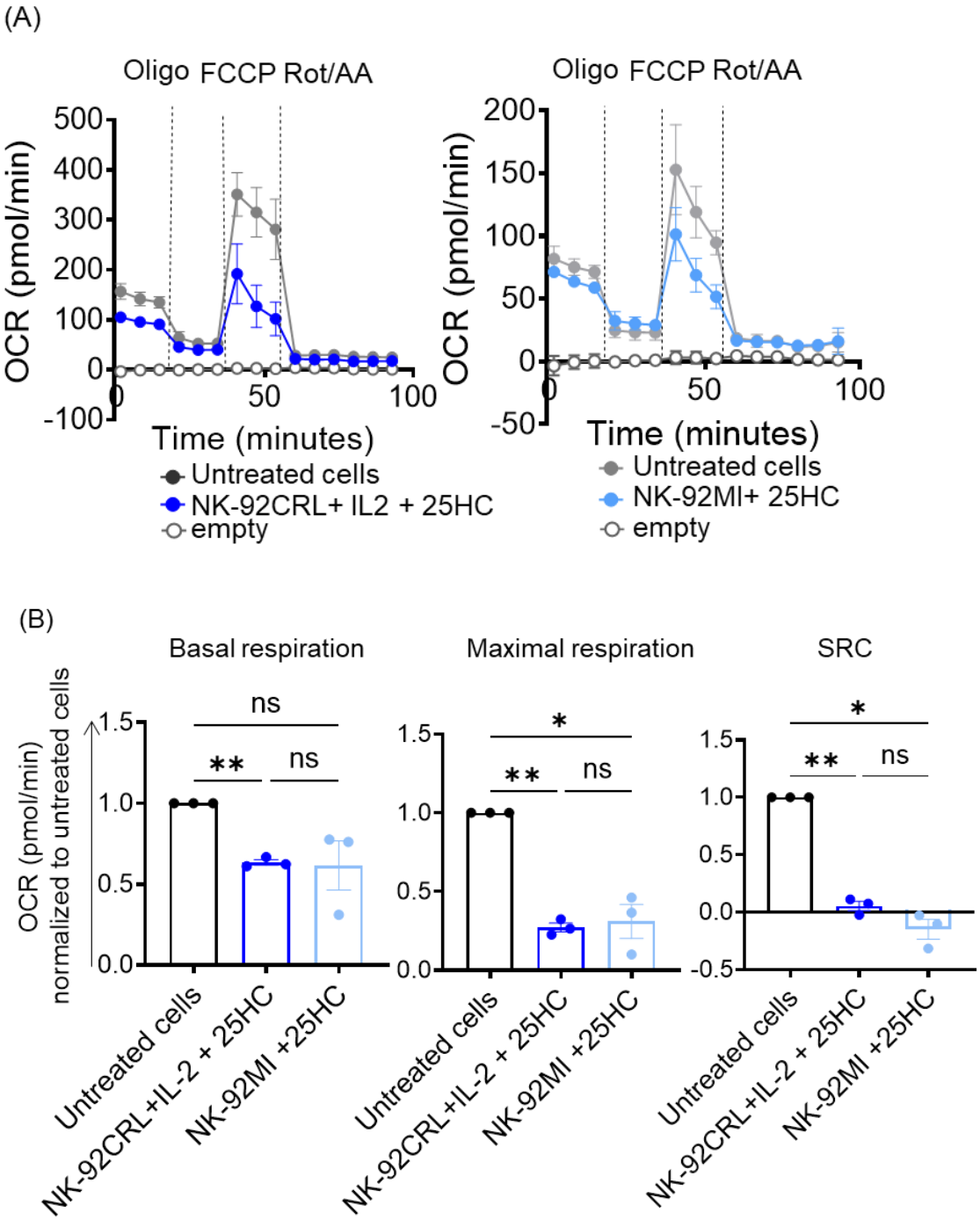

Figure 5.5: NK-92MI OxPhos is inhibited by 18 hours 25-HC pre-treatment.

NK-92 cell lines were cultured with (CRL cells) and without (MI cells) human recombinant IL-2 (100 U/ml) in the presence or absence of 25-HC (2 μM) for 18 hours. NK-92 cells were then plated at 150,000/well in seahorse media (without ant 25-HC) and analyzed using the seahorse extracellular flux analyzer measuring basal oxygen consumption rate (OCR) and rates after sequential injection of oligomycin (2μM), FCCP (0.5μM) and Rotenone/Antimycin A (0.1 /4μM). The data are presented as a representative OCR trace (A) or mean +/- SEM (B) of 3 independent experiments. Statistical analysis was performed using a one-way ANOVA with a Tukey-test for multiple comparisons compared to untreated NK-92 cells. ns, nonsignificant; *p<0.05; **P<0.01; ns, nonsignificant.

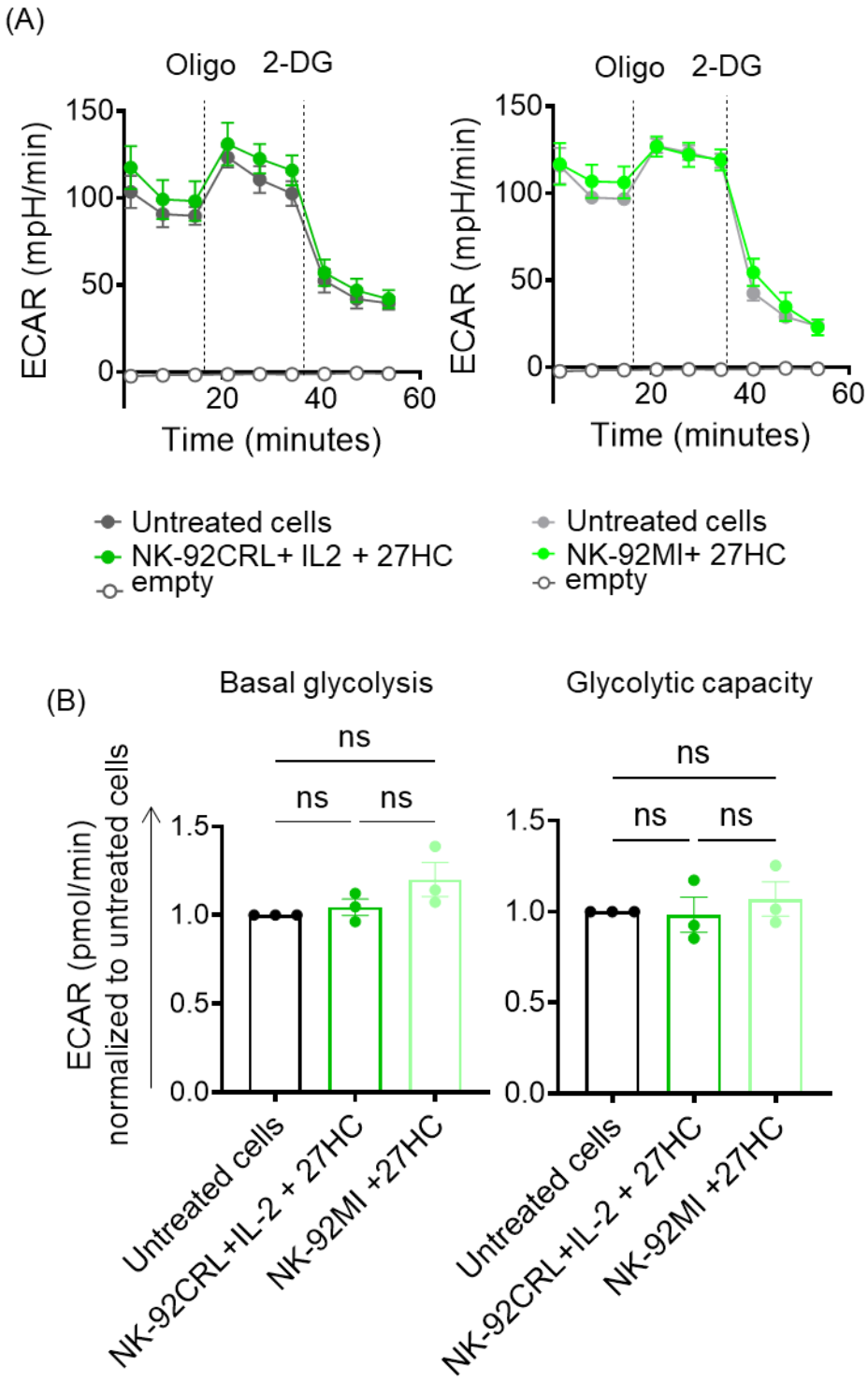
(A)
Oligo
2-DG
ECAR (mpH/min)
150
100
50
0
20
40
60
Time (minutes)
Untreated cells
NK-92CRL+ IL2 + 27HC
empty
Oligo
2-DG
ECAR (mpH/min)
150
100
50
0
20
40
60
Time (minutes)
Untreated cells
NK-92MI+ 27HC
empty
(B)
Basal glycolysis
Glycolytic capacity
ns
ns
ns
ns
ns
ECAR (pmol/min)
normalized to untreated cells
1.5
1.0
0.5
0.0
Untreated cells
NK-92CRL+IL-2 + 27HC
NK-92MI +27HC
Untreated cells
NK-92CRL+IL-2 + 27HC
NK-92MI +27HC

Figure 5.6: Glycolysis is unchanged by 18 hours pre-treatment with 27-HC in NK-92MI cells like NK-92CRL cells.

NK-92 cell lines were cultured with (CRL cells) and without (MI cells) human recombinant IL-2 (100 U/ml) in the presence or absence of 27-HC (5 μM) for 18 hours. NK-92 cells were then plated at 150,000/well in seahorse media (without any 27-HC) and analyzed using the seahorse extracellular flux analyzer measuring basal extracellular acidification rate (ECAR) and rates after sequential injection of oligomycin (2μM), and 2-deoxyglucose (30mM). The data are presented as a representative ECAR trace (A) or (B) mean +/- SEM (B) of 3 independent experiments. Statistical analysis was performed using a one-way ANOVA with a Tukey-test for multiple comparisons compared to untreated NK-92 cells. ns, nonsignificant.

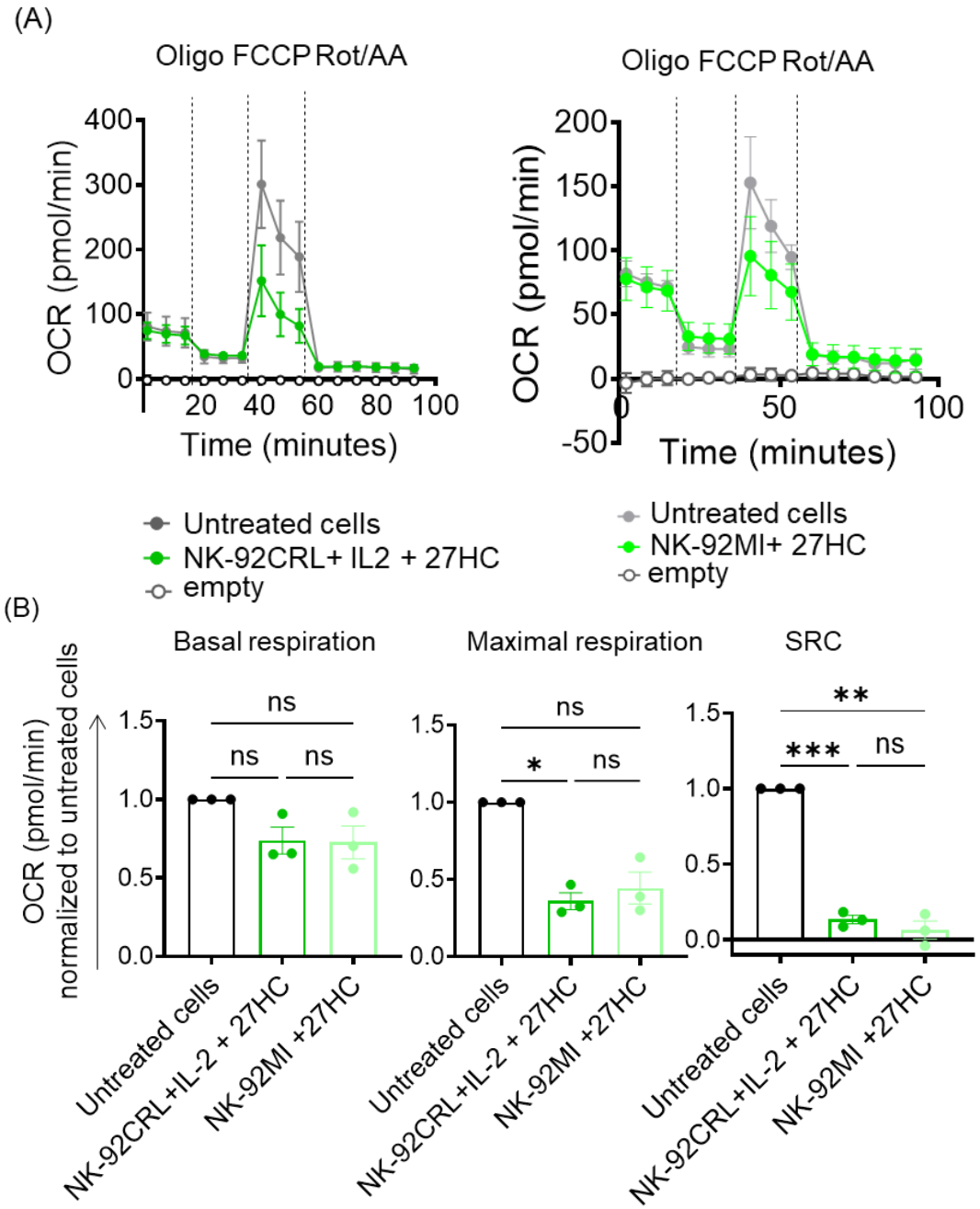

Figure 5.7: NK-92MI OxPhos is inhibited by 18 hours 27-HC pre-treatment like NK-92CRL.

NK-92 cell lines were cultured with (CRL cells) and without (MI cells) human recombinant IL-2 (100 U/ml) in the presence or absence of 27-HC (5 μM) for 18 hours. NK-92 cells were then plated at 150,000/well in seahorse media (without ant 27-HC) and analyzed using the seahorse extracellular flux analyzer measuring basal oxygen consumption rate (OCR) and rates after sequential injection of oligomycin (2μM), FCCP (0.5μM) and Rotenone/Antimycin A (0.1 /4μM). The data are presented as a representative OCR trace (A) or mean +/- SEM (B) of 3 independent experiments. Statistical analysis was performed using a one-way ANOVA with a Tukey-test for multiple comparisons compared to untreated NK-92 cells. ns, nonsignificant; *p<0.05; **P<0.01; ***P,0.001; ns, nonsignificant.

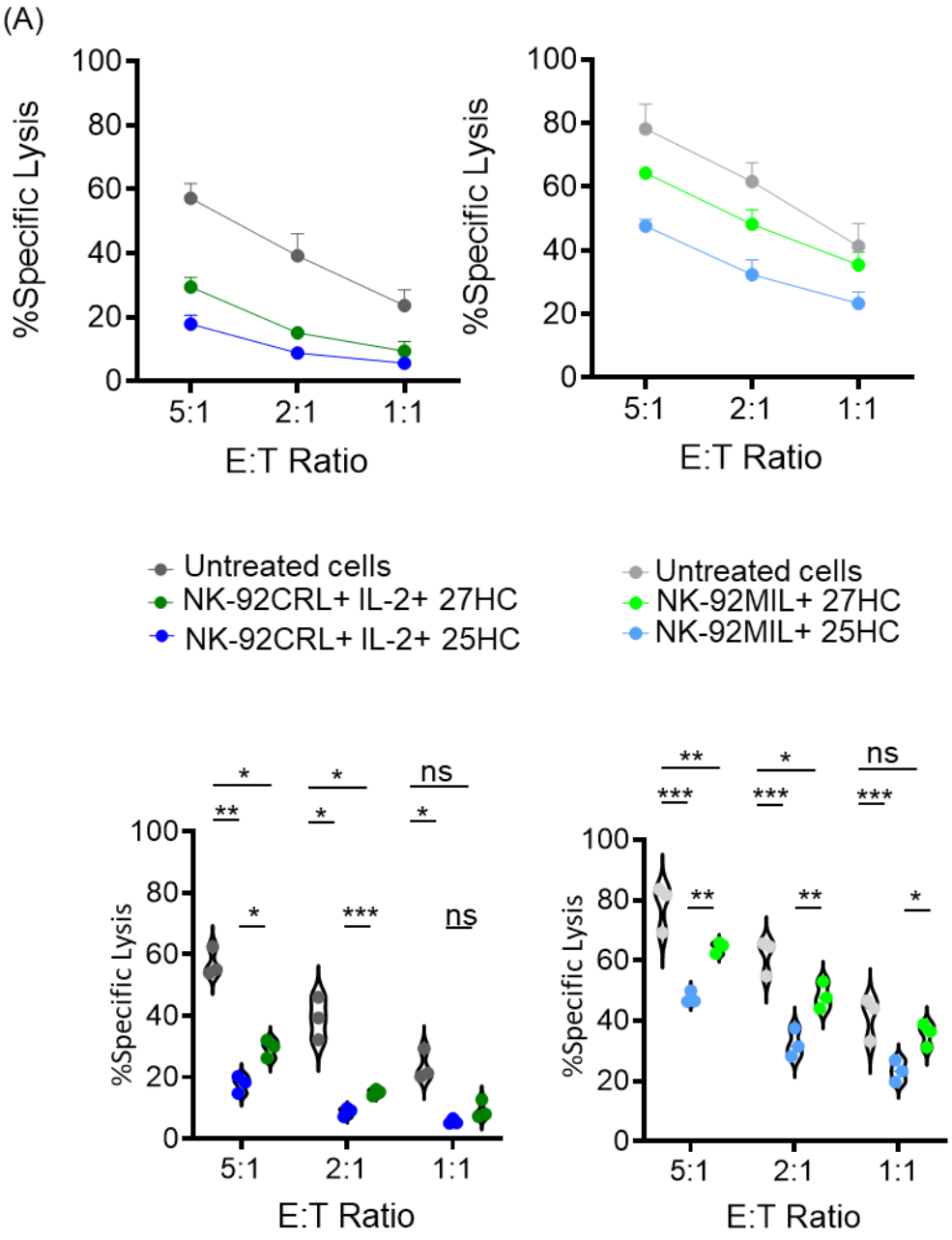
(A)
%Specific Lysis
100
80
60
40
20
0
5:1
2:1
1:1
E:T Ratio
Untreated cells
NK-92CRL+ IL-2+ 27HC
NK-92CRL+ IL-2+ 25HC
Untreated cells
NK-92MIL+ 27HC
NK-92MIL+ 25HC
*
**
***
ns

Figure 5.8: 25-HC and 27-HC pre-treatment for 18 hours inhibits NK-92 cell cytotoxicity in NK-92MI.

NK-92 cell line were cultured with (CRL) and without (MI) IL-2 (100 UI/ml) and treated with or without 25-HC (2μM) or 27-HC (5 μM) for 18 hours prior to assessing *in vitro* cytotoxicity against K562 tumour cells and. Cytotoxicity measured following co-incubation of NK-92 cell with K562 target cells for 4 hours (with no 27-HC present) at the ratios indicated, performed using technical triplicates. The data are presented as violin plot distributions (A*)* at the ratio indicated where each point represents an individual data points (B) of 3 independent experiments. Data was analyzed using a two-way ANOVA with Dunnett-test for multiple comparison compared to +IL-2. ns, nonsignificant; **p<0.01, ****p<0.0001.

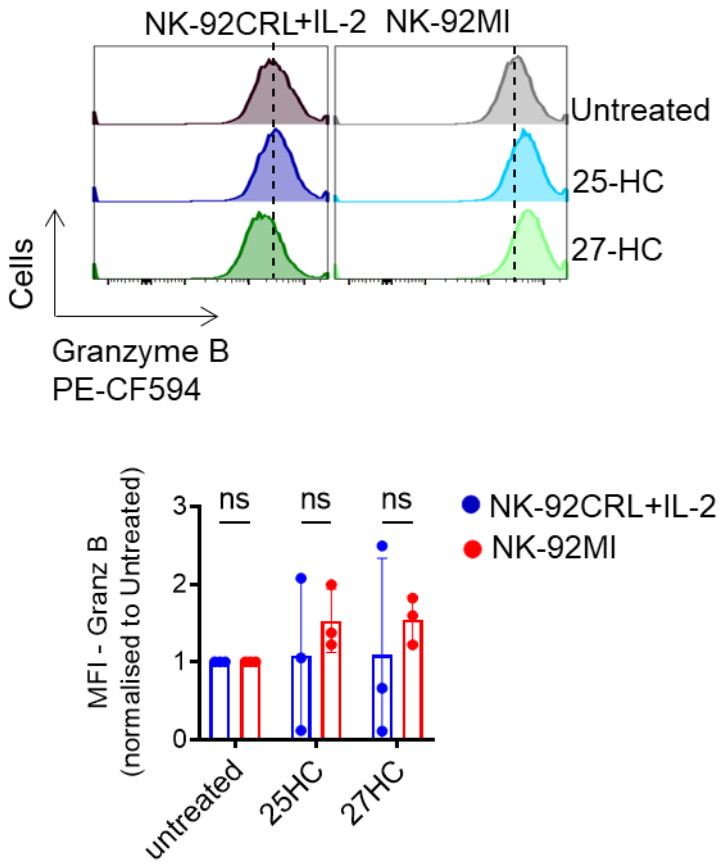

Figure 5.9: 25-HC and 27-HC pre-treatment for 18 hours does not affect granzyme B expression in NK-92MI.

NK-92 cell line were cultured with (CRL) and without (MI) IL-2 (100 UI/ml) and treated with 25-HC (2 μM) or 27-HC (5 μM) for 18 hours prior to analysing by flow cytometry. The level of granzyme B was determined by staining the cells with PE-CF594. Data are presented a representative histogram (above) or mean + /- SEM (bottom) of 3 independent experiments. Data were analyzed using one-way ANOVA with Dunnett-test for multiple comparison compared to untreated cells. The level of granzyme B in treated cells is relative to untreated cells. MFI; mean fluorescence intensity; ns, nonsignificant

5.3 Oxysterols inhibition of cytotoxicity is dose-dependent and time-dependent.

Data so far shows that oxysterols, 25-HC and 27-HC, impact NK-92MI cell OxPhos and cytotoxicity. Oxysterol levels can be enriched in the tumor microenvironment (TME) due to an increase in the expression of enzymes that are responsible for 25-HC and 27-HC synthesis, CH25H and CYP27A1, respectively [183]. The most abundant oxysterol in human serum is 27-HC, found to be ranging from 0.15µM – 0.7 µM while 25-HC spins around 0.1µM – 0.5µM [184], [185]. These concentrations increase three to five-fold in the circulation and tissues of Cyp27a1 and Ch25h overexpressing mice [5], [8]. It is likely that local concentrations of 25-HC and 27-HC within the tumor microenvironment are significantly higher those reported systemically. To further investigate the potential for oxysterol-induced inhibition of NK-92MI cytotoxic response I performed dose response experiments to determine the concentration of each oxysterol required to inhibit NK-92MI cytotoxicity.

NK-92MI cells were cultured in the presence or absence of 25-HC (0.1, 0.25, 1, 2, and 5mM) or 27-HC (0.1, 0.25, 1, 2, 5, and 10mM) for 18 hours and then stained with viability stain (Zombie Near IR) to examine whether NK-92MI cell viability and size is affected. The data shows that oxysterol treatment had no impact on the viability and cell size of the cells at any dose administered **(Figure 5.11 and 5.12). Next,** NK-92MI cells were cultured in the presence or absence of 25-HC (0.1, 0.25, 1, 2, and 5mM) or 27-HC (0.1, 0.25, 1, 2, 5, and 10mM) for 18 hours and then co-cultured with target cancer cell K562 at different effector: target ratio (without any oxysterols in media) for 4 hours. The data reveals that NK-92 cytotoxicity towards K562 target cells is reduced in a dose dependent manner with significant decreases shown for 25-HC treatment at 2 µM and 5 µM **(Figure 5.13)** and for 27-HC HC treatment between 2 µM and 10 µM **(Figure 5. 15).** This reduction of NK-

92 cytotoxicity was not changed granzyme B production in either 25-HC **(Figure 5.14)** and 27-HC **(Figure 5.16)** dose responses.

Next, to investigate the time required for oxysterols to inhibit NK-92 cytotoxicity, NK-92MI cell were cultured in the presence or absence of 25-HC (2 μM) or 27-HC (5 μM) for 1, 4, and 18 hours and then co-cultured with target cancer cell K562 at different effector: target ratio (without any oxysterols in media) for 4 hours. The results show that 1 hour **(Figure 5.17, A)** and 4 hours **(Figure 5.17, B)** exposure to 25HC or 27HC was insufficient to inhibit NK-92MI cytotoxicity against target cells. The data showed again that 18 hours exposure exerts the inhibitory effect of oxysterols in NK-92MI cytotoxicity **(Figure 5.17, C).** To summarize, exposure of NK-92MI cell to 25-HC (1- 2μM) or 27-HC (2- 5μM) for 18 hours results in inhibition of NK-92MI cytotoxic activity toward K562.

From the previous chapter, we noticed that oxysterols have a significant effect on the NK-92 OxPhos rate. I next investigated the impact of oxysterols on NK-92 cytotoxicity due to mitochondrial dysfunction. Firstly, I confirmed the impact of 25-HC and 27-HC treatment on mitochondrial respiration at the two doses that had the greatest impact upon NK-92MI cytotoxicity using the Seahorse Metabolic flux analyzer. Cells cultured in the presence or absence of 25-HC (1- 2μM) or 27-HC (2- 5μM) for 18 hours and plated at 150,000/well. The data show clearly that 25-HC and 27-HC significantly reduced the maximal respiration of NK-92MI at the higher doses of each oxysterol only **(Figure 5.18).**

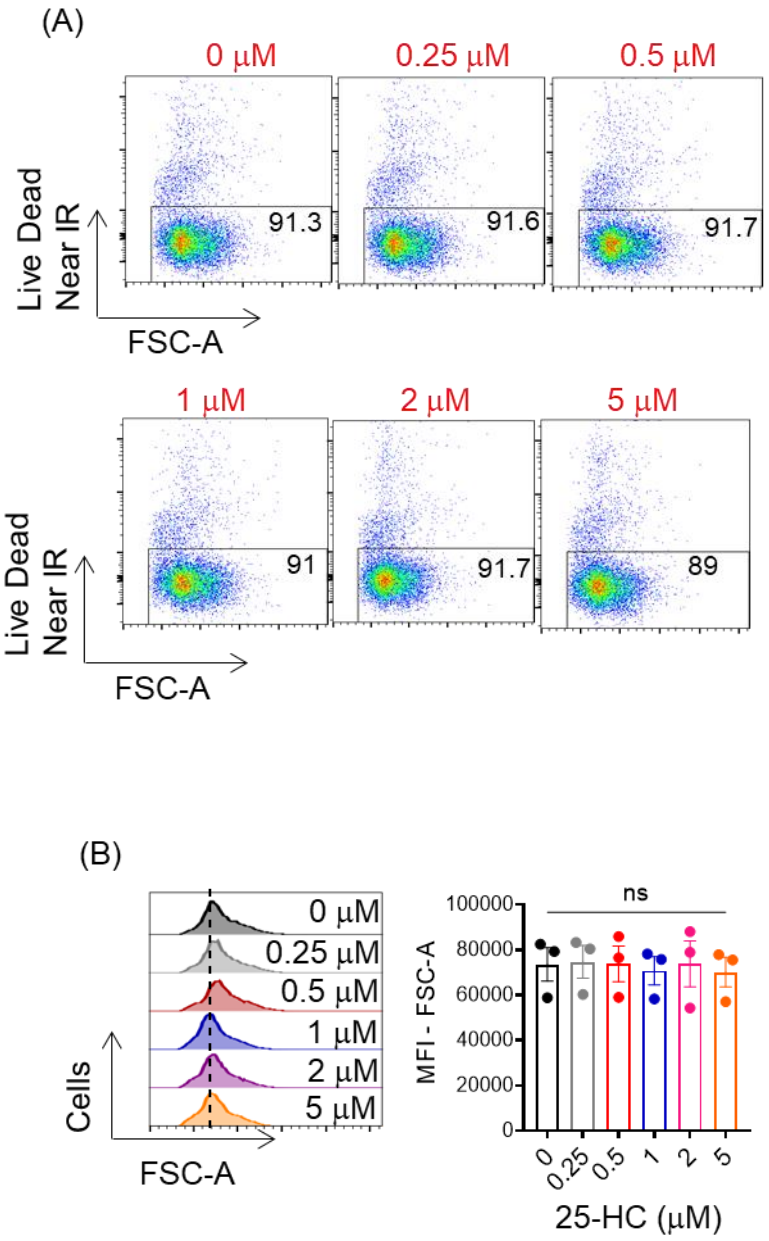
(A)
0 μM
0.25 μM
0.5 μM
Live Dead
Near IR
91.3
91.6
91.7
FSC-A
1 μM
2 μM
5 μM
Live Dead
Near IR
91
91.7
89
FSC-A
(B)
0 μM
0.25 μM
0.5 μM
1 μM
2 μM
5 μM
Cells
FSC-A
ns
MFI - FSC-A
100000
80000
60000
40000
20000
0
0
0.25
0.5
1
2
5
25-HC (μM)

Figure 5.10: The viability and cell size in NK-92MI cells was not affected by 25-HC dose response for 18 hours.

NK-92MI cell lines were cultured in the presence or absence of 25-HC (0.25, 0.5, 1, 2, 5 μM) for 18 hours and analysis by flow cytometry. (A) The viability of NK-92 cell lines was determined by staining the cells with Live Dead (Near IR). (B) NK-92 cells were analyzed for FSC-A as a measure of cell size. Data shown are presented representative (A and B, left) or mean +/- SEM (B, right) of 3 independent experiments. Data was analyzed using one-way ANOVA with a Dunnett-test for multiple comparisons compared to untreated NK-92 cells. ns, nonsignificant.

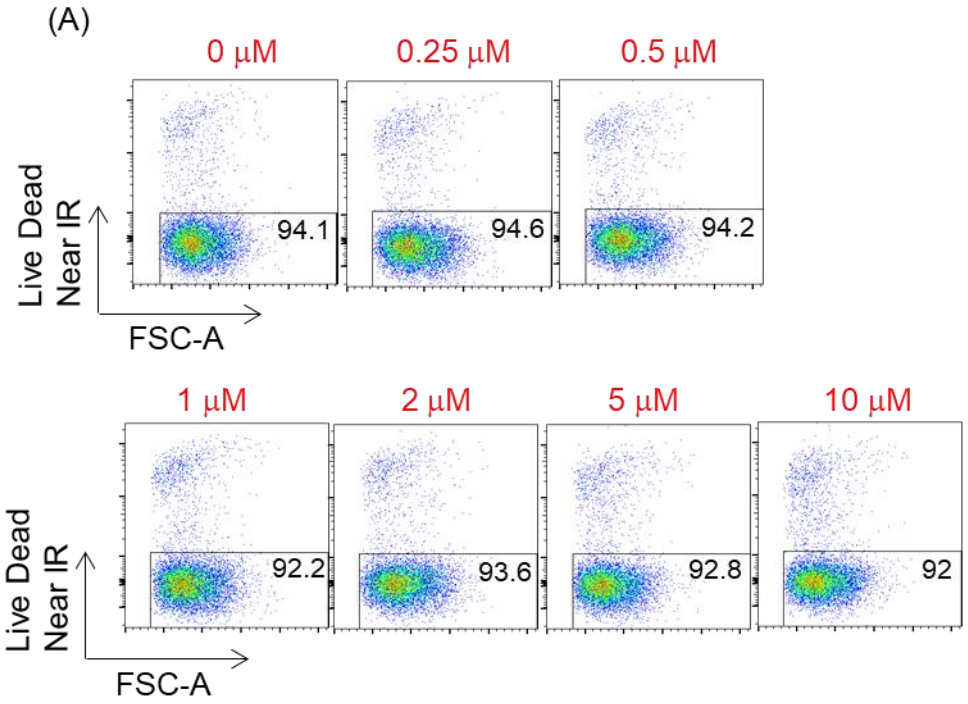
(A)
0 μM
0.25 μM
0.5 μM
Live Dead
Near IR
94.1
94.6
94.2
FSC-A
1 μM
2 μM
5 μM
10 μM
92.2
93.6
92.8
92
Live Dead
Near IR
FSC-A

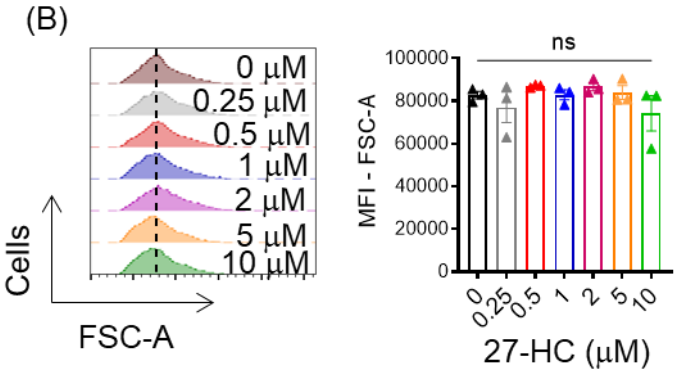
(B)
0 μM
0.25 μM
0.5 μM
1 μM
2 μM
5 μM
10 μM
Cells
FSC-A
ns
MFI - FSC-A
100000
80000
60000
40000
20000
0
0
0.25
0.5
1
2
5
10
27-HC (μM)

Figure 5.11: The Viability and cell size in NK-92MI was not affected by 18 hours 27-HC dose response.

NK-92MI cell lines were cultured in the presence or absence of 27-HC (0.25, 0.5, 1, 2, 5, 10 μM) for 18 hours prior to analysis by flow cytometry. (A) The viability of NK-92 cell lines was determined by staining the cells with Live Dead (Near IR). (B) NK-92 cells were analyzed for FSC-A as a measure of cell size. Data shown are presented representative (A and B, left) or mean +/- SEM (B, right) of 3 independent experiments. Data was analyzed using one-way ANOVA with a Dunnett-test for multiple comparisons compared to untreated NK-92 cells. ns, nonsignificant.

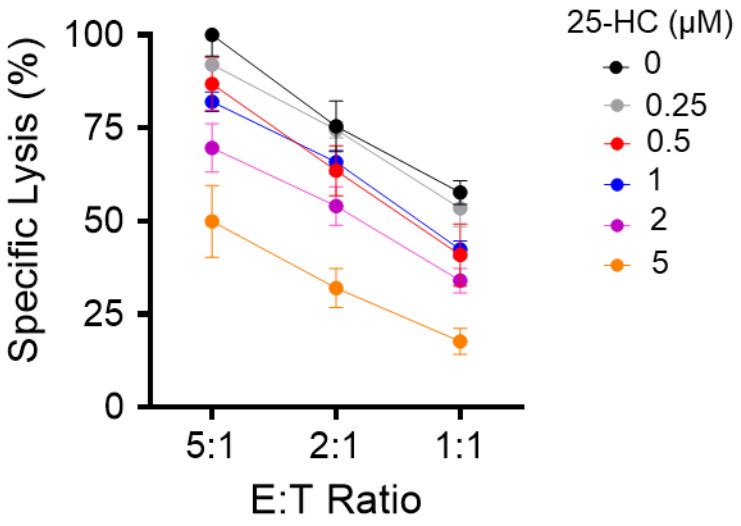
Specific Lysis (%)
100
75
50
25
0
5:1
2:1
1:1
E:T Ratio
25-HC (μM)
0
0.25
0.5
1
2
5

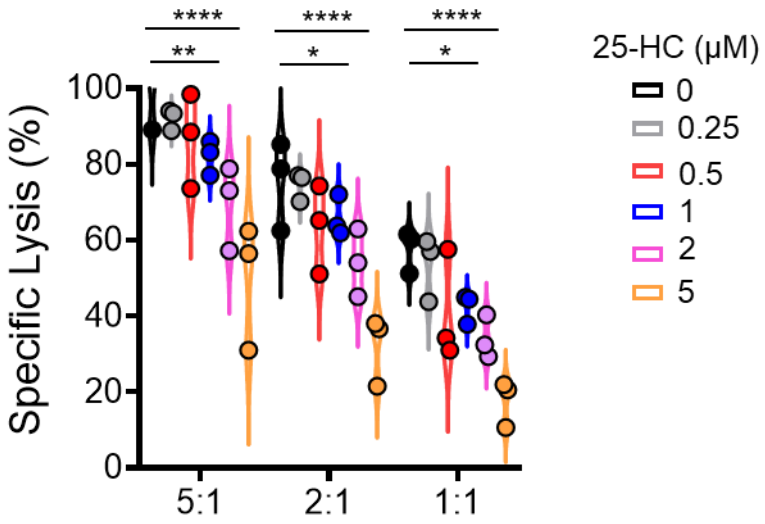
****
**
****
*
****
*
Specific Lysis (%)
100
80
60
40
20
0
5:1
2:1
1:1
25-HC (μM)
0
0.25
0.5
1
2
5

Figure 5.12: 25-HC dose response for 18 hours inhibits NK-92MI cell cytotoxicity at multiple doses.

NK-92MI cell line were cultured and treated with or without 25-HC (0.25, 0.5, 1, 2,5 μM) for 18 hours prior to assessing *in vitro* cytotoxicity against K562 tumour cells and. Cytotoxicity measured following co-incubation of NK-92 cell with K562 target cells for 4 hours (with no 25-HC present) at the ratios indicated, performed using technical triplicates. The data are presented as violin plot distributions (right) at the ratio indicated where each point represents an individual data points (bottom) of 3 independent experiments. Data were analyzed using a two-way ANOVA with Dunnett -test for multiple comparison compared to 0μM. ns, non-significant; *p<0.05; **p<0.01; ****p<0.0001.

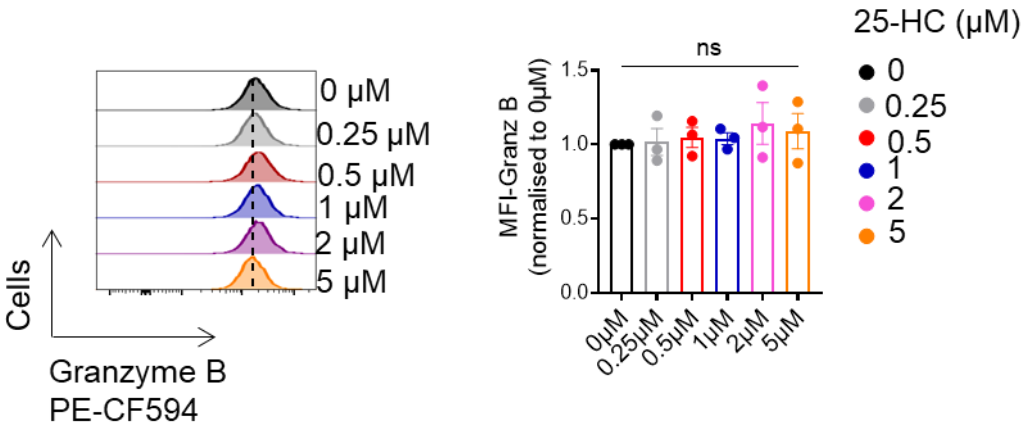

Figure 5.13: 25-HC dose response for 18 hours does not affect granzyme B expression in NK-92MI.

NK-92 cell line were cultured and treated with 25-HC (0.25, 0.5, 1, 2, 5 µM) for 18 hours prior to analysing by flow cytometry. The level of granzyme B was determined by staining the cells with PE-CF594. Data are presented as a representative histogram (above) or mean + /- SEM (bottom) of 3 independent experiments. Data were analyzed using one-way ANOVA with Dunnett-test for multiple comparison compared to untreated cells. The level of granzyme B in treated cells is relative to 0 µM. MFI; mean fluorescence intensity; ns, nonsignificant.

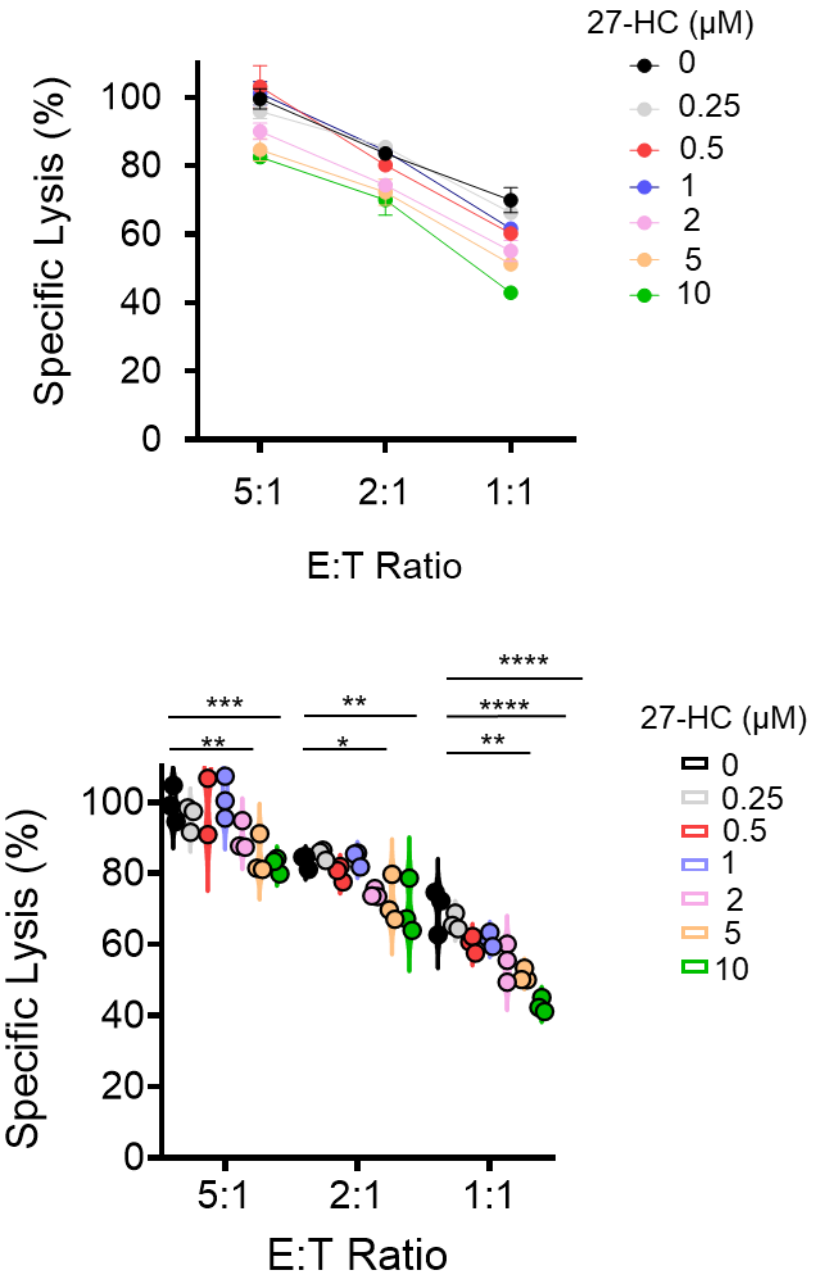
27-HC (μM)
0
0.25
0.5
1
2
5
10
Specific Lysis (%)
100
80
60
40
20
0
5:1
2:1
1:1
E:T Ratio
****
***
**
****
**
*
**
27-HC (μM)
0
0.25
0.5
1
2
5
10
Specific Lysis (%)
100
80
60
40
20
0
5:1
2:1
1:1
E:T Ratio

Figure 5.14: 27-HC dose response for 18 hours inhibits NK-92MI cell cytotoxicity at multiple doses.

NK-92MI cell line were cultured and treated with or without 27-HC (0.25, 0.5, 1, 2,5, 10 μM) for 18 hours prior to assessing in vitro cytotoxicity against K562 tumour cells and. Cytotoxicity measured following co-incubation of NK-92 cell with K562 target cells for 4 hours (with no 27-HC present) at the ratios indicated, performed using technical triplicates. The data are presented as violin plot distributions (right) at the ratio indicated where each point represents an individual data points (bottom) of 3 independent experiments. Data were analysed using a two-way ANOVA with Dunnett -test for multiple comparison compared to 0 μM. ns, nonsignificant; *p<0.05; **p<0.01; ***p<0.001; ****p<0.0001.

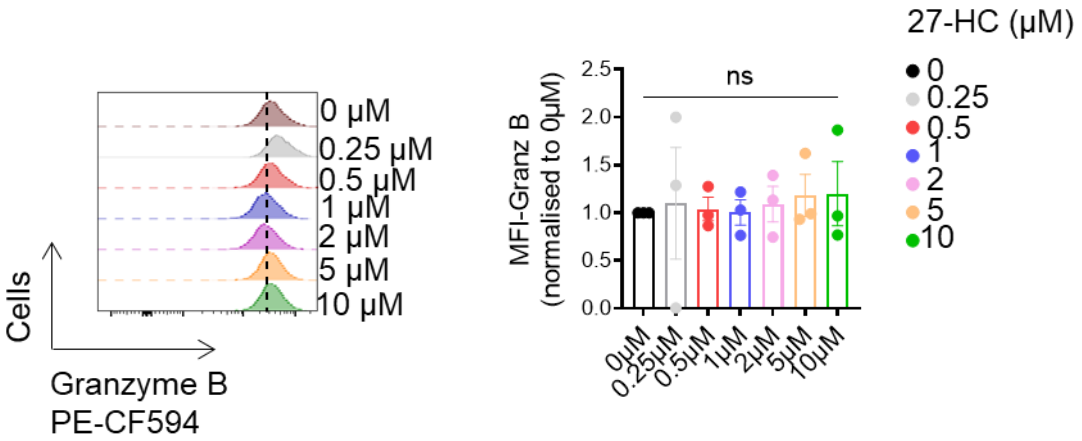

Figure 5.15: 27-HC dose response for 18 hours does not affect granzyme B expression in NK-92MI.

NK-92 cell line were cultured and treated with 25-HC (0.25, 0.5, 1, 2, 5, 10 μM) for 18 hours prior to analysing by flow cytometry. The level of granzyme B was determined by staining the cells with anti-granzyme B PE-CF594. Data are a representative histogram (above) or mean + /- SEM (bottom) of 3 independent experiments. Data were analyzed using one-way ANOVA with Dunnett-test for multiple comparison compared to untreated cells. The level of granzyme B in treated cells is relative to 0 μM. MFI; mean fluorescence intensity; ns, nonsignificant.

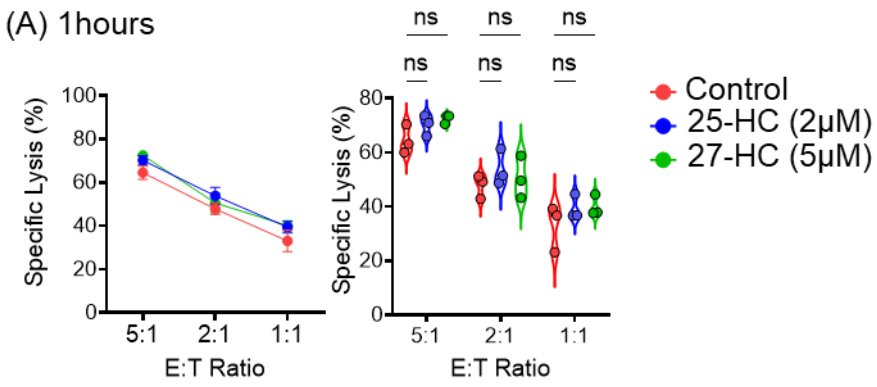

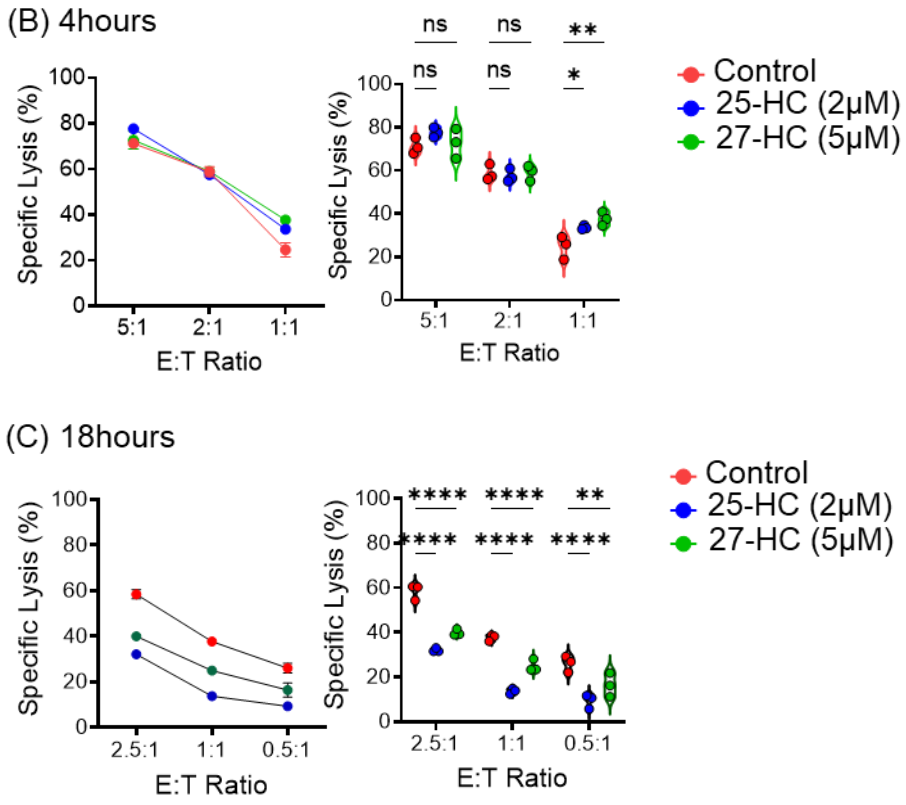

Figure 5.16: Pre-treatment for 18 hours is required to exhibit the effect of 25-HC and 27-HC on NK-92MI cell cytotoxicity.

NK-92MI cell line were cultured and treated with or without 25-HC (2 μM) or 27-HC (5 μM) for 1(A), 4(B), and 18(C) hours prior to assessing *in vitro* cytotoxicity against K562 tumour cells and. Cytotoxicity measured following co-incubation of NK-92 cell with K562 target cells for 4 hours (with no 25-HC or 27-HC present) at the ratios indicated, performed using technical triplicates The data are presented as violin plot distributions (right of A, B, and C) at the ratio indicated where each point represents

an individual data points (right of A, B, and C) of 3 independent experiments. Data were analyzed using a two-way ANOVA with Dunnett -test for multiple comparison compared to control . ns, nonsignificant; *p<0.05; **p<0.01; ****p<0.0001.

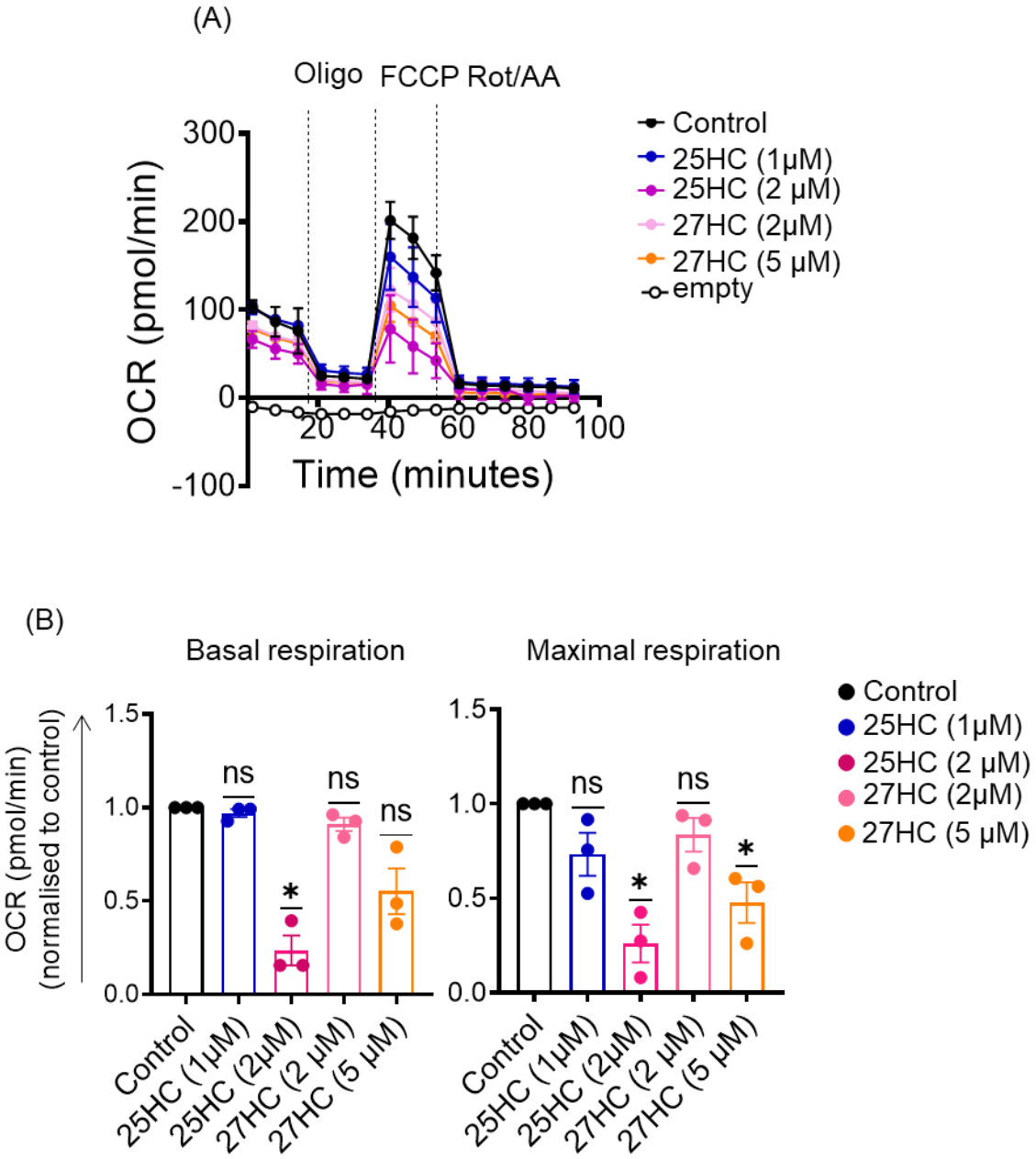
(A)
Oligo
FCCP
Rot/AA
OCR (pmol/min)
300
200
100
0
-100
20
40
60
80
100
Time (minutes)
Control
25HC (1μM)
25HC (2 μM)
27HC (2μM)
27HC (5 μM)
empty
(B)
Basal respiration
Maximal respiration
OCR (pmol/min)
(normalised to control)
1.5
1.0
0.5
0.0
ns
*
Control
25HC (1μM)
25HC (2μM)
27HC (2 μM)
27HC (5 μM)

Figure 5.17: 25-HC and 27-HC inhibit NK-92MI maximal respiration rate at the highest doses by 18 hours.

NK-92MI cell lines were cultured in the presence or absence of 25-HC (1, 2 μM) or 27-HC (2, 5 μM) for 18 hours. NK-92 cells were then plated at 150,000/well in seahorse media (without any 25-HC or 27-HC) and analyzed using the seahorse extracellular flux analyzer measuring basal oxygen consumption rate (OCR) and rates after sequential injection of oligomycin (2μM), FCCP (0.5μM) and Rotenone/Antimycin A (0.1 /4μM). The data are presented as a representative OCR trace (A) or mean +/- SEM (B) of 3 independent experiments. Statistical analysis was performed using a one sample t test against a hypothetical value of 1. ns, non-significant; *p<0.05; **P<0.01.

5.4 25-HC treatment inhibits other Mitochondrial parameters.

To further investigate the effect of 25-HC and 27-HC on mitochondrial metabolism, I used flow cytometry to investigate mitochondrial parameters such as mitochondrial volume, membrane potential, and mitochondrial reactive oxygen species (mtROS) production. NK-92MI cells were cultured in the presence or absence of 25-HC (1, 2 mM) or 27-HC (2, 5 mM) for 18 hours, and stained with mitochondrial dye before analyzing by flow cytometry. Mitochondrial volume can be quantified using MitoTracker™ Green, a is a carbocyanine-based dye that localizes mitochondria in live cells. The potential across the mitochondrial inner membrane was investigated using Tetramethyl rhodamine (TMRM), a mitochondrial stain located to the mitochondria in a manner proportional to the mitochondrial inner membrane potential. The accumulation of mitochondrial ROS that was measured using the probe MitoSOX™ Red.

The data shows oxysterols-treated cells had reduced mitochondrial volume when assessed with MitoTracker™ Green **(Figure 5.19)**. However, there was no observed impact on the potential across mitochondrial inner membrane, measured using TMRM, compared to untreated controls **(Figure 5.20)**. Finally, the data show that there is an increase abundance of mitochondrial ROS-producing cells in the presence of 25-HC (1, 2 mM) but not 27-HC (2, 5 mM) when compared to untreated controls **(Figure 5.21).** When considering changes in mtROS it is important to consider the mitochondrial mass associated with those reading. In this context the reduced volume of mitochondria in 25HC treated cells is making more mtROS than control cells that have more mitochondria. Therefore, the mtROS per mitochondria is even more significantly increased. Taken together, 25-HC has a clear impact on mitochondrial metabolism but the data for impact of 27-HC on mitochondrial metabolism and health is less compelling.

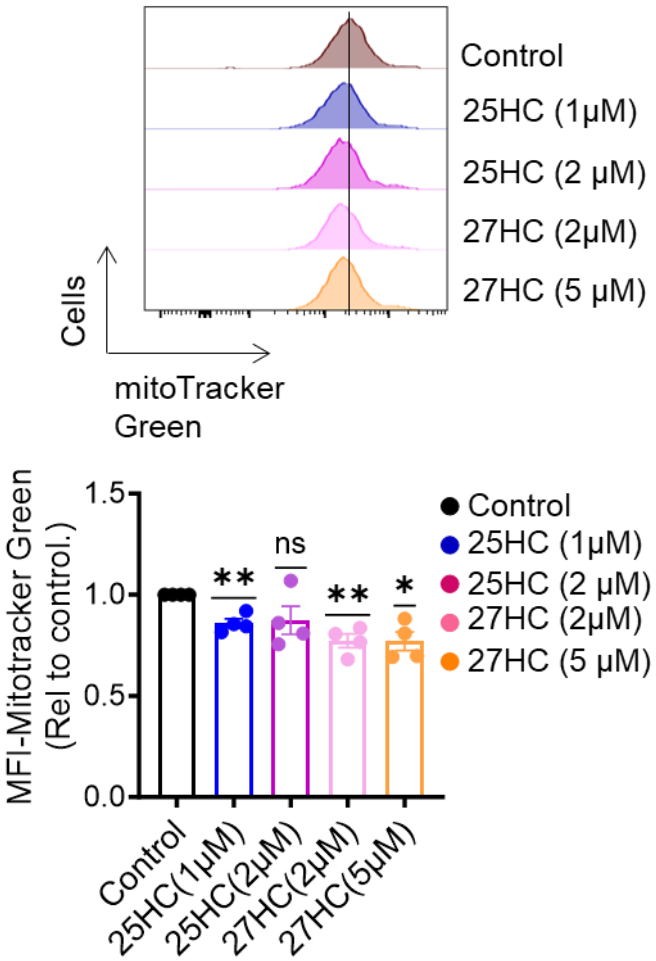

Figure 5.18: 25-HC and 27-HC reduce mitochondrial volume in NK-92MI cells.

NK-92MI cell lines were cultured in the presence or absence of 25-HC (1, 2 μM) or 27-HC (2, 5 μM) for 18 hours. Mitochondrial mass was measured by flow cytometry using MitoTracker™ green dye. Data are presented as a representative (above) or mean +/- SEM (bottom) of 4 independent experiments. Statistical analysis was performed using one-sample t-test versus a theoretical value of 1. ns, non-significant; *p<0.05; **P<0.01.

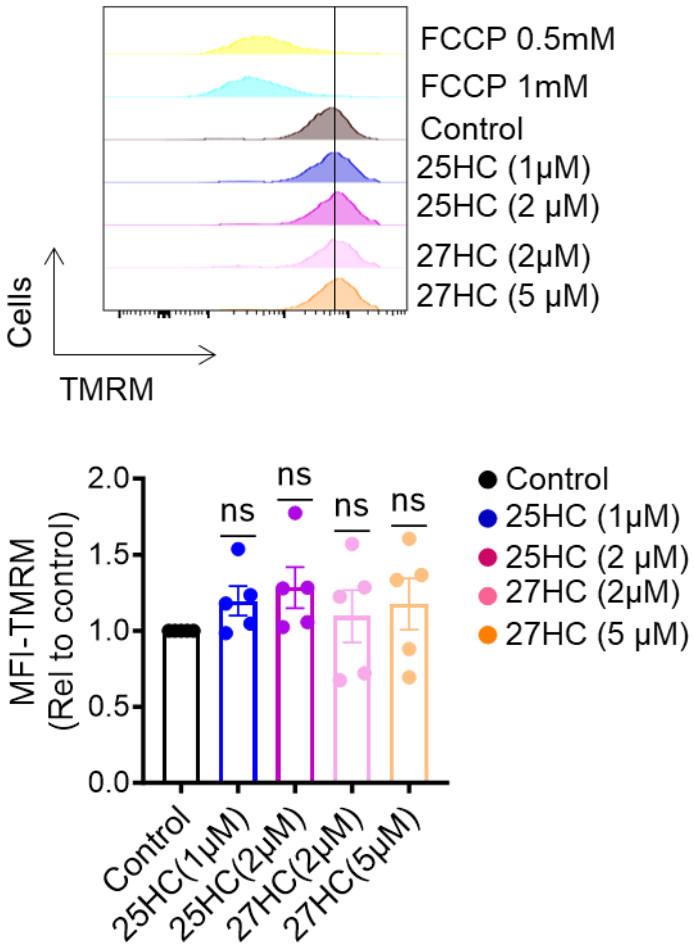

Figure 5.19: 25-HC and 27-HC does not affect mitochondrial membrane potential in NK-92MI cells.

NK-92MI cell lines were cultured in the presence or absence of 25-HC (1, 2 μM) or 27-HC (2, 5 μM) for 18 hours. Membrane potential was measured by flow cytometry using TMRM dye. Data are presented as a representative (above) or mean +/- SEM (bottom) of 4 independent experiments. Statistical analysis was performed using one-sample t-test versus a theoretical value of 1. ns, non-significant.

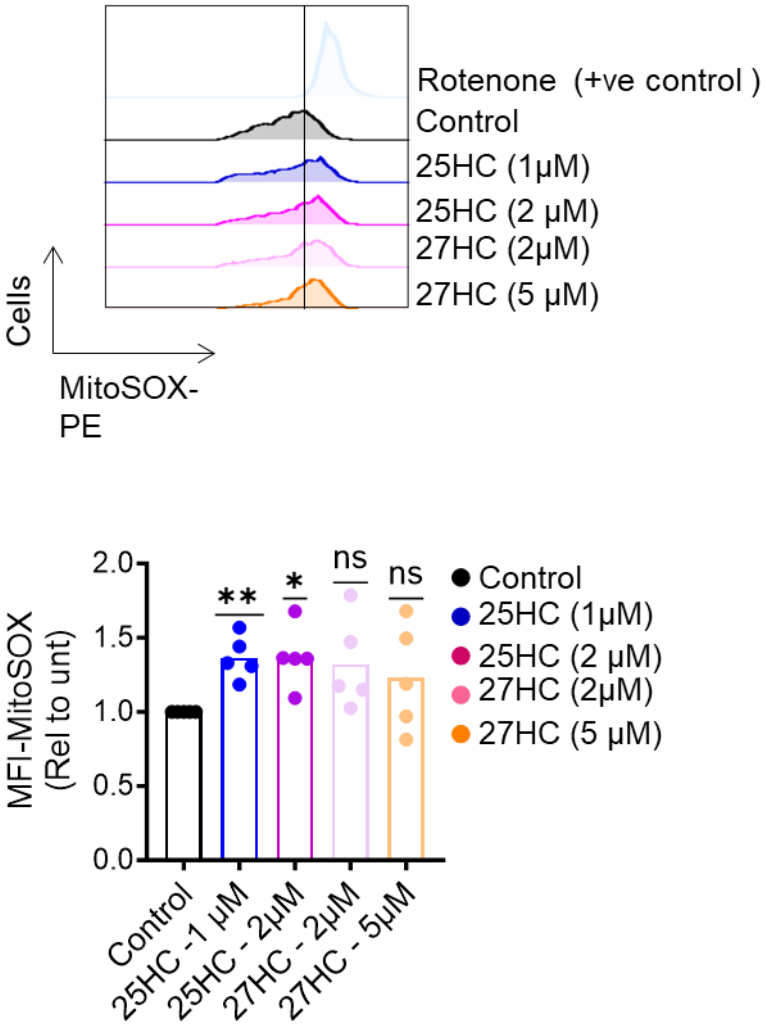

Figure 5.20: 25-HC but not 27-HC increase the frequency of NK-92MI producing mitochondrial ROS following treatment for 18 hours.

NK-92MI cell lines were cultured in the presence or absence of 25-HC (1, 2 μM) or 27-HC (2, 5 μM) for 18 hours. Mitochondrial ROS production was measured by flow cytometry using MitoSOX Red. Data are presented as a representative (above) or mean +/- SEM (bottom) of 5 independent experiments. Statistical analysis was performed using one-sample t-test versus a theoretical value of 1. ns, non-significant; *p<0.05; **p<0.01.

5.5 25-HC treatment affects the structure of the NK92 plasma membrane.

Oxysterols can insert into the plasma membrane and considering the presence of additional hydrophilic functional groups, these sterols with addition hydrophilic groups can affect the membrane packing and the overall order of the membrane lipids (**Figure 5.21**). Therefore, we considered whether the impact of 25HC and 27HC on NK92 cytotoxicity might be associated with oxysterol mediated changes in plasma membrane structure. Plasma membrane structure can be assessed by flow cytometry using the dye di-4-ANEPPDHQ. This is a member of the aminonaphthylethenylpyridinium (ANEP) family of membrane potential-sensitive dyes, that is used to measure the order of lipid domains, such as the plasma membrane structure **(Figure 5.22)** [186]. Firstly, to assess whether the dye di-4-ANEPPDHQ can be used, I used 7-ketocholesterol (10 mM), a positive control, as it is shown that a high concentration of 7-KC can strongly inhibit the organization of membrane lipid order [183], [184].

When NK-92MI cell were treated with 7-KC for 18 hours there was a clear decrease in the plasma membrane order **(Figure 5.23),** which provided confidence that the di-4-ANEPPDHQ dye can be used to assess membrane order in NK-92MI cells. NK-92MI cells were then cultured in the presence or absence of 25-HC (1, 2 mM) or 27-HC (2, 5 mM) for 18 hours, and stained with di-4-ANEPPDHQ dye for 20 min before analyzing by flow cytometry. There was a significant decrease in membrane order when NK-92 cells were treated with either 25-HC and 27-HC concentration for 18 hours **(Figure 5. 25).** Interestingly, the inhibition of SREBP activation using PF429242 or the activation of LXR using GW3965 did not alter the membrane order of NK-92MI cells **(Figure 5.25)** suggesting that these effects of 25HC and 27HC are direct upon the membrane rather than due to changes in SREBP/LXR signaling. Taken

together, the data shows that 25-HC and 27-HC affect membrane order in NK92MI cells and that this is likely due to direct interactions between the oxysterol and the plasma membrane composition.

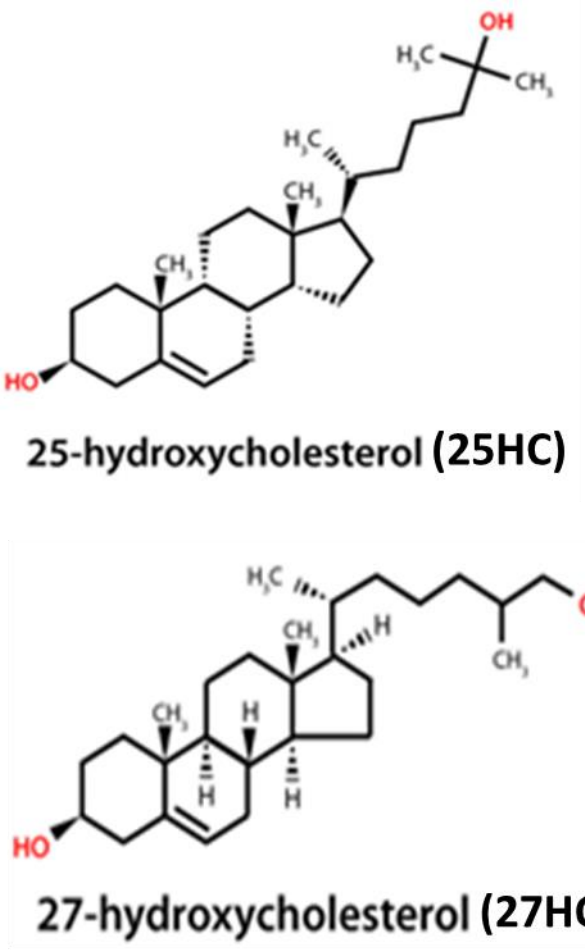

Figure 5. 21: Oxysterols structure.

Both 25HC and 27HC are oxysterols, which are derivatives of cholesterol oxidized at specific positions on the cholesterol molecule. 25-hydroxycholesterol (25HC) involves a hydroxyl (-OH) group attached at the 25th carbon atom on the cholesterol molecule. 27-hydroxycholesterol (27HC) involves a hydroxyl group attached at the 27th carbon atom on the cholesterol. molecule. These modifications result in different properties and biological activities for each oxysterol, impacting their functions in various physiological processes.

(A)

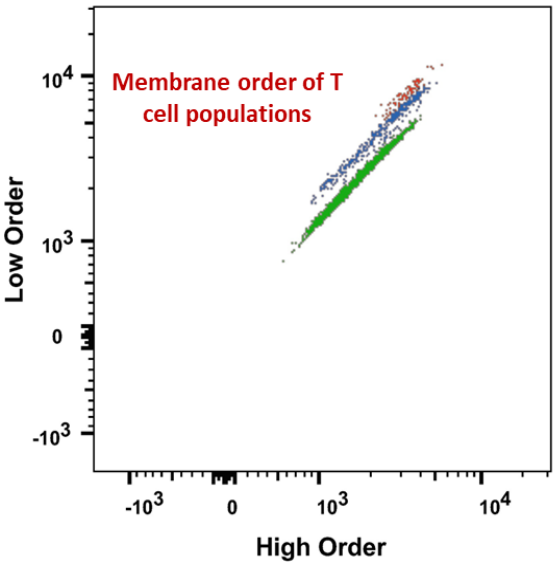

Membrane dye: Di-4-ANEPPDHQ

	Subset Name	Freq. of Parent
■	High Order	96.2
■	Intermediate Order	3.09
■	Low order	0.66

(B)

$$rGP = \frac{MFI_{Ch1} - MFI_{Ch2}}{MFI_{Ch1} + MFI_{Ch2}}$$

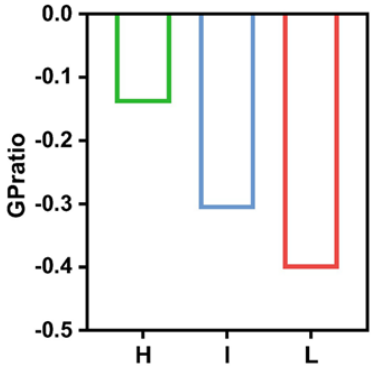

Figure 5. 22: Assessing T-Cell Plasma Membrane Lipids via Flow Cytometry utilizing the membrane dye Di-4-ANEPPDHQ.

The dot plot illustrates distinct T cell groups categorized by their plasma membrane lipid accessed through the Di-4-ANEPPDHQ dye. This membrane dye alters its fluorescence across two distinct channels relative to membrane organization. T cell populations exhibiting high membrane order are depicted in green, intermediate order in blue, and low order in red (A). The bar graph results from the calculation of the rGP ratio (B).

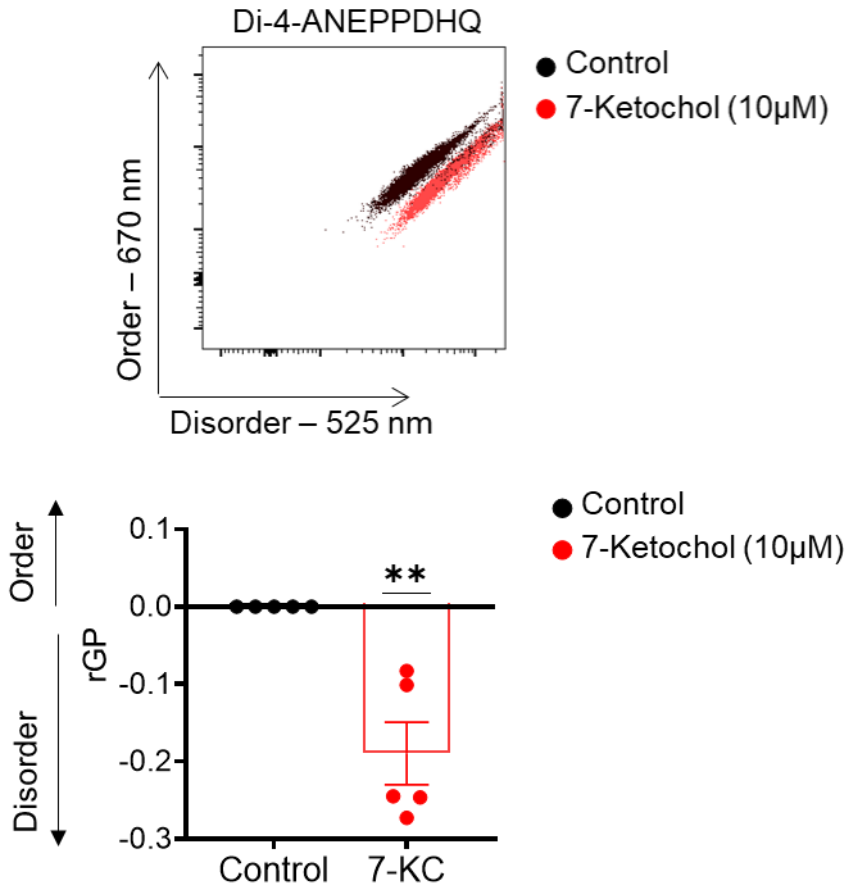

Figure 5. 23: Di-4-ANEPPDHQ can be used to assess NK-92 cell membrane order by flow cytometry.

NK-92MI cell lines were cultured in the presence or absence of 7-KC (10 μM) for 18 hours before the cells were analysed for Di-4-ANNEPDHQ staining by flow cytometry. The dye was excited at 488 nm and the ordered and disordered phases of the dye were measured at 620 nm and 525 nm respectively. The data are presented as a representative (above) or mean +/- SEM (bottom) of 5 independent experiments. Statistical analysis was performed using a one-sample t-test versus a theoretical value of 0. Ns, non-significant; **p<0.01.

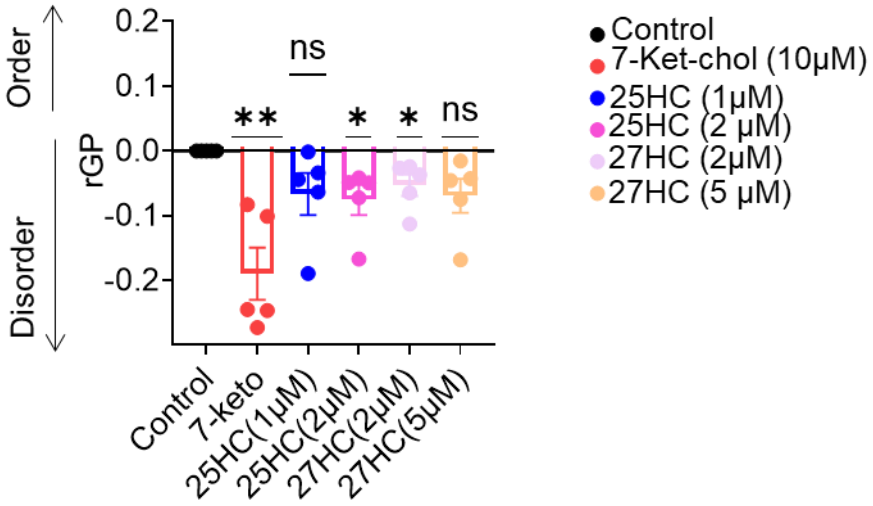

Figure 5.24: 25-HC and 27-HC at 2μM decrease plasma membrane order in NK-92MI cells treated for 18 hours.

NK-92MI cell lines were cultured in the presence or absence of 25-HC (1, 2 μM) or 27-HC (2, 5 μM) for 18 hours before the cells were analysed for Di-4-ANNEPDHQ staining by flow cytometry. The dye was excited at 488 nm and the ordered and disordered phases of the dye were measured at 620 nm and 525 nm respectively. The data are presented as mean +/- SEM of 5 independent experiments. Statistical analysis was performed using a one-sample t-test versus a theoretical value of 0. ns, non-significant; *p< 0.5; **p<0.01.

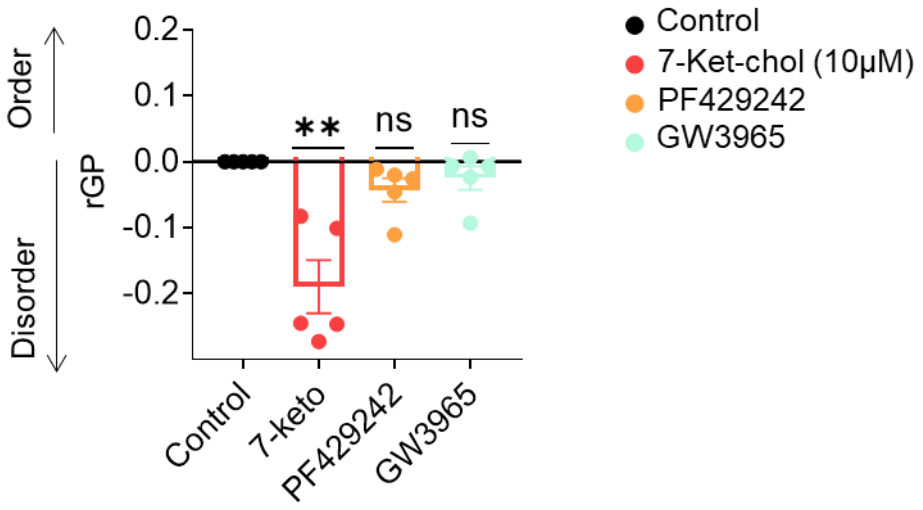

Figure 5.25: GW 3965 and PF429242 does not decrease the plasma membrane order in NK-92MI treated 18 hours.

NK-92MI cell lines were cultured in the presence or absence of 25-HC (1, 2 μM), 27-HC (2, 5 μM), PF429242, or GW3965 (2 μM) for 18 hours before the cells were analysed for Di-4-ANNEPDHQ staining by flow cytometry. The dye was excited at 488 nm and the ordered and disordered phases of the dye were measured at 620 nm and 525 nm respectively. The data are presented as a mean +/- SEM of 5 independent experiments. Statistical analysis was performed using a one-sample t-test versus a theoretical value of 0. ns, non-significant; **p<0.01.

5.6 Discussion of Chapter 5

NK-92 cell line (ATCC® CRL-2408TM)-NK-92MI- was derived by transfecting the parental NK-92 cell line (ATCC® CRL-2407TM)-NK-92CRL- with human IL-2 cDNA in the retroviral MFG-hIL-2 vector using a particle-induced gene transfer technology [179]. This IL-2-independent NK-92 cell should allow elongated treatment with fully activated NK-92 cells without needing an external source of IL-2 [179]. The comparative studies of NK-92CRL and NK-92MI in this report revealed that they display similar surface markers such as CD56, TRAIL, and NKp44, and both lack the expression of CD3, FASL, and other activating receptors. Additionally, both cell lines have the same biological responses, but NK-92MI can be extended *in vitro* without exogenous IL-2. We shifted to use NK-92MI as they exert a higher cytotoxic activity and more closely match the NK92 cells that are being used therapeutically [183]. Many preclinical researches have been conducted on CAR-engineered NK-92 cells, where CAR-targeted antigens include CD33, CD19, CD20, CD138 and CS-1 specific [184], [185], [187], [188]. The first phase I clinical trial with CD33-modified CAR NK-92 cells has been initiated [6]. NK-92 cells have shown promising candidate for adaptive cellular immunotherapy, mainly when the CAR-engineered NK-92 cells can additionally boost their anti-cancer activity with tumor antigen [6], [9] which makes them the first ‘off-the-shelf’ cellular product for cancer immunotherapy [185]. In this study, we used NK-92MI to investigate the mechanism of oxysterol-mediated cytotoxicity inhibition as such knowledge could be used to genetically modify CAR-NK-92MI to boost their anti-tumor activity to become more efficient even in harsh conditions like solid tumors.

Herein, I provided also clear evidence of the effect of oxysterols, 25HC and 27HC, on NK-92MI metabolic responses, which is critical for the effective functioning of NK-92 cells. To examine the effect of oxysterols on NK-92MI, we aimed to demonstrate the minimum concentration of 25-HC and 27-HC that display a potent action on NK-92 cytotoxicity without impact on the basic

cell biology of the cell line, therefore, I consider 1- 2µM for 25-HC and 2- 5µM for 27-HC are an optimal dose that reflect plausible local concentrations in TME. Several studies show that mitochondrial dysfunction affects the anti-tumor activity of human NK cells. For instance, human NK cells from breast cancer patients had clear metabolic defects including dysfunctional mitochondrial that involved structural changes in mitochondrial morphology [189]. Based on our results in the previous chapter, we suggested that these oxysterols impaired mitochondrial function. Indeed, the data clearly shows that 25-HC and 27-HC significantly reduced the maximal respiration of NK-92MI at the higher doses of each oxysterol. There was also an associated decrease in mitochondrial volume. In addition, I measured increased mitochondrial reactive oxygen species (mtROS) in 25HC treated NK92, a feature consistent with mitochondrial dysfunction and with observations in NK cells from patients with breast cancer [189]. When analyzing mtROS production one should take into consideration and changes in mitochondrial mass that might mean an increased mtROS per volume of mitochondrial. Here, 25HC-treated cells with less mitochondrial volume produced more mtROS compared with control cells. While the increase in mtROS in 27HC treated cells was not significant is should be noted that 27HC had significantly reduced mitochondrial volume and so mitochondria under these conditions are most likely producing elevated ROS per unit of mitochondrial volume. However, Mitotracker Green, a Carbocyanine-based dye used to assess mitochondrial volume, exhibits an inclination to accumulate within live cell mitochondria owing to the presence of the mitochondrial membrane potential. Consequently, its accumulation is reliant upon this potential and is not self-sufficient. (Accumulation is impeded in the presence of FFCP, so it would be useful if we used FCCP as a control). This particular dye functions as a marker for mitochondria due to its capability to engage with thiol groups once internalized. This interaction allows the dye to remain within the matrix after fixation, unlike other dyes that tend to diffuse out of the organelle.

Consequently, the intensity of the dye may not only correspond to its extent of reaction with mitochondrial proteins but also to the potency of the membrane potential. It holds significance because there's an indication of variance in mtROS levels observed in cells treated with 25HC versus 27HC due to the decreased mitochondrial volume in the 25HC-treated cells.

Cholesterol is a crucial component of the plasma membrane and oxysterols can also insert into lipid bilayers though they do so in a different way to cholesterol due to an extra hydrophilic group. I hypothesized that some of the effects of oxysterols could be due to effects on plasma membrane order/disorder. Oxysterols like 25-HC and 27-HC are known to insert into the plasma membrane and because these oxysterols possess additional hydrophilic functional group, they are not able to insert effectively into hydrophobic regions of the membrane. As a result, they have a profound effect on membrane structure and dynamics [190]‑[192]. 7-Ketocholesterol, an oxysterol produced from nonenzymatic cholesterol oxidation, is well-known for its potent effect in the disruption of membrane order

7-Ketocholesterol (7KC), an oxysterol formed from the nonenzymatic oxidation of cholesterol, is a potent disruptor of membrane order [190] [191], [193]‑[195], and was used as a positive control to validate using Di-4-ANEPPDHQ dye in the assessment of NK-92 membrane order. 7-KC caused a significant shift towards membrane disorder which is consistent with previous studies. The data show that 25-HC and 27-HC affect membrane order in NK92MI cells, and this is likely due to direct interactions between the oxysterol and the plasma membrane rather than due to changes in SREBP/LXR signaling. There is emerging evidence revealed that the integrity of plasma membrane structure in terms of lipid organization is integrity for regulating NK cell cytolytic function which is a highly regulated multistep process. For instance, NK cell is protected from death during degranulation of their perforin toward target cells through tightly packed and highly ordered

presynaptic lipid membrane. By disrupting this packed lipid membrane, NK cells become susceptible to auto-lysis [196].

To conclude, this chapter showed that the distinct impact of these oxysterols on cytotoxicity is evident (Figure 5.12) and (Figure 5.14), where 27-HC (Figure 5.14) is notably less potent compared to 25HC (Figure 5.12). The data from the Di-4-ANEPPDHQ dye assay indicates that the heightened influence of 25HC on cytotoxicity is improbable to result from an impact on plasma membrane structure, as both oxysterols demonstrate this effect.

Chapter 6 – Overall Discussion

An emerging number of research studies and clinical reports have shown promising anit-tumor effects when utilizing NK cell-based immunotherapy [193]. Currently, multiple approaches are used to develop and enhance the number and function of NK cells [193], [194]. However, NK cells from a patient's blood represent only 10% of the lymphocytes and frequently they are dysfunctional thus one of the technical challenges is to collect adequate numbers of NK cells. Alternatively, taking NK cells from healthy donors requires depletion of the allogeneic T cells to avoid graft-host reaction [195]. To overcome these clinical challenges, cytotoxic cell lines were established from a patient who was diagnosed with NK-lymphoma [196]–[200]. Among these NK cell lines, the NK-92 cell line exerts highly and consistently cytotoxic activity against a wide range of target cells [198]. NK-92 cell lines have engaged in immense preclinical development [201], [202] and completed phase I trials in patients with cancer [203], [204]; (NCT00900809) and (NCT00990717). There is a growing number of strategies applied to enhance and develop NK-92 cell-based therapy. The field of immunometabolism has rapidly extended in recent years. It has been shown that cellular metabolism is integral for the effector function of the immune cells and each cell type has its metabolic signature to support their functions. The ability of NK cells to recruit their metabolic profile is not only dependent on the amount of energy they produce but is dependent on a distinct metabolic pathway and biosynthetic precursors that sustain cell growth, proliferation, and produce effector molecules and therefore they can sustain their normal effector function. An intensive immunosuppressor microenvironment like TME impairs the NK cell function. The TME is a rich environment with different factors that can suppress NK effector response. One of the factors that are highly expressed in TME is oxysterols such as 25-HC and 27-HC. Our lab has previously found that oxysterols have an impact on murine and human NK cell metabolism and function through SREBP-dependent mechanism [169]. Herein, we investigated the metabolic profile of the NK-92 cell line and measured the consequence of oxysterol

treatment on NK-92 metabolism and cytotoxicity. This study pinpoints the potential mechanism of 25-HC that disrupts NK-92 metabolism and cytotoxicity, and that such knowledge should be considered in the future of NK-92-based immunotherapy. The ultimate aim is to establish a novel strategy enabling NK-92 cells to resist the harmful effect of the TME.

My research on the NK-92 cell line was consistent with what has been found previously in our lab regarding the oxysterols impairing the metabolism and effector function of NK-92. Contrary to our previous work, oxysterols-mediated inhibition of NK-92 cells was independent of SREBP inhibition and LXR activation. Additionally, we observed the intensive effect of oxysterols on mitochondrial respiration rates and that associated with a reduction in mitochondrial parameters such as mitochondrial mass and increased production of mtROS. Moreover, oxysterol treatment significantly disrupted the plasma membrane order, however, LXR agonist GW3965 and SREBP inhibitor PF429242 did not cause plasma membrane disorder. From these results, I suggest that 25-HC and 27-HC impact NK-92 function independent of SREBP inhibition, LXR activation, and lipid/cholesterol biosynthesis. The impact of oxysterols arises from their ability to insert into and modify the structure of tightly packed and organized lipid membranes.

Numerous studies demonstrated that LXR activation is crucial for fatty acid and cholesterol synthesis [205]–[208]. Gene expression analysis in LXR*α and* LXR*β* deficient mice confirmed that LXR mediated several target genes connected in cholesterol and fatty acid metabolism in the liver, macrophages, and intestine. Also, the observation that LXR*α* is reactive to fatty acid as well as expressed in metabolic tissue proposes that it also has a role in lipid metabolism [208]. Moreover, SREPB has an essential role in lipid homeostasis [209]–[212]. In this report inhibition of SREBP, by using an S1P inhibitor PF429242, did not affect plasma lipid order, additionally, treatment with LXR agonist GW3965 did not impact

membrane order. Taking together, the inhibition of NK-92 cytotoxicity by oxysterols does not occur via lipid inhibition.

Clear evidence from this report suggested that the potential mechanism of oxysterols involves the insertion and disruption of densely packed plasma lipid order. This occurs due to the hydrophilic nature of the side-chains of 25-HC and 27-HC, preventing their proper incorporation. [186], [190]. The NK cells are well-known for their lytic activity, they can recognize and produce lytic granules toward a target cell through a dynamic process called degranulation. Upon recognition of the target cells, the NK cells formed an immunological synapse to initiate a tight series of controlled downstream events [213]. This involves the movement of lytic granules that are stored cytoplasm of NK cell for secretion purposes. Then, these lytic granules initially converge to the microtubule organizing centre (MTOC) and polarize with the MTOC toward the synapse that forms with the target cells [214]. The lytic granules travel a meshwork of filamentous actin and find a way to be secreted through the NK cell membrane and this movement is supported by myosin-II that motor deliver the vehicle to the site where they are secreted [215]. By this, the lytic granules fuse with the plasma membrane to excrete their contents into synapses between NK cells and target cells [216], [217], [192]. Any defect in the NK-92 plasma membrane may interfere with the ability of NK-92 to kill against target cells. Interestingly, after degranulation, NK cells ensure their own survival due to a membrane-protective mechanism that shields them from the released perforin within the synapse [192].

It has found lytic granules have endogenously intensively packed lipid membranes and that was investigated by using high-resolution imaging and lipidomic analysis. Upon degranulation, fusion between the lytic granule and cell membrane reinforces the presynaptic packing of the membrane. This reinforces membrane protection in specific areas where NK cells anticipate a high concentration of perforin [192]. Disrupting membrane lipid order, NK cells became to be more susceptible to secreted perforin thereby impairing NK function [192]. All this evidence highlighted the significant role of NK plasma membrane structure on NK effector function.

With the recent growing number of studies in development of NK cell-based immunotherapy, NK-92 cells is well positioned to produce off-the-shelf cellular therapy. The future advantage of NK-92 cells are that their potential to generate by genetic manipulation to generate a resistant NK-92 cell inTME.

Chapter 7 – Bibliography

[1] I. Prager *et al.*, “NK cells switch from granzyme B to death receptor–mediated cytotoxicity during serial killing,” *Journal of Experimental Medicine*, vol. 216, no. 9, pp. 2113–2127, 2019.
[2] K. BİLGİN, “CHAPTER ONE INTRODUCTION TO THE IMMUNE SYSTEM KEMAL BİLGİN,” *Human Autoimmunity and Associated Diseases*, p. 1, 2021.
[3] L. E. Lowry and W. A. Zehring, “Potentiation of natural killer cells for cancer immunotherapy: a review of literature,” *Front Immunol*, vol. 8, p. 1061, 2017.
[4] J. S. Marshall, R. Warrington, W. Watson, and H. L. Kim, “An introduction to immunology and immunopathology,” *Allergy, Asthma & Clinical Immunology*, vol. 14, no. 2, pp. 1–10, 2018.
[5] F. A. Bonilla and H. C. Oettgen, “Adaptive immunity,” *Journal of Allergy and Clinical Immunology*, vol. 125, no. 2, Supplement 2, pp. S33–S40, 2010, doi: https://doi.org/10.1016/j.jaci.2009.09.017.
[6] D. L. Hermanson and D. S. Kaufman, “Utilizing chimeric antigen receptors to direct natural killer cell activity,” *Front Immunol*, vol. 6, p. 195, 2015.
[7] L. Chiossone, P.-Y. Dumas, M. Vienne, and E. Vivier, “Natural killer cells and other innate lymphoid cells in cancer,” *Nat Rev Immunol*, vol. 18, no. 11, pp. 671–688, 2018.
[8] M. Luetke-Eversloh *et al.*, “NK cells gain higher IFN-γ competence during terminal differentiation,” *Eur J Immunol*, vol. 44, no. 7, pp. 2074–2084, 2014.
[9] S. Q. Crome *et al.*, “A distinct innate lymphoid cell population regulates tumor-associated T cells,” *Nat Med*, vol. 23, no. 3, pp. 368–375, 2017.
[10] E. Vivier *et al.*, “Innate or adaptive immunity? The example of natural killer cells,” *Science (1979)*, vol. 331, no. 6013, pp. 44–49, 2011.
[11] J. Tabiasco *et al.*, “Human decidual NK cells: unique phenotype and functional properties–a review,” *Placenta*, vol. 27, pp. 34–39, 2006.
[12] S. M. Poznanski and A. A. Ashkar, “What defines NK cell functional fate: phenotype or metabolism?,” *Front Immunol*, vol. 10, p. 1414, 2019.
[13] J. E. Boudreau and K. C. Hsu, “Natural killer cell education in human health and disease,” *Curr Opin Immunol*, vol. 50, pp. 102–111, 2018.
[14] H. S. Lawrence, “Cellular and humoral aspects of the hypersensitive states: a symposium held at the New York Academy of Medicine,” *(No Title)*, 1959.
[15] R. M. Loftus *et al.*, “Amino acid-dependent cMyc expression is essential for NK cell metabolic and functional responses in mice,” *Nat Commun*, vol. 9, no. 1, p. 2341, 2018.
[16] T. L. Geiger and J. C. Sun, “Development and maturation of natural killer cells,” *Curr Opin Immunol*, vol. 39, pp. 82–89, 2016.
[17] M. K. Kennedy *et al.*, “Reversible defects in natural killer and memory CD8 T cell lineages in interleukin 15–deficient mice,” *J Exp Med*, vol. 191, no. 5, pp. 771–780, 2000.
[18] A. Chan *et al.*, “CD56bright human NK cells differentiate into CD56dim cells: role of contact with peripheral fibroblasts,” *The Journal of Immunology*, vol. 179, no. 1, pp. 89–94, 2007.
[19] E. Takahashi *et al.*, “Induction of CD16+ CD56bright NK cells with antitumour cytotoxicity not only from CD16− CD56bright NK cells but also from CD16− CD56dim NK cells,” *Scand J Immunol*, vol. 65, no. 2, pp. 126–138, 2007.
[20] K. Hudspeth *et al.*, “Human liver-resident CD56bright/CD16neg NK cells are retained within hepatic sinusoids via the engagement of CCR5 and CXCR6 pathways,” *J Autoimmun*, vol. 66, pp. 40–50, 2016.

[21] K. Rezvani and R. H. Rouce, “The application of natural killer cell immunotherapy for the treatment of cancer,” *Front Immunol*, vol. 6, p. 578, 2015.
[22] A. Poli, T. Michel, M. Thérésine, E. Andrès, F. Hentges, and J. Zimmer, “CD56bright natural killer (NK) cells: an important NK cell subset,” *Immunology*, vol. 126, no. 4, pp. 458–465, 2009.
[23] W. Carson and M. Caligiuri, “Natural killer cell subsets and development,” *Methods*, vol. 9, no. 2, pp. 327–343, 1996.
[24] C. J. Chan, M. J. Smyth, and L. Martinet, “Molecular mechanisms of natural killer cell activation in response to cellular stress,” *Cell Death Differ*, vol. 21, no. 1, pp. 5–14, 2014.
[25] A. M. Chambers, K. B. Lupo, and S. Matosevic, “Tumor microenvironment-induced immunometabolic reprogramming of natural killer cells,” *Front Immunol*, vol. 9, p. 2517, 2018.
[26] K. Kärre, H. G. Ljunggren, G. Piontek, and R. Kiessling, “Selective rejection of H–2-deficient lymphoma variants suggests alternative immune defence strategy,” *Nature*, vol. 319, no. 6055, pp. 675–678, 1986.
[27] H. Peng and Z. Tian, “Diversity of tissue-resident NK cells,” in *Seminars in immunology*, Elsevier, 2017, pp. 3–10.
[28] E. Hashemi and S. Malarkannan, “Tissue-resident NK cells: development, maturation, and clinical relevance,” *Cancers (Basel)*, vol. 12, no. 6, p. 1553, 2020.
[29] K. Burrows, P. Chiaranunt, L. Ngai, and A. Mortha, “Rapid isolation of mouse ILCs from murine intestinal tissues,” in *Methods in Enzymology*, vol. 631, Elsevier, 2020, pp. 305–327.
[30] L. K. Mackay *et al.*, “Hobit and Blimp1 instruct a universal transcriptional program of tissue residency in lymphocytes,” *Science (1979)*, vol. 352, no. 6284, pp. 459–463, 2016.
[31] D. Cibrián and F. Sánchez-Madrid, “CD69: from activation marker to metabolic gatekeeper,” *Eur J Immunol*, vol. 47, no. 6, pp. 946–953, 2017.
[32] W. Salzberger *et al.*, “Tissue-resident NK cells differ in their expression profile of the nutrient transporters Glut1, CD98 and CD71,” *PLoS One*, vol. 13, no. 7, p. e0201170, 2018.
[33] A. D. Barrow and M. Colonna, “Exploiting NK cell surveillance pathways for cancer therapy,” *Cancers (Basel)*, vol. 11, no. 1, p. 55, 2019.
[34] N. Assmann *et al.*, “Srebp-controlled glucose metabolism is essential for NK cell functional responses,” *Nat Immunol*, vol. 18, no. 11, pp. 1197–1206, 2017.
[35] M. G. Morvan and L. L. Lanier, “NK cells and cancer: you can teach innate cells new tricks,” *Nat Rev Cancer*, vol. 16, no. 1, pp. 7–19, 2016.
[36] S. Bournazos, T. T. Wang, R. Dahan, J. Maamary, and J. V Ravetch, “Signaling by antibodies: recent progress,” *Annu Rev Immunol*, vol. 35, pp. 285–311, 2017.
[37] K. Hr, “Fc gammaRIIIa-158 V/F polymorphism influences the binding of IgG by natural killer cell Fc gammaRIIIa, independently of the Fc gammaRIIIa-48L/R/H phenotype,” *Blood*, vol. 90, pp. 1109–1114, 1997.
[38] H. Peng and Z. Tian, “Diversity of tissue-resident NK cells,” in *Seminars in immunology*, Elsevier, 2017, pp. 3–10.
[39] K. C. Conlon *et al.*, “Redistribution, hyperproliferation, activation of natural killer cells and CD8 T cells, and cytokine production during first-in-human clinical trial of recombinant human interleukin-15 in patients with cancer,” *Journal of clinical oncology*, vol. 33, no. 1, p. 74, 2015.
[40] J. S. Miller *et al.*, “A first-in-human phase I study of subcutaneous outpatient

recombinant human IL15 (rhIL15) in adults with advanced solid tumors," *Clinical Cancer Research*, vol. 24, no. 7, pp. 1525–1535, 2018.
[41] C. Guillerey, N. D. Huntington, and M. J. Smyth, "Targeting natural killer cells in cancer immunotherapy," *Nat Immunol*, vol. 17, no. 9, pp. 1025–1036, 2016.
[42] O. Melaiu, V. Lucarini, L. Cifaldi, and D. Fruci, "Influence of the tumor microenvironment on NK cell function in solid tumors," *Front Immunol*, vol. 10, p. 3038, 2020.
[43] E. Batlle and J. Massagué, "Transforming growth factor-β signaling in immunity and cancer," *Immunity*, vol. 50, no. 4, pp. 924–940, 2019.
[44] M. A. Friese *et al.*, "RNA interference targeting transforming growth factor-β enhances NKG2D-mediated antiglioma immune response, inhibits glioma cell migration and invasiveness, and abrogates tumorigenicity in vivo," *Cancer Res*, vol. 64, no. 20, pp. 7596–7603, 2004.
[45] C. A. Crane, S. J. Han, J. J. Barry, B. J. Ahn, L. L. Lanier, and A. T. Parsa, "TGF-β downregulates the activating receptor NKG2D on NK cells and CD8+ T cells in glioma patients," *Neuro Oncol*, vol. 12, no. 1, pp. 7–13, 2010.
[46] R. Castriconi *et al.*, "Transforming growth factor β1 inhibits expression of NKp30 and NKG2D receptors: consequences for the NK-mediated killing of dendritic cells," *Proceedings of the National Academy of Sciences*, vol. 100, no. 7, pp. 4120–4125, 2003.
[47] K. Slattery *et al.*, "TGFβ drives NK cell metabolic dysfunction in human metastatic breast cancer," *J Immunother Cancer*, vol. 9, no. 2, 2021.
[48] A. Y. Ho, S. Tabrizi, S. A. Dunn, and H. L. McArthur, "Current advances in immune checkpoint inhibitor combinations with radiation therapy or cryotherapy for breast cancer," *Breast Cancer Res Treat*, pp. 1–13, 2022.
[49] K. L. O'Brien and D. K. Finlay, "Immunometabolism and natural killer cell responses," *Nature Reviews Immunology*, vol. 19, no. 5. Nature Publishing Group, pp. 282–290, May 01, 2019. doi: 10.1038/s41577-019-0139-2.
[50] D. Wang and H. Wei, "Natural killer cells in tumor immunotherapy," *Cancer Biol Med*, vol. 20, no. 8, p. 539, 2023.
[51] Y. Wang, X. Li, and S. Ren, "Cholesterol metabolites 25-hydroxycholesterol and 25-hydroxycholesterol 3-sulfate are potent paired regulators: from discovery to clinical usage," *Metabolites*, vol. 11, no. 1, p. 9, 2020.
[52] C. Choi and D. K. Finlay, "Diverse immunoregulatory roles of oxysterols—the oxidized cholesterol metabolites," *Metabolites*, vol. 10, no. 10, p. 384, 2020.
[53] D. O'Shea and A. E. Hogan, "Dysregulation of natural killer cells in obesity," *Cancers (Basel)*, vol. 11, no. 4, p. 573, 2019.
[54] J. Cong, "Metabolism of natural killer cells and other innate lymphoid cells," *Front Immunol*, vol. 11, p. 1989, 2020.
[55] M. L. Martínez-Chantar, T. C. Delgado, and N. Beraza, "Revisiting the role of natural killer cells in non-alcoholic fatty liver disease," *Front Immunol*, vol. 12, p. 640869, 2021.
[56] K. Solocinski *et al.*, "Overcoming hypoxia-induced functional suppression of NK cells," *J Immunother Cancer*, vol. 8, no. 1, 2020.
[57] K. Solocinski *et al.*, "Overcoming hypoxia-induced functional suppression of NK cells," *J Immunother Cancer*, vol. 8, no. 1, 2020.
[58] A. R. Farina, L. Cappabianca, M. Sebastiano, V. Zelli, S. Guadagni, and A. R. Mackay, "Hypoxia-induced alternative splicing: the 11th Hallmark of Cancer," *Journal of Experimental & Clinical Cancer Research*, vol. 39, pp. 1–30, 2020.

[59] O. Melaiu, V. Lucarini, L. Cifaldi, and D. Fruci, “Influence of the tumor microenvironment on NK cell function in solid tumors,” *Front Immunol*, vol. 10, p. 3038, 2020.
[60] G. Thomas, “Keeping Vaccination Simple: Building French Immunization Schedules, 1959–1999,” *Bull Hist Med*, vol. 94, no. 3, pp. 423–458, 2020.
[61] C. Jochems and J. Schlom, “Tumor-infiltrating immune cells and prognosis: the potential link between conventional cancer therapy and immunity,” *Exp Biol Med*, vol. 236, no. 5, pp. 567–579, 2011.
[62] M. A. Erickson and W. A. Banks, “Age-associated changes in the immune system and blood–brain barrier functions,” *Int J Mol Sci*, vol. 20, no. 7, p. 1632, 2019.
[63] E. A. Futata, A. E. Fusaro, C. A. De Brito, and M. N. Sato, “The neonatal immune system: immunomodulation of infections in early life,” *Expert Rev Anti Infect Ther*, vol. 10, no. 3, pp. 289–298, 2012.
[64] C. Fauriat, E. O. Long, H.-G. Ljunggren, and Y. T. Bryceson, “Regulation of human NK-cell cytokine and chemokine production by target cell recognition,” *Blood, The Journal of the American Society of Hematology*, vol. 115, no. 11, pp. 2167–2176, 2010.
[65] M. C. Ochoa *et al.*, “Antibody-dependent cell cytotoxicity: immunotherapy strategies enhancing effector NK cells,” *Immunol Cell Biol*, vol. 95, no. 4, pp. 347–355, 2017.
[66] D. Pende *et al.*, “Identification and molecular characterization of NKp30, a novel triggering receptor involved in natural cytotoxicity mediated by human natural killer cells,” *J Exp Med*, vol. 190, no. 10, pp. 1505–1516, 1999.
[67] A. Diefenbach, E. R. Jensen, A. M. Jamieson, and D. H. Raulet, “Rae1 and H60 ligands of the NKG2D receptor stimulate tumour immunity,” *Nature*, vol. 413, no. 6852, pp. 165–171, 2001.
[68] L. L. Lanier, “NK cell recognition,” *Annu. Rev. Immunol.*, vol. 23, pp. 225–274, 2005.
[69] F. Garrido, F. Perea, M. Bernal, A. Sánchez-Palencia, N. Aptsiauri, and F. Ruiz-Cabello, “The escape of cancer from T cell-mediated immune surveillance: HLA class I loss and tumor tissue architecture,” *Vaccines (Basel)*, vol. 5, no. 1, p. 7, 2017.
[70] P. Parham, “MHC class I molecules and KIRs in human history, health and survival,” *Nat Rev Immunol*, vol. 5, no. 3, pp. 201–214, 2005.
[71] V. M. Braud *et al.*, “HLA-E binds to natural killer cell receptors CD94/NKG2A, B and C,” *Nature*, vol. 391, no. 6669, pp. 795–799, 1998.
[72] N. Anfossi *et al.*, “Human NK cell education by inhibitory receptors for MHC class I,” *Immunity*, vol. 25, no. 2, pp. 331–342, 2006.
[73] J. P. Goodridge, B. Önfelt, and K. Malmberg, “Newtonian cell interactions shape natural killer cell education,” *Immunol Rev*, vol. 267, no. 1, pp. 197–213, 2015.
[74] P. Parham, “MHC class I molecules and KIRs in human history, health and survival,” *Nat Rev Immunol*, vol. 5, no. 3, pp. 201–214, 2005.
[75] C. Fauriat, E. O. Long, H.-G. Ljunggren, and Y. T. Bryceson, “Regulation of human NK-cell cytokine and chemokine production by target cell recognition,” *Blood, The Journal of the American Society of Hematology*, vol. 115, no. 11, pp. 2167–2176, 2010.
[76] M. Terme, E. Ullrich, N. F. Delahaye, N. Chaput, and L. Zitvogel, “Natural killer cell–directed therapies: moving from unexpected results to successful strategies,” *Nat Immunol*, vol. 9, no. 5, pp. 486–494, 2008.
[77] K. Imai, S. Matsuyama, S. Miyake, K. Suga, and K. Nakachi, “Natural cytotoxic

activity of peripheral-blood lymphocytes and cancer incidence: an 11-year follow-up study of a general population," *The lancet*, vol. 356, no. 9244, pp. 1795–1799, 2000.
[78] K. Imai, S. Matsuyama, S. Miyake, K. Suga, and K. Nakachi, "Natural cytotoxic activity of peripheral-blood lymphocytes and cancer incidence: an 11-year follow-up study of a general population," *The lancet*, vol. 356, no. 9244, pp. 1795–1799, 2000.
[79] E. G. Iliopoulou *et al.*, "A phase I trial of adoptive transfer of allogeneic natural killer cells in patients with advanced non-small cell lung cancer," *Cancer immunology, immunotherapy*, vol. 59, pp. 1781–1789, 2010.
[80] S. A. Rosenberg *et al.*, "Observations on the systemic administration of autologous lymphokine-activated killer cells and recombinant interleukin-2 to patients with metastatic cancer," *New England journal of medicine*, vol. 313, no. 23, pp. 1485–1492, 1985.
[81] E. A. Grimm *et al.*, "Lymphokine-activated killer cell phenomenon," *J exp Med*, vol. 157, pp. 884–897, 1983.
[82] L. J. Burns *et al.*, "IL-2-based immunotherapy after autologous transplantation for lymphoma and breast cancer induces immune activation and cytokine release: a phase I/II trial," *Bone Marrow Transplant*, vol. 32, no. 2, pp. 177–186, 2003.
[83] N. Kobayashi, "Artificial cells for the development of cell therapy," *Cell Transplant*, vol. 17, no. 1–2, pp. 3–9, 2008.
[84] A. M. Chambers, K. B. Lupo, and S. Matosevic, "Tumor microenvironment-induced immunometabolic reprogramming of natural killer cells," *Front Immunol*, vol. 9, p. 2517, 2018.
[85] T. Tonn, S. Becker, R. Esser, D. Schwabe, and E. Seifried, "Cellular immunotherapy of malignancies using the clonal natural killer cell line NK-92," *J Hematother Stem Cell Res*, vol. 10, no. 4, pp. 535–544, 2001.
[86] G. JH, "Characterization of a human cell line (NK-92) with phenotypical and functional characteristics of activated natural killer cells," *Leukemia*, vol. 8, pp. 652–658, 1994.
[87] M. J. Robertson, K. J. Cochran, C. Cameron, J. M. Le, R. Tantravahi, and J. Ritz, "Characterization of a cell line, NKL, derived from an aggressive human natural killer cell leukemia.," *Exp Hematol*, vol. 24, no. 3, pp. 406–415, 1996.
[88] S. Meng, X. Wu, J. Fan, W. Xiao, J. Ma, and Z. Tian, "223. Consideration for Quality Control of NKG Cell Line Used for Adoptive Cellular Therapy," *Molecular Therapy*, vol. 23, pp. S87–S88, 2015.
[89] J. Yodoi *et al.*, "TCGF (IL 2)-receptor inducing factor (s). I. Regulation of IL 2 receptor on a natural killer-like cell line (YT cells).," *J Immunol*, vol. 134, no. 3, pp. 1623–1630, 1985.
[90] Y. Kagami *et al.*, "Establishment of an IL-2-dependent cell line derived from 'nasal-type'NK/T-cell lymphoma of CD2+, sCD3−, CD3ε+, CD56+ phenotype and associated with the Epstein-Barr virus," *Br J Haematol*, vol. 103, no. 3, pp. 669–677, 1998.
[91] M. Yagita *et al.*, "A novel natural killer cell line (KHYG-1) from a patient with aggressive natural killer cell leukemia carrying a p53 point mutation," *Leukemia*, vol. 14, no. 5, pp. 922–930, 2000.
[92] J. Tsuchiyama *et al.*, "Characterization of a novel human natural killer-cell line (NK-YS) established from natural killer cell lymphoma/leukemia associated with Epstein-Barr virus infection," *Blood, The Journal of the American Society of Hematology*,

vol. 92, no. 4, pp. 1374–1383, 1998.
[93] Y. K. Tam, B. Miyagawa, V. C. Ho, and H.-G. Klingemann, “Immunotherapy of malignant melanoma in a SCID mouse model using the highly cytotoxic natural killer cell line NK-92,” *J Hematother*, vol. 8, no. 3, pp. 281–290, 1999.
[94] K. V Konstantinidis, E. Alici, A. Aints, B. Christensson, H.-G. Ljunggren, and M. S. Dilber, “Targeting IL-2 to the endoplasmic reticulum confines autocrine growth stimulation to NK-92 cells,” *Exp Hematol*, vol. 33, no. 2, pp. 159–164, 2005.
[95] G. Maki, H.-G. Klingemann, J. A. Martinson, and Y. K. Tam, “Factors regulating the cytotoxic activity of the human natural killer cell line, NK-92,” *J Hematother Stem Cell Res*, vol. 10, no. 3, pp. 369–383, 2001.
[96] S. Heidenreich *et al.*, “Impact of the NK cell receptor LIR-1 (ILT-2/CD85j/LILRB1) on cytotoxicity against multiple myeloma,” *Clin Dev Immunol*, vol. 2012, 2014.
[97] S. Arai *et al.*, “Infusion of the allogeneic cell line NK-92 in patients with advanced renal cell cancer or melanoma: a phase I trial,” *Cytotherapy*, vol. 10, no. 6, pp. 625–632, 2008.
[98] Y. K. Tam, B. Miyagawa, V. C. Ho, and H.-G. Klingemann, “Immunotherapy of malignant melanoma in a SCID mouse model using the highly cytotoxic natural killer cell line NK-92,” *J Hematother*, vol. 8, no. 3, pp. 281–290, 1999.
[99] H.-G. Ljunggren and K.-J. Malmberg, “Prospects for the use of NK cells in immunotherapy of human cancer,” *Nat Rev Immunol*, vol. 7, no. 5, pp. 329–339, 2007.
[100] T. Sutlu and E. Alici, “Natural killer cell-based immunotherapy in cancer: current insights and future prospects,” *J Intern Med*, vol. 266, no. 2, pp. 154–181, 2009.
[101] F. Bibeau *et al.*, “Impact of FcγRIIa-FcγRIIIa polymorphisms and KRAS mutations on the clinical outcome of patients with metastatic colorectal cancer treated with cetuximab plus irinotecan,” *Journal of clinical oncology*, vol. 27, no. 7, pp. 1122–1129, 2009.
[102] R. J. Taylor *et al.*, “FcγRIIIa polymorphisms and cetuximab induced cytotoxicity in squamous cell carcinoma of the head and neck,” *Cancer Immunology, Immunotherapy*, vol. 58, pp. 997–1006, 2009.
[103] A.-C. Tran, D. Zhang, R. Byrn, and M. R. Roberts, “Chimeric zeta-receptors direct human natural killer (NK) effector function to permit killing of NK-resistant tumor cells and HIV-infected T lymphocytes.,” *J Immunol*, vol. 155, no. 2, pp. 1000–1009, 1995.
[104] L. Boissel, M. Betancur, W. S. Wels, H. Tuncer, and H. Klingemann, “Transfection with mRNA for CD19 specific chimeric antigen receptor restores NK cell mediated killing of CLL cells,” *Leuk Res*, vol. 33, no. 9, pp. 1255–1259, 2009.
[105] Y. Chu *et al.*, “Targeting CD20+ aggressive B-cell non–Hodgkin lymphoma by anti-CD20 CAR mRNA-modified expanded natural killer cells in vitro and in NSG mice,” *Cancer Immunol Res*, vol. 3, no. 4, pp. 333–344, 2015.
[106] S. Gilfillan, E. L. Ho, M. Cella, W. M. Yokoyama, and M. Colonna, “NKG2D recruits two distinct adapters to trigger NK cell activation and costimulation,” *Nat Immunol*, vol. 3, no. 12, pp. 1150–1155, 2002.
[107] E. A. Futata, A. E. Fusaro, C. A. De Brito, and M. N. Sato, “The neonatal immune system: immunomodulation of infections in early life,” *Expert Rev Anti Infect Ther*, vol. 10, no. 3, pp. 289–298, 2012.
[108] Z. Wei, X. Liu, C. Cheng, W. Yu, and P. Yi, “Metabolism of amino acids in cancer,” *Front Cell Dev Biol*, vol. 8, p. 603837, 2021.
[109] J. Oberlies *et al.*, “Regulation of NK cell function by human granulocyte arginase,”

The Journal of Immunology, vol. 182, no. 9, pp. 5259–5267, 2009.
[110] N. Kedia-Mehta and D. K. Finlay, “Competition for nutrients and its role in controlling immune responses,” *Nat Commun*, vol. 10, no. 1, p. 2123, 2019.
[111] R. M. Loftus *et al.*, “Amino acid-dependent cMyc expression is essential for NK cell metabolic and functional responses in mice,” *Nat Commun*, vol. 9, no. 1, p. 2341, 2018.
[112] I. Terrén, A. Orrantia, J. Vitallé, O. Zenarruzabeitia, and F. Borrego, “NK cell metabolism and tumor microenvironment,” *Front Immunol*, vol. 10, p. 2278, 2019.
[113] R. M. Loftus *et al.*, “Amino acid-dependent cMyc expression is essential for NK cell metabolic and functional responses in mice,” *Nat Commun*, vol. 9, no. 1, p. 2341, 2018.
[114] J. H. Gong, G. Maki, and H. G. Klingemann, “Characterization of a human cell line (NK-92) with phenotypical and functional characteristics of activated natural killer cells,” *Leukemia*, vol. 8, no. 4, pp. 652–658, 1994, [Online]. Available: http://europepmc.org/abstract/MED/8152260
[115] T. Tonn, S. Becker, R. Esser, D. Schwabe, and E. Seifried, “Cellular immunotherapy of malignancies using the clonal natural killer cell line NK-92,” *J Hematother Stem Cell Res*, vol. 10, no. 4, pp. 535–544, 2001.
[116] H. Y. Shin *et al.*, “Cytokine engineered NK-92 therapy to improve persistence and anti-tumor activity,” *Theranostics*, vol. 13, no. 5, p. 1506, 2023.
[117] Q. Xiong *et al.*, “A novel membrane-bound interleukin-2 promotes NK-92 cell persistence and anti-tumor activity,” *Oncoimmunology*, vol. 11, no. 1, p. 2127282, 2022.
[118] N. J. MacIver, S. R. Jacobs, H. L. Wieman, J. A. Wofford, J. L. Coloff, and J. C. Rathmell, “Glucose metabolism in lymphocytes is a regulated process with significant effects on immune cell function and survival,” *Journal of Leucocyte Biology*, vol. 84, no. 4, pp. 949–957, 2008.
[119] W. Zhang, H. Cai, and W.-S. Tan, “Dynamic suspension culture improves ex vivo expansion of cytokine-induced killer cells by upregulating cell activation and glucose consumption rate,” *J Biotechnol*, vol. 287, pp. 8–17, 2018.
[120] J. Jung, H. Zeng, and T. Horng, “Metabolism as a guiding force for immunity,” *Nat Cell Biol*, vol. 21, no. 1, pp. 85–93, 2019.
[121] H. Sohn and M. A. Cooper, “Metabolic regulation of NK cell function: implications for immunotherapy,” *Immunometabolism (Cobham (Surrey, England)*, vol. 5, no. 1, p. e00020, 2023.
[122] Y.-Y. Gong *et al.*, “Na/H-exchanger 1 Enhances Antitumor Activity of Engineered NK-92 Natural Killer Cells,” 2022.
[123] Y. Peng *et al.*, “Engineering c-Met-CAR NK-92 cells as a promising therapeutic candidate for lung adenocarcinoma,” *Pharmacol Res*, vol. 188, p. 106656, 2023, doi: https://doi.org/10.1016/j.phrs.2023.106656.
[124] X. Song, C. Xu, X. Wu, X. Zhao, J. Fan, and S. Meng, “The potential markers of NK-92 associated to cytotoxicity against K562 cells,” *Biologicals*, vol. 68, pp. 46–53, 2020.
[125] M. Chrobok *et al.*, “Functional assessment for clinical use of serum-free adapted NK-92 cells,” *Cancers (Basel)*, vol. 11, no. 1, Jan. 2019, doi: 10.3390/cancers11010069.
[126] Y. Yang, L. Chen, B. Zheng, and S. Zhou, “Metabolic hallmarks of natural killer cells in the tumor microenvironment and implications in cancer immunotherapy,” *Oncogene*, vol. 42, no. 1, pp. 1–10, 2023.

[127] L. Zhi *et al.*, “Intrinsic and extrinsic factors determining natural killer cell fate: Phenotype and function,” *Biomedicine & Pharmacotherapy*, vol. 165, p. 115136, 2023.
[128] T. G. Poehlmann *et al.*, “Inhibition of term decidual NK cell cytotoxicity by soluble HLA-G1,” *American journal of reproductive immunology*, vol. 56, no. 5-6, pp. 275–285, 2006.
[129] D. I. Sokolov *et al.*, “Phenotypic and functional characteristics of microvesicles produced by natural killer cells,” *Медицинская иммунология*, vol. 21, no. 4, pp. 669–688, 2019.
[130] N. Du, F. Guo, Y. Wang, and J. Cui, “NK cell therapy: A rising star in cancer treatment,” *Cancers (Basel)*, vol. 13, no. 16, p. 4129, 2021.
[131] X. Song, C. Xu, X. Wu, X. Zhao, J. Fan, and S. Meng, “The potential markers of NK-92 associated to cytotoxicity against K562 cells,” *Biologicals*, vol. 68, pp. 46–53, 2020.
[132] D. K. Finlay *et al.*, “PDK1 regulation of mTOR and hypoxia-inducible factor 1 integrate metabolism and migration of CD8+ T cells,” *Journal of Experimental Medicine*, vol. 209, no. 13, pp. 2441–2453, 2012.
[133] W. Salzberger *et al.*, “Tissue-resident NK cells differ in their expression profile of the nutrient transporters Glut1, CD98 and CD71,” *PLoS One*, vol. 13, no. 7, p. e0201170, 2018.
[134] M. Shipkova and E. Wieland, “Surface markers of lymphocyte activation and markers of cell proliferation,” *Clinica chimica acta*, vol. 413, no. 17–18, pp. 1338–1349, 2012.
[135] B. Lo, “The requirement of iron transport for lymphocyte function,” *Nat Genet*, vol. 48, no. 1, pp. 10–11, 2016.
[136] H.-G. Klingemann, E. Wong, and G. Maki, “A cytotoxic NK-cell line (NK-92) for ex vivo purging of leukemia from blood.,” *Biol Blood Marrow Transplant*, vol. 2, no. 2, pp. 68–75, 1996.
[137] C. M. Gardiner, “NK cell metabolism,” *J Leukoc Biol*, vol. 105, no. 6, pp. 1235–1242, 2019.
[138] R. P. Donnelly and D. K. Finlay, “Glucose, glycolysis and lymphocyte responses,” *Mol Immunol*, vol. 68, no. 2, pp. 513–519, 2015.
[139] R. M. Loftus and D. K. Finlay, “Immunometabolism: cellular metabolism turns immune regulator,” *Journal of Biological Chemistry*, vol. 291, no. 1, pp. 1–10, 2016.
[140] O. Warburg, K. Gawehn, and A. W. Geissler, “Metabolism of leukocytes,” *Z Naturforsch B*, vol. 13, no. 8, pp. 515–516, 1958.
[141] D. A. Hume, J. L. Radik, E. Ferber, and M. J. Weidemann, “Aerobic glycolysis and lymphocyte transformation,” *Biochemical Journal*, vol. 174, no. 3, pp. 703–709, 1978.
[142] R. P. Donnelly *et al.*, “mTORC1-dependent metabolic reprogramming is a prerequisite for NK cell effector function,” *The Journal of Immunology*, vol. 193, no. 9, pp. 4477–4484, 2014.
[143] A. Marçais *et al.*, “The metabolic checkpoint kinase mTOR is essential for IL-15 signaling during the development and activation of NK cells,” *Nat Immunol*, vol. 15, no. 8, pp. 749–757, 2014.
[144] D. K. Finlay *et al.*, “Temporal differences in the dependency on phosphoinositide-dependent kinase 1 distinguish the development of invariant Vα14 NKT cells and conventional T cells,” *The Journal of Immunology*, vol. 185, no. 10, pp. 5973–5982, 2010.

[145] J. Shin, S. Wang, W. Deng, J. Wu, J. Gao, and X.-P. Zhong, “Mechanistic target of rapamycin complex 1 is critical for invariant natural killer T-cell development and effector function,” *Proceedings of the National Academy of Sciences*, vol. 111, no. 8, pp. E776–E783, 2014.
[146] R. P. Donnelly *et al.*, “mTORC1-dependent metabolic reprogramming is a prerequisite for NK cell effector function,” *The Journal of Immunology*, vol. 193, no. 9, pp. 4477–4484, 2014.
[147] J. D. Powell, K. N. Pollizzi, E. B. Heikamp, and M. R. Horton, “Regulation of immune responses by mTOR,” *Annu Rev Immunol*, vol. 30, pp. 39–68, 2012.
[148] N. Nandagopal, A. K. Ali, A. K. Komal, and S.-H. Lee, “The critical role of IL-15–PI3K–mTOR pathway in natural killer cell effector functions,” *Front Immunol*, vol. 5, p. 187, 2014.
[149] G. Andrejeva and J. C. Rathmell, “Similarities and distinctions of cancer and immune metabolism in inflammation and tumors,” *Cell Metab*, vol. 26, no. 1, pp. 49–70, 2017.
[150] C. J. Fox, P. S. Hammerman, and C. B. Thompson, “Fuel feeds function: energy metabolism and the T-cell response,” *Nat Rev Immunol*, vol. 5, no. 11, pp. 844–852, 2005.
[151] S. E. Keating *et al.*, “Metabolic reprogramming supports IFN-γ production by CD56bright NK cells,” *The Journal of Immunology*, vol. 196, no. 6, pp. 2552–2560, 2016.
[152] N. Assmann *et al.*, “Srebp-controlled glucose metabolism is essential for NK cell functional responses,” *Nat Immunol*, vol. 18, no. 11, pp. 1197–1206, 2017.
[153] F. A. de Freitas, D. Levy, C. O. Reichert, E. Cunha-Neto, J. Kalil, and S. P. Bydlowski, “Effects of oxysterols on immune cells and related diseases,” *Cells*, vol. 11, no. 8, p. 1251, 2022.
[154] L. Reinmuth, C.-C. Hsiao, J. Hamann, M. Rosenkilde, and J. Mackrill, “Multiple targets for oxysterols in their regulation of the immune system,” *Cells*, vol. 10, no. 8, p. 2078, 2021.
[155] F. A. de Freitas, D. Levy, C. O. Reichert, E. Cunha-Neto, J. Kalil, and S. P. Bydlowski, “Effects of oxysterols on immune cells and related diseases,” *Cells*, vol. 11, no. 8, p. 1251, 2022.
[156] C. Choi and D. K. Finlay, “Diverse immunoregulatory roles of oxysterols—the oxidized cholesterol metabolites,” *Metabolites*, vol. 10, no. 10, p. 384, 2020.
[157] S. He and E. R. Nelson, “27-Hydroxycholesterol, an endogenous selective estrogen receptor modulator,” *Maturitas*, vol. 104, pp. 29–35, 2017.
[158] A. Reboldi, E. V Dang, J. G. McDonald, G. Liang, D. W. Russell, and J. G. Cyster, “25-Hydroxycholesterol suppresses interleukin-1–driven inflammation downstream of type I interferon,” *Science (1979)*, vol. 345, no. 6197, pp. 679–684, 2014.
[159] J. G. Cyster, E. V Dang, A. Reboldi, and T. Yi, “25-Hydroxycholesterols in innate and adaptive immunity,” *Nat Rev Immunol*, vol. 14, no. 11, pp. 731–743, 2014.
[160] A. Biever, E. Valjent, and E. Puighermanal, “Ribosomal protein S6 phosphorylation in the nervous system: from regulation to function,” *Front Mol Neurosci*, vol. 8, p. 75, 2015.
[161] Q. Cao, Z. Liu, Y. Xiong, Z. Zhong, and Q. Ye, “Multiple roles of 25-hydroxycholesterol in lipid metabolism, antivirus process, inflammatory response, and cell survival,” *Oxid Med Cell Longev*, vol. 2020, 2020.
[162] R. A. Saxton and D. M. Sabatini, “mTOR signaling in growth, metabolism, and disease,” *Cell*, vol. 168, no. 6, pp. 960–976, 2017.

[163] M. A. MacMullan, P. Wang, and N. A. Graham, “Phospho-proteomics reveals that RSK signaling is required for proliferation of natural killer cells stimulated with IL-2 or IL-15,” *Cytokine*, vol. 157, p. 155958, 2022.
[164] D. Gotthardt and V. Sexl, “STATs in NK-cells: the good, the bad, and the ugly,” *Front Immunol*, vol. 7, p. 694, 2017.
[165] R. Morris, N. J. Kershaw, and J. J. Babon, “The molecular details of cytokine signaling via the JAK/STAT pathway,” *Protein Science*, vol. 27, no. 12, pp. 1984–2009, 2018.
[166] K. S. Wang, J. Ritz, and D. A. Frank, “IL-2 induces STAT4 activation in primary NK cells and NK cell lines, but not in T cells,” *The Journal of Immunology*, vol. 162, no. 1, pp. 299–304, 1999.
[167] D. Gotthardt, J. Trifinopoulos, V. Sexl, and E. M. Putz, “JAK/STAT cytokine signaling at the crossroad of NK cell development and maturation,” *Front Immunol*, p. 2590, 2019.
[168] N. Assmann *et al.*, “Srebp-controlled glucose metabolism is essential for NK cell functional responses,” *Nat Immunol*, vol. 18, no. 11, pp. 1197–1206, 2017.
[169] W.-R. Lee, T. Ishikawa, and M. Umetani, “The interaction between metabolism, cancer and cardiovascular disease, connected by 27-hydroxycholesterol,” *Clin Lipidol*, vol. 9, no. 6, pp. 617–624, 2014.
[170] N. Zelcer, C. Hong, R. Boyadjian, and P. Tontonoz, “LXR regulates cholesterol uptake through Idol-dependent ubiquitination of the LDL receptor,” *Science (1979)*, vol. 325, no. 5936, pp. 100–104, 2009.
[171] V. M. Olkkonen, O. Béaslas, and E. Nissilä, “Oxysterols and their cellular effectors,” *Biomolecules*, vol. 2, no. 1, pp. 76–103, 2012.
[172] K. E. Waddington *et al.*, “LXR directly regulates glycosphingolipid synthesis and affects human CD4+ T cell function,” *Proceedings of the National Academy of Sciences*, vol. 118, no. 21, p. e2017394118, 2021.
[173] C. Fontaine *et al.*, “Liver X receptor activation potentiates the lipopolysaccharide response in human macrophages,” *Circ Res*, vol. 101, no. 1, pp. 40–49, 2007.
[174] D. Töröcsik *et al.*, “Activation of liver X receptor sensitizes human dendritic cells to inflammatory stimuli,” *The Journal of Immunology*, vol. 184, no. 10, pp. 5456–5465, 2010.
[175] D. Y. Grinman *et al.*, “Liver X receptor-α activation enhances cholesterol secretion in lactating mammary epithelium,” *American Journal of Physiology-Endocrinology and Metabolism*, vol. 316, no. 6, pp. E1136–E1145, 2019.
[176] L. Boissel *et al.*, “An ‘off the shelf,’GMP-grade, IL-2-independent NK cell line expressing the high-affinity Fc-receptor to augment antibody therapeutics,” *Cancer Res*, vol. 76, no. 14_Supplement, p. 2302, 2016.
[177] B. Zhang, J. Zhang, and Z. Tian, “Comparison in the effects of IL-2, IL-12, IL-15 and IFNα on gene regulation of granzymes of human NK cell line NK-92,” *Int Immunopharmacol*, vol. 8, no. 7, pp. 989–996, 2008.
[178] H. Klingemann, “The NK-92 cell line—30 years later: its impact on natural killer cell research and treatment of cancer,” *Cytotherapy*, 2023.
[179] Y. K. Tam, G. Maki, B. Miyagawa, B. Hennemann, T. Tonn, and H.-G. Klingemann, “Characterization of genetically altered, interleukin 2-independent natural killer cell lines suitable for adoptive cellular immunotherapy,” *Hum Gene Ther*, vol. 10, no. 8, pp. 1359–1373, 1999.
[180] M. J. Robertson, K. J. Cochran, C. Cameron, J. M. Le, R. Tantravahi, and J. Ritz, “Characterization of a cell line, NKL, derived from an aggressive human natural

killer cell leukemia.," *Exp Hematol*, vol. 24, no. 3, pp. 406–415, 1996.
[181] M. Yagita *et al.*, "A novel natural killer cell line (KHYG-1) from a patient with aggressive natural killer cell leukemia carrying a p53 point mutation," *Leukemia*, vol. 14, no. 5, pp. 922–930, 2000.
[182] J. Tsuchiyama *et al.*, "Characterization of a novel human natural killer-cell line (NK-YS) established from natural killer cell lymphoma/leukemia associated with Epstein-Barr virus infection," *Blood, The Journal of the American Society of Hematology*, vol. 92, no. 4, pp. 1374–1383, 1998.
[183] Y. Chen *et al.*, "Gene-modified NK-92MI cells expressing a chimeric CD16-BB-ζ or CD64-BB-ζ receptor exhibit enhanced cancer-killing ability in combination with therapeutic antibody," *Oncotarget*, vol. 8, no. 23, p. 37128, 2017.
[184] X. Tang *et al.*, "First-in-man clinical trial of CAR NK-92 cells: safety test of CD33-CAR NK-92 cells in patients with relapsed and refractory acute myeloid leukemia," *Am J Cancer Res*, vol. 8, no. 6, p. 1083, 2018.
[185] G. Suck *et al.*, "NK-92: an 'off-the-shelf therapeutic'for adoptive natural killer cell-based cancer immunotherapy," *Cancer immunology, immunotherapy*, vol. 65, pp. 485–492, 2016.
[186] K. E. Waddington, I. Pineda-Torra, and E. C. Jury, "Analyzing T-cell plasma membrane lipids by flow cytometry," *Lipid-Activated Nuclear Receptors: Methods and Protocols*, pp. 209–216, 2019.
[187] H. Jiang *et al.*, "Transfection of chimeric anti-CD138 gene enhances natural killer cell activation and killing of multiple myeloma cells," *Mol Oncol*, vol. 8, no. 2, pp. 297–310, 2014.
[188] P. Oberoi and W. S. Wels, "Arming NK cells with enhanced antitumor activity: CARs and beyond," *Oncoimmunology*, vol. 2, no. 8, p. e25220, 2013.
[189] K. Slattery *et al.*, "TGFβ drives mitochondrial dysfunction in peripheral blood NK cells during metastatic breast cancer," *Biorxiv*, p. 648501, 2019.
[190] H. Ohvo-Rekilä, B. Ramstedt, P. Leppimäki, and J. P. Slotte, "Cholesterol interactions with phospholipids in membranes," *Prog Lipid Res*, vol. 41, no. 1, pp. 66–97, 2002.
[191] S. E. Gale *et al.*, "Side chain oxygenated cholesterol regulates cellular cholesterol homeostasis through direct sterol-membrane interactions," *Journal of Biological Chemistry*, vol. 284, no. 3, pp. 1755–1764, 2009.
[192] B. N. Olsen, P. H. Schlesinger, and N. A. Baker, "Perturbations of membrane structure by cholesterol and cholesterol derivatives are determined by sterol orientation," *J Am Chem Soc*, vol. 131, no. 13, pp. 4854–4865, 2009.
[193] A. Magenau *et al.*, "Phagocytosis of IgG-coated polystyrene beads by macrophages induces and requires high membrane order," *Traffic*, vol. 12, no. 12, pp. 1730–1743, 2011.
[194] R. Filomenko, C. Fourgeux, L. Bretillon, and S. Gambert-Nicot, "Oxysterols: Influence on plasma membrane rafts microdomains and development of ocular diseases," *Steroids*, vol. 99, pp. 259–265, 2015.
[195] S. M. Lu and G. D. Fairn, "7-Ketocholesterol impairs phagocytosis and efferocytosis via dysregulation of phosphatidylinositol 4, 5-bisphosphate," *Traffic*, vol. 19, no. 8, pp. 591–604, 2018.
[196] Y. Li and J. S. Orange, "Degranulation enhances presynaptic membrane packing, which protects NK cells from perforin-mediated autolysis," *PLoS Biol*, vol. 19, no. 8, p. e3001328, 2021.